DESIGN OF COANDA INTAKES FOR OPTIMUM SEDIMENT RELEASE EFFICIENCIES AND WATER CAPTURE PERFORMANCES

A Thesis Submitted to
the Graduate School of Engineering and Sciences of
İzmir Institute of Technology
in a Partial Fulfillment of the Requirements for the Degree of

MASTER OF SCIENCE

in Civil Engineering

by
Oğuz HAZAR

May 2020
İZMİR

ACKNOWLEDGEMENTS

I would like to express my gratitude to everyone who contributed to help me to finish my thesis. I wish to thank my advisors Prof. Dr. Gökmen Tayfur and Co-advisor Prof. Dr. Şebnem Elçi for all their precious supports. Additionally, I would like to thank my family who was always with me during my studies and offered endless support to me. Finally, I would like to express my special thanks to my grandfather Recep Yamanlar who always supported me with his extensive knowledge.

ABSTRACT

DESIGN OF COANDA INTAKES FOR OPTIMUM SEDIMENT RELEASE EFFICIENCIES AND WATER CAPTURE PERFORMANCES

Bottom type water intake structures are frequently preferred in the case of flows containing high levels of sediment in case where it is not possible to construct settling pool or if their construction costs are high. Coanda and Tyrolean type water intake structures are the most commonly used bottom type intake structures. It has been observed in a limited number of studies that Coanda type water intakes are superior to the Tyrolean type water intakes both in terms of withdrawing the design amount of flow and excluding the sediment as much as possible. However, the biggest obstacle to the widespread usage of Coanda type water intake is their complex design and difficulties of the analysis. It has been observed that there are no formula or numerical studies that calculate the water Capture Performance (WCP) and Sediment Release Efficiency (SRE) of the Coanda screens. In order to overcome this gap in the literature, six different Coanda screens have been tested for both WCP and SRE using various incoming flows and sediment compositions. The data obtained as a result of the experimental studies were analyzed using statistical analysis method and two different equations were obtained that enable to find the WCP and SRE. In a situation where the incoming flow conditions and screen parameters are known, someone can gain a preliminary knowledge about the screen performance by using these equations. As a result of this study, adding new data to the literature and eliminating the mentioned lack in the literature was aimed.

ÖZET

COANDA TİPİ SU ALMA YAPILARININ SEDİMENT GEÇİRME VERİMLİLİĞİ VE SU ALMA PERFORMANSINA GÖRE OPTİMUM TASARIMLARININ YAPILMASI

Tabandan su alma yapıları, sediment yoğunluğunun yüksek olduğu ve çökeltme havuzu benzeri yapıların inşa edilmesinin mümkün olmadığı ya da yapımlarının yüksek maliyetli olması durumlarında sıklıkla tercih edilen yapılardır. Coanda ve Tirol tipi su alma yapıları en çok tercih edilen tabandan su alma yapılarıdır. Coanda ızgaraların hem istenilen tasarım debisini çekme konusunda hem de çekilen debinin sediment ve diğer katı cisimlerden mümkün olduğunca arındırılması bakımından Tirol tipi ızgaralardan daha üstün olduğu yapılmış olan sınırlı sayıda ki çalışmalarda görülmüştür. Ancak Coanda ızgaraların kullanılması konusunda ki en büyük engel tasarım ve analizlerinin oldukça karmaşık olmasıdır. Coanda ızgaralar ile ilgili yapılmış olan önceki çalışmalar incelendiğinde her ne kadar yalnızca temiz su koşulları için ve sadece ızgaraların su çekme performansını ortaya koyan bir program olduğu görülmüş olsa da hem temiz su koşulları hem de sediment etkisini gözeterek ızgaraların su çekme performansı ve sediment uzaklaştırma verimliliğini hesaplamaya yarayan bir formül çalışmasının olmadığı görülmüştür. Literatürde ki bu eksikliği gidermek amacıyla farklı ızgara parametrelerine sahip altı Coanda ızgara değişik debiler ve sediment kompozisyonları kullanılarak su çekme performansı (WCP) ve sediment uzaklaştırma verimliliği (SRE) için test edilmiştir. Deneysel çalışmalar sonucunda elde edilen veriler sayısal analiz yöntemi kullanılarak analiz edilmiş ve su çekme performansı ve sediment geçirme verimliliğini bulmayı sağlayan iki farklı bağıntı elde edilmiştir. Akım koşulları ve ızgara parametreleri bilinen bir durumda kullanıcı bu bağıntıları kullanarak ızgara performansı hakkında bir ön bilgi edinebilmektedir. Bu çalışma neticesinde hem literatüre veri katkısı yapılmış hem de elde edilen bağıntılar sayesinde literatürde saptanan ve sözü edilen eksikliğin giderilmesi amaçlanmıştır.

TABLE OF CONTENTS

LIST OF FIGURES

Figures **Page**

LIST OF TABLES

Table **Page**

LIST OF SYMBOLS

C = Discharge coefficient for weir equation

C_d = Discharge coefficient or (concentration of diverted flow)

C_{d0} = Discharge coefficient calculated under static conditions

C_{in} = Diverted flow concentration

C_q = Discharge coefficient

C_{qh} = Discharge coefficient on the current location

C_{qH} = Discharge coefficient on the energy level

C_{q0} = Discharge coefficient under static conditions due to kinetic energy

C_{CV} = Coefficient for the velocity reduction and contraction

CF = Coefficient which is dependent to Froude number and geometry of the screen

D = Flow rate

D_x = Local flow depth

F = Froude number

Fre = Froude number based on bar spacing

F_{H0} = Froude number at the beginning of the screen

H = Hydraulic head or (weir head for the weir equation)

H_0 = Specific flow depth that is approaching to rack

L = Wetted screen length

L_{total} = Total screen length

L_{net} = Net screen length

ΔL = Section length

R = Reynolds number or screen curvature radius

SRE = Sediment Release Efficiency

SRE_C = Sediment Release Efficiency based on concentration

Si and Sd = Diverted sediment amount

St and Sd = Incoming sediment amount in the main channel

V = Velocity of the incoming flow

Q_{in} = Approaching flow rate

Q_t = Total incoming flow

Q_1 = Total approximation flow

Qi and Qd = diverted water discharge

Qt and Qin = Incoming water discharge

W = Weber number

WCP = Water Capture Performance

X = Sagging distance

θ = Screen inclination

Ø = Wire tilt angle

β = constant takes 2,42 for T-shape bars, and takes 1,79 for circular bars

a = Empirical coefficient equal to – 0,1056 or distance between centerline of two consecutive bars

$\mathbf{b_0}$ = Empirical coefficient equal to 1,5

$\mathbf{b_1}$ = Empirical coefficient equal to 0,478

b = Width of the channel or (the crest width for the weir equation)

dq / dx = Diverted discharge for unit width for length dx

$\mathbf{d_{50}}$ = Median of the sediment diameter

e = Distance between two consecutive bars

f = coefficient that reduces to the effective opening

g = Gravitational acceleration

h = average flow depth

$\mathbf{h_0}$ = is the water colum height at the beginning of the screen

k = coefficient that reduces the effective area on the rack

m = Void ratio

m' = $m * C_{qh}$

p = Screen porosity or accelerator plate height

s = Sloth width

$\mathbf{q_0}$ = specific flow rate at the beginning of the screen

Δqd = Flow that is derived from the length of the segment

w = wire width

α = wire tilt angle

ρ = Density of water

$\mathbf{\rho_s}$ **=** Density of sediment

υ = kinematic viscosity

σ = Surface tension

$\mathbf{\sigma_D}$ **=** Uniformity coefficient

λ = Pressure coefficient in the energy equation

CHAPTER 1

INTRODUCTION

1.1. General Information

Water is the source of life and it is an essential substance for living things. Both water scarcity and excessive amounts cause serious problems for people and other living things. In the world, many people suffer from water scarcity due to the unconscious use of water resources while others also suffer from floods and other problems which are a result of an excessive amount of water. Because its absence or excessive amount is so important, people have tried to reach water resources and controlled its power for ages.

Some archeological evidence proof that even in ancient times, people constructed barriers for preventing the floods and they constructed dams, reservoirs, wells, and cisterns for using water in irrigation and domestic usage. Sad-el-Kaffara which is constructed at the time of ancient Egypt is accepted as one of the earliest dams in the world (Figure 1).

Figure 1. Sadd-el-Kafara Dam (Source: https://structurae.net/en/structures/sadd-el-kafara-dam)

In addition to this, according to the evidence Central and South American civilizations started to construct dam type buildings during the Pre-Colombian period. Dams are not only structures that were constructed at an early age but, also cisterns, wells, and artificial reservoirs were constructed. Mayans, for example, an important civilization that constructed these kinds of structures. In Anatolia region, many irrigation canals, tunnels and small dams that are dating from the time of the Hittites were found. Among the ancient time civilizations, Roman civilization has an important place in the field of engineering. They brought millions of liters of water to the cities of the Roman Empire with constructing aqueducts (Figure 2). Lots of more examples can be given for the application of water-related structures that have been constructed so far. When we examine the usage area of the water at an early age, it can be concluded that water was used for irrigation and domestic usages.

Figure 2.Roman Aqueduct (Source: https://www.nationalgeographic.org/ encyclopedia/ roman-aqueducts/)

With the development of technology, people figured out that water is also be used in power generation besides irrigation and domestic usage by using its kinetic energy or using its vapor pressure. Energy production stages are carried out with the turbines and other high-value machinery in the power plants. These types of machinery designed for work under clear water conditions that bear negligibly little or no particle inside. Particles in the water cause damage to the turbines, pumps and other electronic devices that are

used in the plant and decrease their life span resulting in both reduced productivity and economic losses. Since these types of machinery are sensitive to the solid particles in the water, the quality of the water which is transmitted from reservoirs or rivers must be well purified from the particles as much as possible.

It is also important that the water required for drinking and general use is well purified from sediment and turbidity for both in terms of aesthetics and health aspects. Turbidity which is caused by the reflection of light suspended or dissolved substances in water is not always a definite indicator of a health hazard, but studies have shown that this kind of water has the potential to carry disease risk. It is known that heavy metals attached to particles can be transported over very long distances. In addition, these particles serve as both food sources and shelter for harmful and pathogenic bacteria and microorganisms. This makes it difficult to eradicate pathogens and therefore causes water-borne diseases.

For these reasons, it is important that water is free from particles and materials as much as possible during the initial withdrawn. Intake structures on in channels or in reservoirs are frequently used to divert or withdraw a certain amount of water discharge for various purposes such as irrigation, potable water supply and generation of hydroelectric power. Different types of intake structures can be used for that purpose. Frontal, lateral and bottom type intake structures are most widely used for that process. Sugözü regulator (Figure 3) that was constructed in Turkey is an example of the lateral intake structure.

Figure 3. Sugözü Regulatör is an example of lateral intake (Source: http://www.ressiad.org.tr /images/genel/gzp01.jpg)

Hydrologic, geotechnical, topographic and climatic factors directly affect the type of intake structures that is to be constructed. Factors such as excessive rain or snowmelt and greater river bed slope which can be a cause of high flow rate make impossible to use the frontal and lateral intake structures. When the water has to be diverted from a turbid source having a great number of suspended materials, and if it is not possible to construct any settling pool or settling basin due to the economical or topographic factors bottom intake structures such as Coanda and Tyrolean types (Figure 4 and Figure 5) are preferred.

For performing this task, diverted water is captured by a transversal rack and a gallery located in the control crest is utilized. With a proper design of the intake, the quality of the diverted water can be increased by screening out most of the sediments in the flow. In the design of the structure, it is necessary to consider different aspects. The efficiency of the intake structure depends on various factors such as the shape of the bar, the clear spacing between the bars (void ratio), flow approximation conditions and quantity, the angle of the rack, length, sediment rate, and composition, etc.

Figure 4. An example of Coanda type intake (Source: http://www.hydroscreen.com/#sthash.fFGLJ11I.dpbs)

Figure 5. Tyrolean intake (Source: https://www.braun- tech.com/upload/filecache/ Basochhu_1_4eb43d92e9a2bc8ff3922a78b0c6a30a.jpg)

There are serious differences between the designs of Coanda and Tyrolean intake structures. Before starting to focus on the main differences between these two kinds of bottom intake structures, it is important to explain meaning of Coanda effect. The Coanda effect (Figure 6) is the tendency of the fluid jet to stay attached to a convex surface as described by its inventor Henry Coanda. As the Coanda effect is used in different areas, one of its applications is the Coanda type water intake structures. The racks of the Coanda intake create curvature shape (Figure 7) rather than straight screen shape as Tyrolean intake. In addition to this, racks of the Tyrolean intakes are placed parallel to the flow direction. Opposite of this, racks of the Coanda intakes (Figure 8) are placed perpendicular to the flow direction in order to create an extra shear force to divert additional inflow.

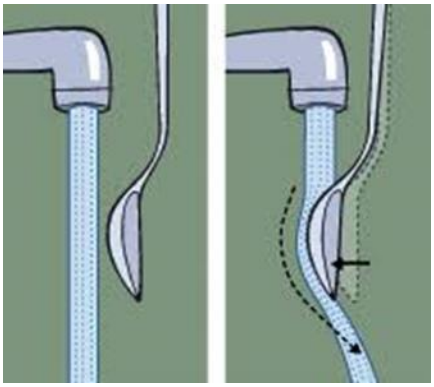

Figure 6. illustration of the Coanda effect (Source: researchgate.net/figure/f-Falling-water-being-re-directed-by-a-spoon-As-there-is-a-lack-of-appropriate-data-and_fig4_338117108

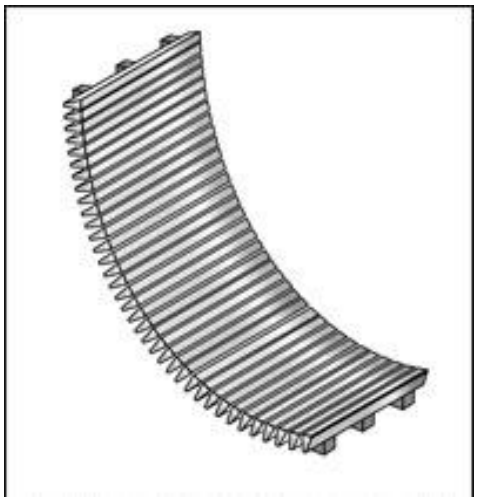

Figure 7. Curved screen shape (Source: http://www.plastok.co.uk/wp- content/ uploads/2014/06/wedge_wire_03.jpg)

Figure 8. Example of the Coanda intake rack (Source: https://encrypted- tbn0.gstatic. com/images?q=tbn:ANd9GcRPcPnNxd3duUObfo1CcPM2o_3SxJL09lX5YR XfuGZB715SlMZe0g&s)

Another important feature of the Coanda intake is that the screen has self-cleaning ability due to its curvature screen shape and the position of the racks. While the design amount of flow is diverted from the weir, most of the sediment passes over the screen (Figure 9) and carried through the downstream with the by-pass flow. Additionally, Coanda intakes are environment-friendly structures that help to pass fish and fish eggs from upstream of the river to downstream and also, help sediment continuity in the river.

Figure 9. Sediment movement on Coanda intake (Source: https://www.wild-metal.com/sites/default/files/styles/contentbilder/public/referenzbilder/prischeralm_wildmetal_stahlwasserbau.jpg?itok=t6TEy0qN)

Another important thing is the mechanisms that govern water withdrawn from the intake structures. Both for Coanda and Tyrolean intakes, one of the important mechanisms that govern the water withdrawn is the orifice effect. Water column height on the screen directly affects the amount of orifice flow that is taken through the screen. The water column height is increasing while the screen inclination is decreasing. On the other hand, decreasing the screen inclination causes decreasing the flow velocity which is passing over the screen and the risk of clogging becomes apparent. Especially for the Tyrolean type intakes, there must be necessary screen inclination for decreasing the clogging probability. According to study of (Castillo, García and Carrillo 2013.) that was conducted with the flow that contains sediment, maximum water capturing performances obtained when the screen slope %30 and the worst performance was obtained when the screen angle %0. However, in the clear water test, the maximum performance was obtained at %0 screen inclination and the worst performance was obtained %33 screen inclination. This subject will be discussed in the literature review part of the thesis and more information will be given about this subject. As a result, the Tyrolean type intakes should be designed with the necessary screen slope to overcome from clogging problem but this reduces the water height on the screen and also decrease the orifice effect.

Therefore, withdrawn or capturing flow is decreasing. On the other hand, if Coanda type intakes are used instead of the Tyrolean type intakes, the water capturing performances would be still high even in steep slopes because of the shear effect which occurs due to the perpendicular placed racks. The shear effect increases with the increasing screen slope. In the study of (T. L. Wahl 2003), which is presented by USBR, the relation between diverted discharge and screen slope is proposed as Figure 10. In this graph, it is clearly seen that a small amount of decrement observed while the screen slope is increasing. On the other hand, even this small amount of the decrement can be tolerated by increasing the wire tilt angle and porosity. The wire tilt angle can be expressed as the angle of individual wires with a horizontal plane. It increases the shear effect and also, increases the withdrawn water.

As a result, it can be said that Coanda type intake structures are an advanced version of Tyrolean type intake structures. Although both types of intakes are economical and they do not use any energy source for operation, the Coanda type intakes are more efficient structures than Tyrolean type intake structures. The self-cleaning feature makes the screen more durable to clogging and helps to keep water capture performance high. It also reduces maintenance costs.

Despite these advantages, Tyrolean type intakes have been the most widely preferred structures in Turkey and all around the world. The main reason for this is that the analysis affecting the design and performance of the Coanda screen is more complicated than Tyrolean type intakes. However, the usage of the Coanda type intakes has increased through the world due to its advanced features over the Tyrolean intake.

Some examples for the application of Coanda intakes can be given;

- Aybige Regulator in Turkey
- Murat – 1 and Murat – 2 hydroelectric power plants in Turkey
- Gökböğet regulator and hydroelectric power plant in Turkey
- Wahianoa Intake in New Zeleand in New Zealand
- City Creek Intake in Utah in U.S.A
- Rock Mountain Arsenal in Colorado in U.S.A
- Stand – Alone Hydro Intake in Scotland
- Center of Alternative in Wales

Many examples for the application of the Coanda intakes in projects can be given from both Turkey and all around the world.

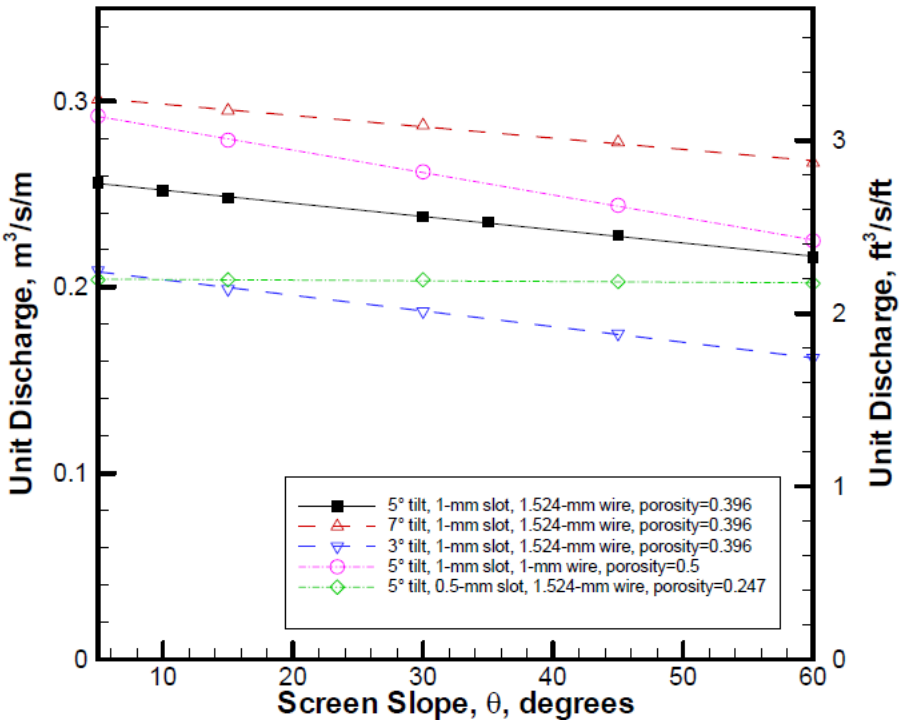

Figure 10. Relation between screen slope and diverted discharge (Source: Wahl, L. Design guidance for Coanda-effect screens. Bureau of Reclamation, Technical Service Center, Water Resources Research Laboratory, Denver, 2003.)

In this part of Chapter-1 general information has been given so far which consists of the importance of the water for humans and the development of the water-related structures and usage purposes of water until today. Also, intake structure types such as frontal, lateral and bottom type intakes have been discussed. Finally, Coanda and Tyrolean type bottom intakes and their differences have been discussed very briefly so far. In the literature review part, the previous studies related to both Coanda and Tyrolean types will be investigated. Although this presented study focuses on the optimum design of the Coanda water intake structure and its both water capturing performance and sediment release efficiency, previous studies about the Tyrolean intakes are important. Because there are some formulations proposed for Coanda intakes are derived from the Tyrolean weir formulations. When the necessary information and previous studies are examined in the literature review part, the aim and motivation of the presented study will be explained in detail. In Chapter 3 experimental setup of the presented study will be proposed. Finally, in Chapters (4 and 5) results that are gained from the experiments and statistical analysis will be presented and discussed. In Chapter 6, conclusion will be presented.

CHAPTER 2

LITERATURE REVIEW

2.1. Previous Studies Related with Tyrolean Intakes

Many researchers have studied on bottom intake structures and they have proposed some equations and formulations on their research subjects so far. As mentioned before the discharge rate and efficiency of an intake structure depend on some parameters. These parameters can be list as; incoming flow rate, screen void ratio, the width of sloth, the width of the wire, screen length and screen slope for both Coanda and Tyrolean type of intakes and wire tilt angle and screen curvature radius for Coanda type intakes. Additionally, two mechanisms govern the withdrawn water. These mechanisms are the orifice effect (orifice flow) and the shear effect. The orifice flow occurs for both Coanda and Tyrolean type intakes. On the other hand, shear effect is only valid for Coanda type intakes due to the its curvature shape, wire (rack) position to the incoming flow and wire tilt angle. Generally, the rate of the diverted flow for all orifice structure can be expressed by Equation 2.1;

$$\frac{dq}{dx} = C_d \, m \sqrt{2 \, g \, H} \tag{2.1}$$

dq/dx = diverted discharge for unit width for length dx; C_d = discharge coefficient; m = void ratio is the ratio of the opening area to the total area of the screen; H=hydraulic head.

Several researchers (Garot 1939; Bouvard 1953; Noseda 1956b; Mostkow 1957; Brunella, Hager and Minor 2003; Marchi and G. 1947) tried to modify Equation 1.1 and they proposed equations for the rate of diverted flow through a bottom intake structure. These equations are proposed for Tyrolean type intake structures and they are listed below in Table 1.

Table 1. Proposed unit discharge equations for Tyrolean intakes

Author	dq/dx	Cd
(Garot 1939)	$C_d\ m\ \sqrt{2gD}$	Constant (1)
(Marchi and G. 1947)	$C_d\ m\ \sqrt{2gHo}$	Constant (1)
(Bouvard 1953)	$C_{d0}\ m\ \sqrt{2gD(x)cos\theta}$	Constant (1)
(Noseda 1956b)	$C_d\ m\ \sqrt{2gD(x)}$	$\alpha\ (D_x / B)^{-0,13}$
(Mostkow 1957)	$C_d\ m\ \sqrt{2gHo}$	Constant (2)
(Brunella, Hager and Minor 2003)	$C_{d0}\ m\ \sqrt{2gD(x)cos\theta}$	Constant (3)

Where dq/dx = discharge through the grid per unit width; C_d = discharge coefficient; C_{d0} = discharge coefficient calculated under static conditions; m = void ratio; D = flow rate; D_x = local flow depth; H_0 = specific flow depth that is approaching to the rack; Constant (1) = it is constant value but not specified; Constant (2) = C_d is suggested (Orth, Chardonnet and Meynardi 1954) to vary in the range of 0.514 – 0.609 for horizontal racks and 0.441 – 0.519 for racks inclined at 1/5 slope; Constant (3) = C_{d0} is measured under static conditions, it is mainly depend on porosity and slightly depend on orifice Reynold number.

For theoretical studies, two kinds of approaches have been preferred. In this part, the necessary rack length equations that have been proposed so far will be discussed according to the approaches given below. These approaches are;

- Constant Energy Level (Energy Grade Line is horizontal)
- Constant Energy Head (Energy Grade Line is parallel to the trash rack)

2.1.1. Constant Energy Level Approaches for Rack Length

One of the theoretical analysis approaches is the Constant Energy Level approach (Figure 11). Some of the researchers (Marchi and G. 1947; Noseda 1956a; Dagan 1963; Krochin and Sviatoslav 1978) preferred the Constant Energy Level approach for

theoretical analysis of the intake structure. Researchers proposed formulas for the wetted length and discharge coefficient. These formulas and equations were proposed for Tyrolean type intake structures.

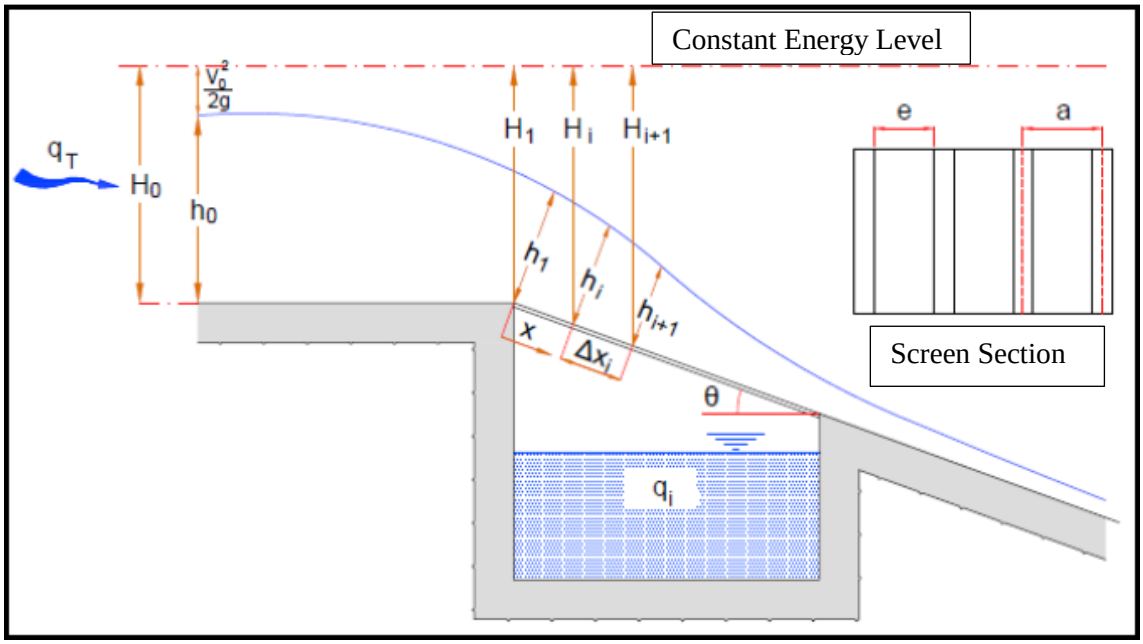

Figure 11. Constant Energy Level approach (Source: Maraş 2017)

(Noseda 1956a) proposed equations that are related to wetted screen length. According to his studies, the wetted length of the screen depends on the flow regime. These equations are given by Equation 2.2 and Equation 2.3.

$$L=0.3994\frac{H_0}{C_{qh}.m}$$

For subcritical flow case

(2.2)

$$L=1.1848\frac{H_0}{C_{qh}.m}$$

For critical flow case

(2.3)

Where L = wetted rack length; H_0 = water height at the beginning of the rack; C_{qh} = discharge coefficient on the current location; m = void ratio.

According to (Mostkow 1957) the wetted length is defined as;

$$L=\frac{Q_1}{C_{qH}\, b\, m\, \sqrt{2gH_0}} \tag{2.4}$$

Q_1 = total approximation flow; C_{qH} = discharge coefficient on the energy level; b= width of the channel; m = void ratio; H_0 = water height at the beginning of the rack.

(Dagan 1963) proposed another equation to describe the wetted length as in Equation 2.5. He developed a coefficient, Ψ, from experimental studies. In Figure 12 the relation of Ψ with another dimensionless parameter can be seen.

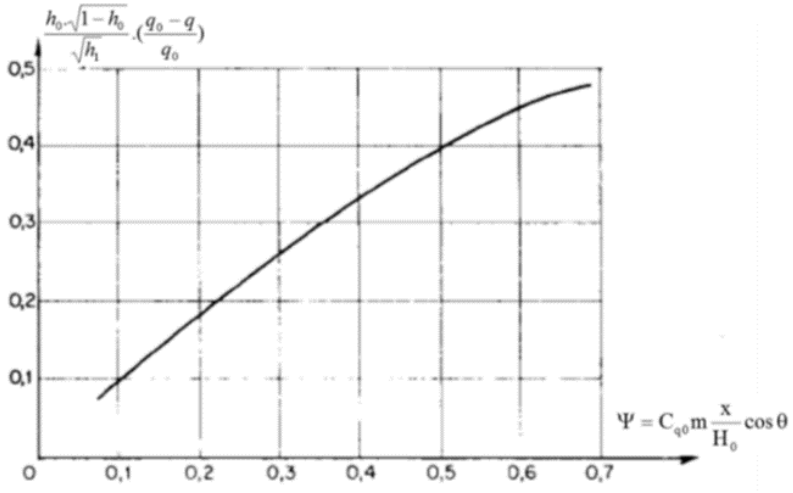

Figure 12. Relation between Ψ and other dimensionless parameters

$$L=\Psi\frac{H_0}{Cq_0\, m\, \cos\theta} \tag{2.5}$$

Where, C_{q0} = discharge coefficient under static conditions due to kinetic energy; m = void ratio; H_0 = water height at the beginning of the rack. Dagan estimated that C_{q0} = 0.72 which is determined by (Noseda 1956).

Another approach for the wetted length was derived from (Krochin and Sviatoslav 1978) and given by Equation 2.6.

$$L=\left[\frac{0.313\ q_l}{(C_{qH}\ k)^{1.5}}\right]^{\frac{2}{3}} \tag{2.6}$$

k = coefficient that reduces the effective area on the rack and defined as k = (1-f) m; f = coefficient that reduces to the effective opening %15 to %30 due to the clogging. Krochin's approach has an important place in the literature because the equation considers the clogging effect which is caused by sedimentation and it differs from the other wetted length formulas in this way.

2.1.2. Constant Energy Head Approach for Rack Length

Another method for the theoretical approach of a Tyrolean intake is the Constant Energy Head Approach. Some researchers (Bouvard 1953; Frank, Von and Erlangen 1956; Brunella, Hager and Minor 2003; Righetti and Lanzoni 2008) performed their studies based on this approach. The representative drawing of this approach is given in Figure 13.

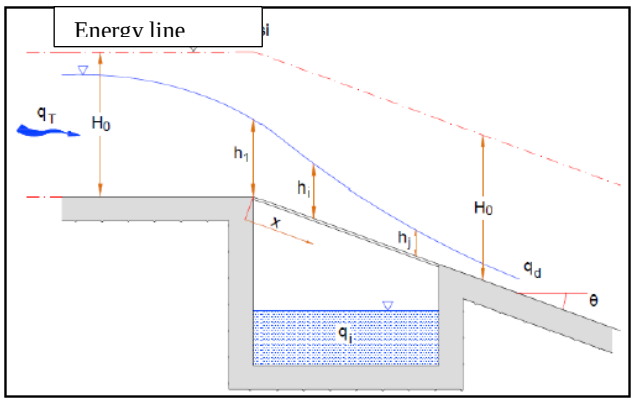

Figure 13. Constant Energy Head Approach (Source: Maraş 2017)

(Bouvard 1953) proposed the rack length equation as;

$$L=\left\{\frac{1}{2m'}\left[\left(j+\frac{1}{2j^2}\right)\arcsin\sqrt{\frac{j}{j+(1/2j^2)}}+3\sqrt{\frac{1}{2j}}\right]+\left(\frac{0,303}{m'^2}+\frac{2j^3-3j^2+1}{4j^2}\right)\tg\theta\right\}h_1\cos\theta \quad (2.7)$$

Where m' = mC_{qh} and it indicates that the equation considers the sedimentation and clogging of the screen racks. $j = h_1 / h_c$.

One of the other important studies was performed by (Frank, Von and Erlangen 1956) which considers that the energy head is constant and the flow profile of the fluid is elliptic arch as seen in Figure 14. The equation which is about the necessity rack length is given by Equation 2.8.

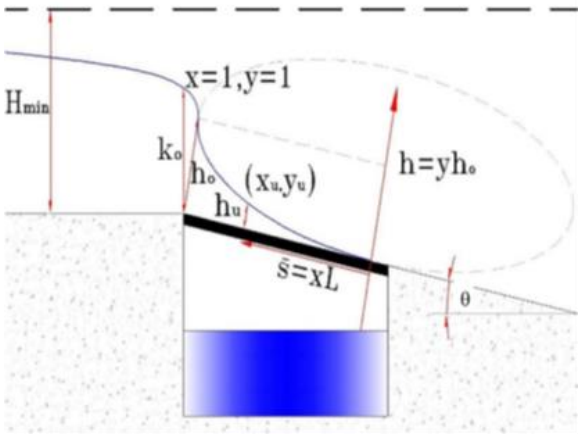

Figure 14. Representative drawing of the elliptic arc flow (Source: Castillo and Bermejo 2016)

$$L=2.561\frac{q_0}{\lambda\sqrt{h_0}} \quad (2.8)$$

Where q_0 is the specific flow rate at the beginning of the screen. h_0 is the water column height at the beginning of the screen that is measured perpendicular to the rack and λ is the pressure coefficient in the energy equation. Brunella was another important researcher

who studied on this topic and he developed his own rack length equation based on the Constant Energy Head Approach. The equation is given by Equation 2.9.

$$L=\frac{0.83\ H_0}{C_{q0}\ m} \tag{2.9}$$

Where H_0 is the energy head at the beginning of the screen. C_{q0} is the discharge coefficient under static conditions and m is the void ratio.

2.1.3. Other Equations Related with Rack Length

(Chow 1959) proposed an equation after investigating the previous studies which are performed by (Garot 1939; Frank, Von and Erlangen 1956; Noseda 1956; Mostkow 1957). His equation about the screen length for longitudinal bars is given by Equation 2.10.

$$L=\frac{Q_1}{C_{qH}.b.m\sqrt{2gH_0}} \tag{2.10}$$

Where Q_1 is the flow rate at the beginning of the screen; C_{qH} is the discharge coefficient considering that the load equal to the height of the energy line; H_0 is the height of the energy which is measured at the beginning of the screen; m is the void ratio of the intake. (Drobir, Kienberger and Krouzecky 1999) defines the rack lengths needed to capture a certain amount of flow. In this definition, he distinguishes two different lengths L_1 and L_2 for the first time. L_1 corresponds to a flow where the gravitational component predominates over the inertial component. In the measurements, he confirms that the difference in the derived flow between the lengths L_1 and L_2 can differ by up to 23%. The representative drawing for the wetted lengths L_1 and L_2 is given in Figure 15.

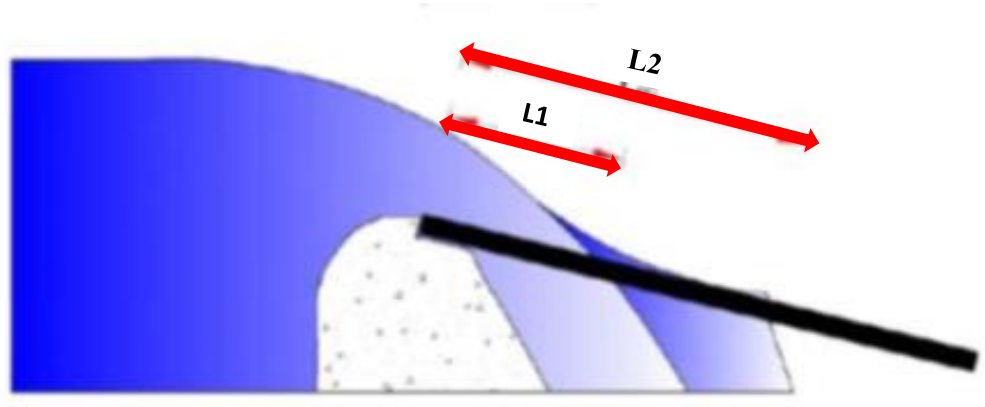

Figure 15. Representative Drawing for the L1 and L2 lengths (Source: Castillo and Bermejo 2016)

Equations that are proposed by (Drobir, Kienberger and Krouzecky 1999) for the L_1 and L_2 are given in Equation 2.11 and Equation 2.12 respectively.

$$L_1=0.9088\ q_1^{0.4993} \tag{2.11}$$

$$L_2=1.7205\ q_1^{0.4296} \tag{2.12}$$

(Gherardelli 1956) proposed an equation for the necessity rack length that is presented in Equation 2.13.

$$L=\frac{0.675\ H_0}{m\ K} \tag{2.13}$$

Where $K=0{,}66m^{-0.16}\left(\frac{b_c}{Ho}\right)^{-0.13}$

According to part of his hypothesis (Vargas 1998) stated that the velocity is uniformly distributed in the cross-section and based on the experimental measurements, he proposed Equation 2.14.

$$L(wet)=K_2\sqrt{\frac{2\cos\theta\, q_1^2}{m\, g\, h_0}} \tag{2.14}$$

Where K_2 is a constant that takes the value of 1,1; h_0 is the height of water at the beginning of the screen; q_1 is the approximate flow rate at the angle of inclination of the rack.

So far, previous and pioneer studies related to necessity and wetted rack lengths for the Tyrolean type water intake structures have been presented. As a summary, the researchers who performed these studies consider one of the two main approaches which are Constant Energy Level Approach and Constant Energy Head Approach. In addition to this, some of the other researchers developed and improved these equations. In Table 2 the summary of the previous studies related to rack length for Tyrolean intakes is presented.

Table 2. Summary of Previous Studies Related with Rack Length

Reference	**Wetted Rack Length (m)**
(Mostkow 1935)	$L=\frac{q_d}{C_{qh}\, m\sqrt{2g\frac{h_1+h_2}{2}}}$ $L=\frac{q_d}{C_{qh}\, m\sqrt{2g\, h_1}}$ if $h_1=hc$, $h_2=0$
(Garot 1939)	$L=\frac{H}{C_{qh}\, m}\left[\Phi\left[\frac{h_2}{H}\right]-\left[\frac{h_1}{H}\right]\right]$
(Noseda 1956a)	$L=\frac{H}{C_{qh}\, m}\left[\Phi\left[\frac{h_2}{H}\right]-\left[\frac{h_1}{H}\right]\right]$ $L=0{,}3994\frac{H_0}{C_{qh}.m}$ subcritical flow $L=1{,}1848\frac{H_0}{C_{qh}.m}$ supercritical flow
(Gherardelli 1956)	$L=\frac{0.675\, H_0}{m\, K}$ $K=0.66m^{-0,16}\left(\frac{b_c}{H_0}\right)^{-0,13}$

(Cont. on the next page)

Reference	Wetted Rack Length (m)
(Bouvard 1953)	$L=\left\{\frac{1}{2m'}\left[\left(j+\frac{1}{2j^2}\right)arcsin\sqrt{\frac{j}{j+(1/2j^2)}}+3\sqrt{\frac{1}{2j}}\right]+\left(\frac{0{,}303}{m'^2}+\frac{2j^3-3j^2+1}{4j^2}\right)tg\theta\right\}h1cos\theta$
(Frank, Von and Erlangen 1956)	$L=2.561\frac{q_0}{\lambda\sqrt{h_0}}$ $\lambda=m\,C_{qh}\sqrt{2gcos\theta}$
(Mostkow 1957)	$L=\frac{Q_1}{C_{qH}\,b\,m\sqrt{2gH_0}}$
(Dagan 1963)	$L=\Psi\frac{H_0}{C_{qo}\,m\,cos\theta}$
(Krochin and Sviatoslav 1978)	$L=\left[\frac{0.313\,q_1}{(C_{qH}\,k)^{1,5}}\right]^{\frac{2}{3}}$ $k=(1-f)\,m$
(Drobir 1981)	$L=\frac{0{,}846h}{C_q\times m}$
(Vargas 1998)	$L(wet)=K_2\sqrt{\frac{2cos\theta\,q_1^2}{m\,g\,h_0}}$
(Drobir, Kienberger and Krouzecky 1999)	$L_1=0.9088\,q_1^{0.4993}$ $L_2=1.7205\,q_1^{0.4296}$
(Brunella, Hager and Minor 2003)	$L=\frac{0.83\,H_0}{C_{q0}\,m}$

2.1.4. Studies Related with Discharge Coefficient for Tyrolean Intakes

Another important topic that many researchers have studied is the discharge coefficient C_q. In this part of the thesis, previous studies related to the discharge coefficient for Tyrolean Type intake is presented. Researchers performed experimental studies for developing equations for the discharge coefficient. The value of the discharge coefficient depends on some parameters. Especially, the shape, geometry, and porosity of the bars are very effective on the discharge coefficient as it can be seen on the following equations and formulations. (Garot 1939) proposed the determination of the discharge coefficient by Equation 2.15 by developing (Kirschmer 1926) formula which is used for

calculation of losses of load due to the flow as it passes through bars in water treatment channels.

$$C_{qh}=\sqrt{\frac{1}{\left(\frac{b_1}{b_1+b_w}\right)^2 \beta \left(\frac{b_w}{b_1}\right)^{\left(\frac{4}{3}\right)}}} \tag{2.15}$$

Where β is the constant and takes 2.42 for the T shape bars and it takes 1.79 for circular bars.

(Orth, Chardonnet and Meynardi 1954) studied by testing various types of bars to avoid clogging which is generally observed on the circular shape bars. (Noseda 1956b) performed experiments using T – shape bars for determining the discharge coefficient C_{q0} which is determined under static conditions. (Noseda 1956b) calculated the discharge coefficient $C_{qh}(h)$ and figure out that the coefficient is variable so, for its determination, he measured the flow which is derived per unit of length experimentally in the laboratory and expressed Equation 2.16.

$$C_{qh}(h)=\frac{\Delta q_d}{m\ \Delta L\sqrt{2g\ h}} \tag{2.16}$$

Where Δq_d is the flow that is derived from the length of the segment; h is the average flow depth and ΔL is the section length. (Noseda 1956b) thought that the differences as a result of the variation of the slope are not important and for an approximation flow over the grid in a slow regime, the discharge coefficient is expressed by Equation 2.17.

$$C_{qh}(h)=0.66\ m^{-0.16}\ \left(\frac{h}{l}\right)^{-0.13} \tag{2.17}$$

For an approximation flow on the screen with a fast regime, the discharge coefficient is only defined for the void ratio of m = 0.28 and expressed in Equation 2.18. Both relations for slow or fast regimes must be accepted as valid for range of values which are $0.20 < h/l < 3.50$ and $0.15 < m < 0.30$.

$$C_{qh}(h)=0.78\left(\frac{h}{l}\right)^{-0.13} \tag{2.18}$$

(Frank 1959), under the hypothesis that the profile of the water sheet fits an ellipse, and integrated this hypothesis along with the entire screen and equals the value of the average discharge coefficient C_{qh}. He proposed Equation 2.19.

$$C_{qh}=1.22\ C_{qh}(h_0) \tag{2.19}$$

Where h_0 is the water height at the beginning of the screen and the $C_{qh}(h_0)$ is the Noseda discharge coefficient.

In addition, (Simmler 1978) and (Sotelo 2004) collected a series of static discharge coefficients C_{q0} for various types of screen bar profiles without specifying the gap between the screen bars (racks). As a result, it can be concluded that Cq_0 varies depending on the distance between bars. (Dagan 1963) proposed a constant C_{qh} instead of varying values, since he interprets that it represents the geometric characteristics of the hole in the screen. This parameter coincides with the value of the static discharge coefficient proposed by (Noseda 1956b) and it is equal to $C_{q0} = 0.72$. (Krochin and Sviatoslav 1978) proposed Equation 2.20 for C_{qH} discharge coefficient.

$$C_{qH}=C_0 - 0.325\tan\theta \tag{2.20}$$

Where $\tan\theta$ is the longitudinal slope; $C_0 = 0.60$ for $e/b_1 \geq 4$; $C_0 = 0.50$ for $e/b_1 < 4$; e is the bar edge and b_1 is the space between bars. One of the important things is that this

coefficient valid for only rectangular bars. Circular bars were not used during his studies because they are more likely to clogged due to the sediment effect. (Nakagawa 1969) put forth that there is a relationship between the discharge coefficient and the static discharge coefficient. (Nakagawa 1969) proposed Equation 2.21 which represents this relation.

$$C_{qH}=C_{q0}\ (1{,}103)^{-x} \tag{2.21}$$

(White, Charlton and Ramsay 1972) defined some graphs after performing a series of experimental studies using different screen length and incoming flow rates. The experiments performed for void ratio (m) of 0.333. According to results, they come up with a value of C_{qh} which is 0.815. (Brunella, Hager and Minor 2003) performed a series of experiments using circular shape bars that were placed parallel to the flow direction. They used two different experimental setups whose void ratios were m = 0.35 and m = 0.664. After these experimental studies, they obtained static discharge coefficient values. The value of C_{q0} = 1,1 is obtained for the case of m = 0.35 and C_{q0} = 0.87 is obtained for the case of m = 0.664. (Righetti and Lanzoni 2008) had started to a study with gathering the data from the previous study of (Righetti, Rigon and Lanzoni 2000). In addition to this they performed new experimental studies and combining the whole results they came up with Equation 2.22.

$$C_{qH}=C_{q0}\left(a\frac{x}{H_0}F\,H_0+1\right)\left\{\tanh\left[b_0\sqrt{2}\text{-}F\,H_0\right]\right\}^{b1} \tag{2.22}$$

Where a, b_0 and b_1 are empirical coefficients and their values computed as a = -0.1056; b_0 = 1.5; b_1 = 0.478 and F_{H0} is the Froude number at the beginning of the screen. In the experimental studies that are performed by (Righetti and Lanzoni 2008), the Froude number varies between 1.02 and 2.05.

So far now, the previous studies related to the screen length for the Tyrolean type water intake structures are explained. All studies that are given under this heading are summarized in Table 3.

Table 3. Summary of Previous Studies Related With Discharge Coefficient

Reference	Discharge Coefficient
(Garot 1939)	$C_{qh}=\sqrt{\frac{1}{\left(\frac{b_1}{b_1+b_w}\right)^2 \beta \left(\frac{b_w}{b_1}\right)^{\left(\frac{4}{3}\right)}}}$
(Orth, Chardonnet and Meynardi 1954)	Proposed graphs related to the performance of the flow capture performances of five different types of screen profiles.
(Noseda 1956b)	Slow Flow Regime $C_{qh}(h)=0.66\ m^{-0.16}\left(\frac{h}{l}\right)^{-0.13}$ Fast Flow Regime $C_{qh}(h)=0.78\left(\frac{h}{l}\right)^{-0.13}$
(Frank 1959)	$C_{qh} = 1.22\ C_{qh}(ho)$
(Nakagawa 1969)	$C_{qH} = C_{q0}\ (1.103)^{-x}$
(Krochin and Sviatoslav 1978)	$C_{qH}=C_0-0.325\tan\theta$ $C_0 = 0.60$ for $e/b_1 \geq 4$; $C_0 = 0.50$ for $e/b_1 < 4$
(White, Charlton and Ramsay 1972)	Experiments performed for m = 0.333 $C_{qh} = 0.815$
(Brunella, Hager and Minor 2003)	The value of $C_{q0} = 1.1$ is obtained for the case of m = 0.35 and $C_{q0} = 0.87$ is obtained for the case of m = 0.664
(Righetti and Lanzoni 2008)	$C_{qH}=C_{q0}\left(a\frac{x}{H_0}F\ H_0+1\right)\{\tanh\left[b_0\sqrt{2}\text{-}F\ H_0\right]\}^{b1}$ $a = -0.1056$; $b_0 = 1.5$; $b_1 = 0.478$ Fr varies varies in between 1.02 and 2.05.

2.1.5. Sediment Related and Other Studies for Tyrolean Intakes

According to (Bouvard 1992) necessary slope for avoiding the clogging of the screen should be between 10% and 60%. (Orth, Chardonnet and Meynardi 1954) presented the following observations after gaining experiences from his experimental studies. A bar profile with the rounded top increases the retention of the sediments between the bars. Also, it is possible to reduce the risk of clogging by making an approach channel with a sufficient length and having an identical slope of the screen. (Krochin and Sviatoslav 1978) recommended that the screen bars should be made of iron and their shapes should be rectangular or trapezoidal. In addition to this, the bars of the screen should be placed parallel to the flow direction. Rounded shape bars were not preferred due to their high potential for clogging. (Madoux, et al. 1955) proposed a necessary space between bars. According to this study, the space between the bars should be close to 0,1 m and the slope of the screen should be close to 20%. (Krochin and Sviatoslav 1978) proposed a recommendation for spacing between bars so that the spacing between bars that are used in hydroelectric power plant projects should be ranged in between 0.02 m and 0.06 m and the inclination of the screen should be 20% from the horizontal position. (Bouvard 1992) recommended that space between bars should be closed to 0.1 – 0.12 m for the normal design. On the other hand, for the case of a power plant, the space between bars should be kept as 0.02 – 0.03 m and the slope of the screen should be between 30% - 60%. (Raudkivi 1993) recommended that a spacing of the bars should be at least 0.005 m and slope can be close to 20%. (Yılmaz 2010) performed a series of experiments about the water and sediment capture efficiencies of the Tyrolean weir in the Laboratory of Middle East Technical University. These experiments were performed with both clear and sediment mixed water conditions. According to the results, sediment capture efficiency increases with decreasing the rack of inclination for a given rack length. Sediment capture efficiency decreases with increasing the rack length for a given rack of inclination. In the case of fixed L and θ values, sediment capture efficiency increases as the bar opening increases. According to (Yılmaz 2010), screens that have small bar opening is more susceptible to clogging and 20% performance loss can be observed for water capture efficiency. Yılmaz also suggested that keeping the screen length %20 - %30 greater than the calculated length is more advisable for obtaining the design flow rate.

(Castillo, Carillo and Garcia 2013) performed a series of experiments with both clear and sediment mixed water conditions. According to the results that were obtained from clear water experiments, an increment of the slope of the rack tends to reduce the diverted water. Opposite of this is valid for the experiments that performed under sediment-water mixed conditions. In that situation, maximum efficiency was obtained when the screen slope is 30% and the worst efficiency was obtained with a horizontal rack. The main reason for this is the clogging of the screen racks due to sedimentations. Therefore, there should be a minimum slope for preventing clogging. In addition to these, (Castillo, Carillo and Garcia 2013) stated that the ordinary wetted length formulations which were derived from the clear water experiments differ from the results which were gained from the sediment mixed experiments. They also suggested that in order to improve the design criteria of intake systems, more experimental studies should be performed. (Yılmaz 2010) applied dimensional analysis to the related terms of the system and defined dimensionless terms for water capture efficiency and discharge coefficient. Using these dimensionless parameters (Yılmaz 2010) plotted series of graphs and diagrams. (Yılmaz 2010) stated that using these diagrams anyone can determine the diverted water by a Tyrolean intake whose geometry is known. Another study was performed by (Yıldız 2016). In that study effect of the rack length and the rack slope was investigated by both experimental and numerical modeling studies. In Table 4 a summary of experimental setups for some previous studies is given.

Table 4. Summary of the previous studies' experimental and modeling setups

Researcher	**Experimental Setup**
(Garot 1939)	Q = 30lt/s and B = 50 cm Shape of the screen bars are spherical and conical b_w = 1 cm; b_l = 0.43; 0.402 and 1 cm void ratio (m) = 0.3; 0.402 and 0.5 Fr_0: 1 – 2.2
(Orth, Chardonnet and Meynardi 1954)	Q = 80 lt/s and B = 50 cm '' T '' shape bars were used b_w = 2.5 cm and b_l = 1.3 cm void ratio (m) = 0.311 screen slope (inclination) = 0; 5; 10; 20 % Fr_0 = 2.1 – 2.8
(Mostkow 1957)	There cannot be found any detailed information about the experimental setup

(Cont. on the next page)

Researcher	Experiment Setup
(Noseda 1956b)	Q = 100 lt/s and B = 50 cm ‘’ T ‘’ shape bars are used void ratio (m) = 0.16 – 0.28 Inclination = 0; 10; 20 %
(Frank 1959)	There cannot be found any detailed information about the experimental setup
(Chow 1959)	There cannot be found any detailed information about the experimental setup
(Dagan 1963)	There cannot be found any detailed information about the experimental setup
(Krochin and Sviatoslav 1978)	There cannot be found any detailed information about the experimental setup
(Righetti, Rigon and Lanzoni 2000)	Q = 35 lt/s and B = 25 cm Devices that used in the experiments; Laser Doppler Anemometer (LDA) Particle Image Velocimetry (PIV)
(Brunella, Hager and Minor 2003)	Q = 100 lt/s and B = 50 cm Circular bars were used Three different combination of b_w and b_l ✓ b_l = 1.2 cm; b_w = 0.6 cm and m = 0.352 ✓ b_l = 0.6 cm; b_w = 0.3 cm and m = 0.664 inclination = 0, 7, 19, 28, 35, 39, 44 and 51 degrees
(Righetti and Lanzoni 2008)	Q = 0.35 lt/s and B = 25 cm B_l = 0.5 cm and b_w = 2 cm Laser Doppler Anemometer (LDA) Particle Image Velocimetry (PIV)
(Yılmaz 2010)	The main channel width (B) = 1.98 meter Length of the main channel = 7 meter Slope of the main channel (S) = 0.001 Circular bars were used Diameter of the bars = 1 cm Clear distances between bars (b_w) = 3, 6, 10 mm Screen inclination = 14.477; 9.594; 4.780 degrees
(Yıldız 2016)	The main channel width (B) = 30 cm The main channel length = 210 cm Circular bars were used Diameter of the bars = 1 cm Length of the screen = 30 cm Clear distance between bars (b_w) = 3, 6, 10 mm Screen inclination = 18 and 25 degrees

As can be seen from the previous studies the researchers tried to figure out that the effect and values of some parameters such as necessary screen length, the effect of screen slope, the spacing between the bars, discharge coefficient, and other parameters. Some of the researchers proposed graphs and diagrams for determining the value of diverted discharge from the mainstream. On the other hand, an empirical equation that gives the diverted discharge value is not found in the previous examples. Addition to this, most of the previous studies were performed under clear water condition that does not consider sedimentation and clogging effect. Despite this situation, there can be found some studies which consider the sediment effect. However, there is not any empirical formulation that determines the sediment capturing or sediment exclusion performances.

Although this presented study is related to the determination of the best design of the Coanda type water intake structures, some experimental studies were also performed for Tyrolean intake structures. Using the results that were gained from this study and some other data that were collected from the other studies, an empirical formulation was determined for water capturing performances. More details will be discussed in the next chapters of this study. The next part will continue with the literature review and previous studies of Coanda type water intake structures.

2.2. Previous Studies Related with Coanda Intakes

The purpose of the usage of intake structures is to withdraw the design amount of water from a river or reservoir to use for various purposes. One of the purposes of withdrawing water is to produce energy in hydroelectric power plants. There are different types of water intake structures in the application. Frontal, lateral and bottom type water intake structures are used for these purposes. In the mountainous regions where the water flow discharge and the transported sediment rate is high, bottom intake structures are preferred. Coanda and Tyrolean type water intake structures are the most widely used bottom type intake structures. In the previous part, the literature review about the Tyrolean intakes is given and discussed. In this part, previous studies that were performed for Coanda type water intake structures is discussed.

One of the important issues for the Coanda intakes is accurately predict the diverted discharge through the racks. Because the design of the Coanda intake structures

is more complicated than the traditional water intake structures, the accurate application and derivation of the empirical formulations to the Coanda intake structures are not easy. On the other hand, some theoretical and experimental studies were performed on Coanda intake structures to analyze its performance. These studies can be classified according to some categories such as experimental studies with clear water and experimental studies with sediment mixed water.

2.2.1. Clear Water Studies Related with Coanda Intakes

Before starting with the previous theoretical studies, it is better to remember the general design of the Coanda type intake structures. The Coanda intakes are generally designed with having a concave arc screen shape. Although there is no any restriction about the determination of the screen arc radius, most of the manufacturer companies design their products with having an arc radius of 3 m. Besides, the Coanda effect screens have unique tilted – wire screen panels. This tilt angle can be ranged in between 3^o – 6^o but generally 5^o is preferred. The main purpose of the usage of the tilted – wire screens is to increase the shear effect on the screen. In Figure 16 the typical design of a Coanda screen can be seen.

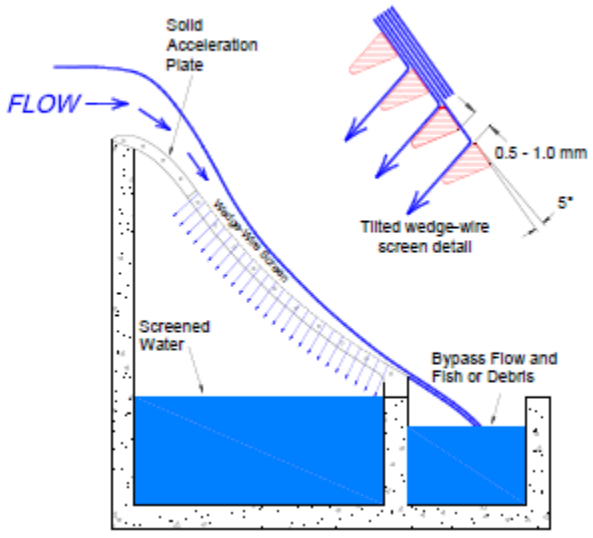

Figure 16. General design of a Coanda Intake (Source: T. L. Wahl 2017)

(T. L. Wahl 2001) indicated Equation 2.23 for the wire tilt angle and the offset distance of the screen bars. The illustration of the tilted – wire screen can be seen in Figure 17.

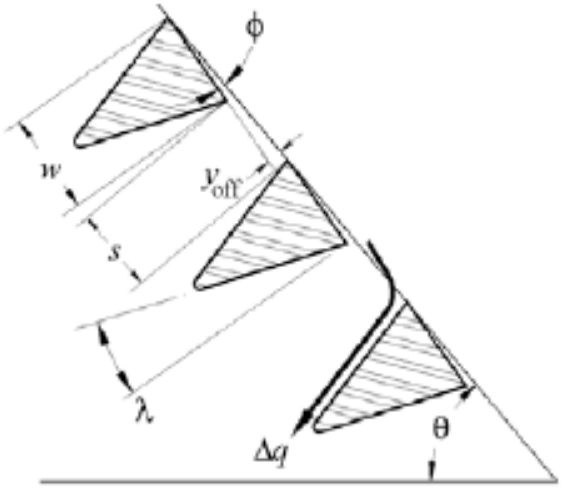

Figure 17. Illustration of tilted - wire screen (Source: T. L. Wahl 2017)

$$y(off)=(s+w\cos Ø)\sin Ø \tag{2.23}$$

Where y(off) = offset height, Ø = wire tilt angle; w = wire width and s = sloth width.

The quantity of water that is diverted from the screen is controlled by two mechanisms. The first one is the flow that withdrawn by the hydrostatic pressure or basically the orifice effect flow and the second one is the flow that occurs due to sharing action at the bottom level of the flow. For the first mechanism (T. L. Wahl 2001) proposed Equation 2.24 which is similar to the ordinary orifice equation.

$$\Delta q=C_{cv}\, C_F\, s'\sqrt{2gE} \tag{2.24}$$

Where C_{cv} is the coefficient for the velocity reduction and contraction; C_F is the coefficient which is depended to Froude number and geometry of the screen; $s' = \sqrt{s^2 + y^2 off}$. The main difference between this equation and the ordinary orifice

equation is the discharge coefficients. (T. L. Wahl 2001) expressed two different discharge coefficients which are C_{cv} and C_F for his equation.

The value of C_F is a function of Froude number and it indicates the screening capacity of slot width. In addition to this, C_F x p indicates the performance of the whole screen surface where p = s / (s+w). In this expression p defines the screen porosity, s indicates the slot width between bars and w indicates the screen wire width. (T. L. Wahl 2001) proposed a diagram that explains the relation between C_F and C_F x p versus Froude number for different screens. This diagram can be seen in Figure 18.

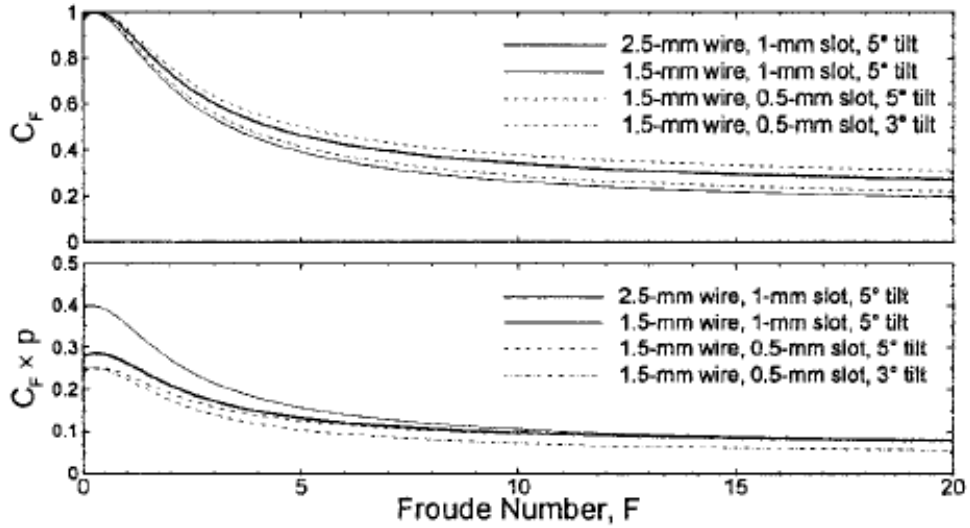

Figure 18. C_F and C_F x p versus Froude Number (F) (Source: T. L. Wahl 2001)

According to (T. L. Wahl 2001), C_F values are almost independent of changes in screen geometry at low Froude number values where the orifice flow is dominant. On the other hand, the value of C_F x p is directly proportional to the wire tilt angle and also independent from the wire width and slot width.

One of the other discharge coefficients proposed by the (T. L. Wahl 2001) is the C_{cv}. A series of experimental studies were performed for determining C_{cv} values in the Bureau of Reclamation's Water Resources Research Laboratory in Denver. The plan drawing and image of the experimental setup are given in Figure 19. The experimental setup consisted of a flume which is 0.30 m wide. Screens were located to the sloped flume at three different locations. The slope of the flume was 37° from the horizontal. In these studies, the flow rate was changing between 0.023 to 0.46 $m^3/s/m$.

In addition to these, according to the measurements, the Froude Number was ranged in between 2.5 and 16 and velocities across the screens ranged in between 2.1 to 4.4 m/s during these studies.

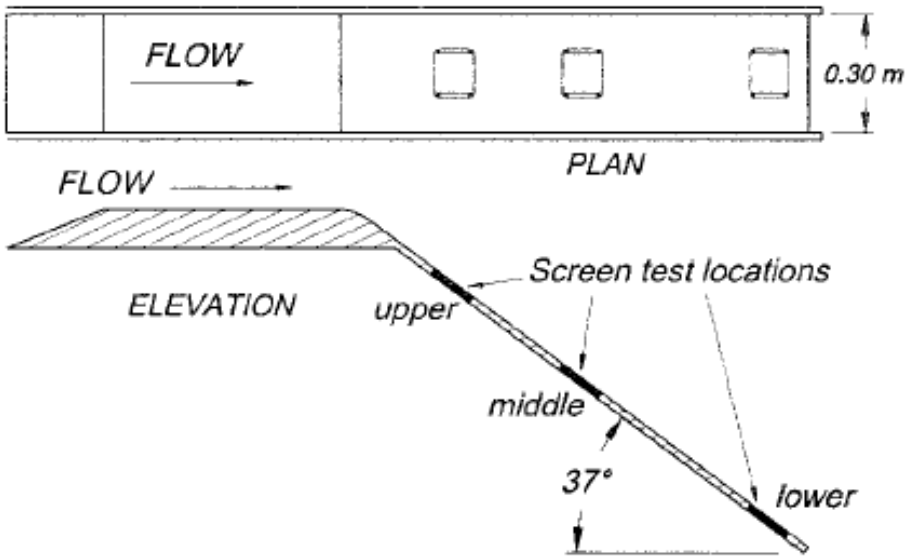

Figure 19. Plan of the experimental setup of Wahl's study (Source: T. L. Wahl 2001)

(T. L. Wahl 2001) indicated that values of the C_{cv} depend on some dimensionless parameters such as; Reynolds Number (R), Weber Number (W), Froude Number (F) and R/W. After performing some regression analysis (T. L. Wahl 2001) proposed Equation 2.25 which determines the C_{cv} values.

$$C_{cv} = 0.210+0.0109\left(\frac{R}{W}\right) + 0.00803(F) \tag{2.25}$$

R=V.s/v and W=(ρV^2s) / σ and V= velocity tangent to screen surface, s= sloth width, v = kinematic viscosity.

Some of the other researchers (Venkataraman 1977, Nasser, Venkataraman and Ramamurthy 1980, Ramamurthy, Zhu and Carballada 1994) also studied for the discharge coefficient of an orifice flow. On the other hand, they used to flow through

parallel bars and they did not consider tilted wires and the wire offset. Therefore, their formulations did not consider the sheared flow which occurs due to the effect of the tilted wire.

(T. L. Wahl 2001) made comments about some of the Coanda intake properties. These parameters are wire tilt angle, screen sloth width and wire size, screen inclination, drop height and arc radius. According to (T. L. Wahl 2001), the wire tilt angle directly affects screen capacity because it is proportional to wire offset height. On the other hand, he explained that increasing the tilt angle can cause some disadvantages on the screen performances such as the sediment retention on the screen which can be increased due to the decrease in the ability of sediment excluding performances.

(T. L. Wahl 2001) commented that changing the sloth width or wire sizes is directly proportional to the screen porosity which affects the flow capacity of the screen. According to (T. L. Wahl 2001), the effects are more dominant at lower Froude numbers over the screen. (T. L. Wahl 2003) proposed a graph that explains the relation between wire tilt angle and unit discharge (Figure 20).

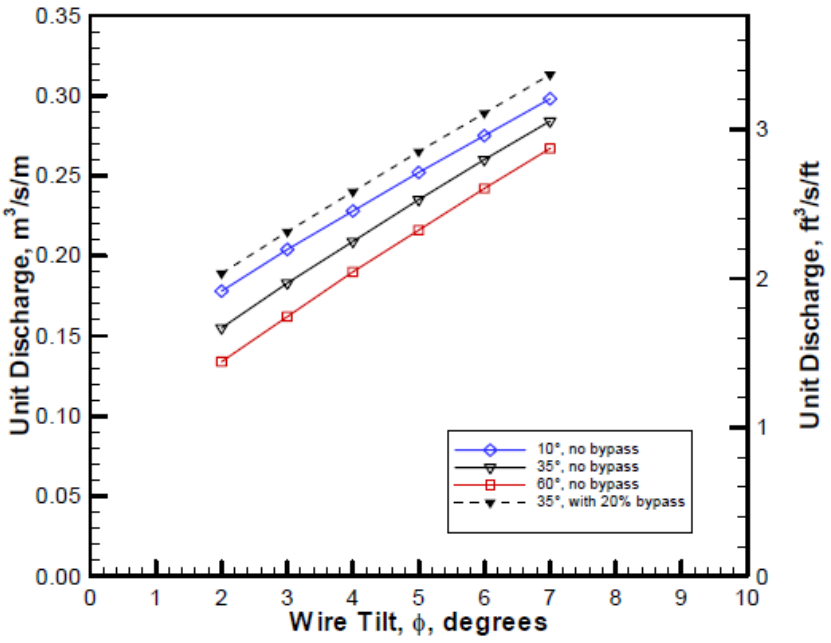

Figure 20. Relation of wire tilt angle and unit discharge (Source: T. L. Wahl 2003)

Another designed parameter that was observed by (T. L. Wahl 2001) is the effect of arc radius on the performance of the screen. According to Wahl's opinion, the concave

screen panels increased the unit flow which is diverted from the main channel due to the increased pressure on the screen. The concave screen panels also increase the screen length, thus this affects the screen capacity in a positive manner. In addition to these, the energy of the flow is dissipated at the downstream part of the screen so, the erosion and scouring problems can be reduced. (T. L. Wahl 2003) proposed a graph for the relationship between the screen arc radius and the unit discharge (Figure 21).

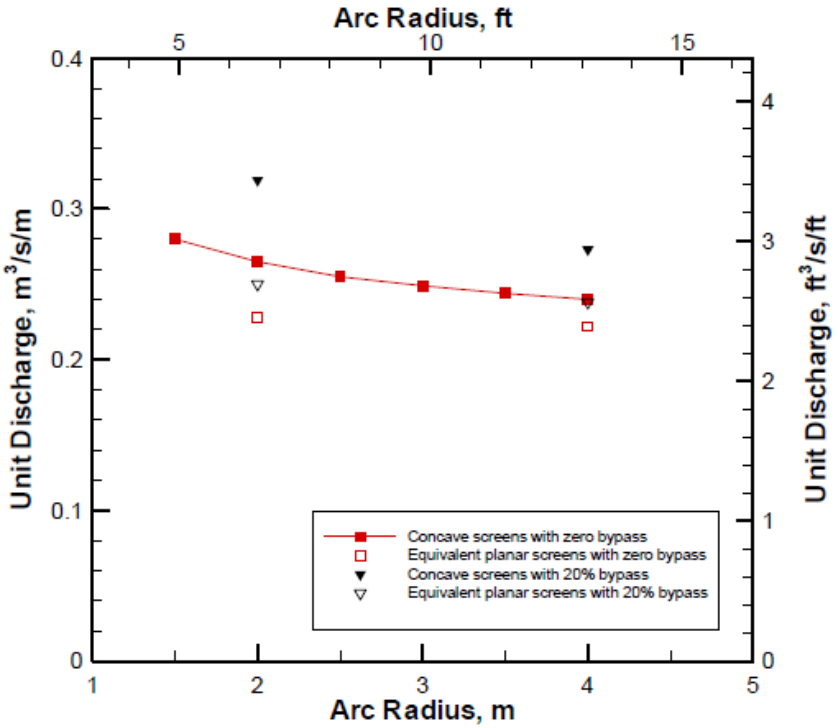

Figure 21. Relation between arc radius and unit discharge (Source: T. L. Wahl 2003)

Screen length is also an important parameter that affects the diverted unit discharge. (T. L. Wahl 2003) expressed a relation related to the screen length and the unit discharge after performing a series of experimental studies. According to these studies, unit discharge increases as a non-linear manner with increasing the screen length. Based on these studies the screening capacity is proportional to $L^{1.24}$. Here L is referring to screen length. On the other hand, (T. L.Wahl 2003) draws attention that changing wire tilt angle, sloth width and wire width could affect this relationship for some degree. (T. L. Wahl 2003) proposed a graph that shows the effect of screen length on the unit discharge (Figure 22).

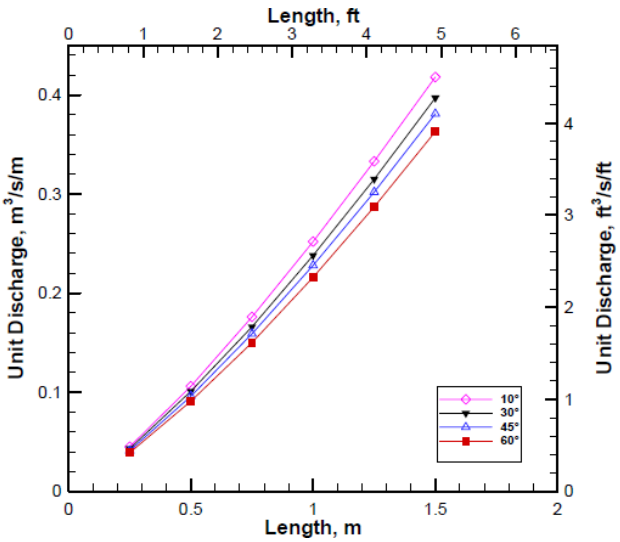

Figure 22. Relation between the screen length and the unit discharge proposed by Wahl (Source: T. L. Wahl 2003)

Another study that is related to the effects of screen slope on the unit discharge was performed by (May 2015). In this experimental study, three coanda screens that have different screen geometry were used. Details of these screens are given in Table 5. During the experiments, the inflow rate was varied between 0 to 1.26 lt/s. the experimental flume was adjusted to the nearly horizontal position and the screen was installed to the experimental model with 45-degree inclination from the horizontal plane. Results showed that the unit discharge increased with a non-linear manner with increasing the screen length which is similar to results of (T. L. Wahl 2003). According to the results of the study of (May 2015), relations were expressed as the unit discharge is proportional with $L^{1.09}$, $L^{1.14}$, $L^{0.99}$ for these three Coanda intakes. May also proposed a graph that explains the relation between screen length and unit discharge (Figure 23).

Table 5. Screen details that were used in the May's experiments (Source: May 2015)

Screen Numbers	Screen 1	Screen 2	Screen 3
Screen specifications	3/16-10-1	3/16-10-0.5	3/16-10-0.3
Tilt angle, φ^o	10	10	10
Sloth width, s (mm)	1	0.5	0.3
Wire thickness w, (inches)	3/16	3/16	3/16

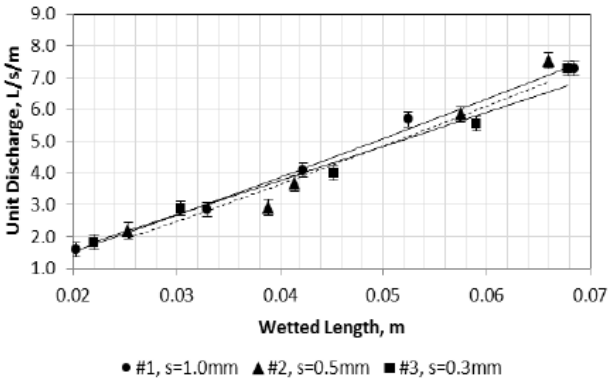

Figure 23. Relation between the screen length and unit discharge proposed by May (Source: May 2015)

In addition to these studies, a computer program was developed under the organization of the United States Bureau of Reclamation. This model was developed based on the data which were gathered from the studies of Wahl. Any user can determine diverted flow from a Coanda screen using this computer program. This program consists of four different sections. These are the section for structural properties, the section for accelerator plate properties, the section for screen properties and the flow condition. Users must enter the necessary information in these sections and then after running the program the results will be shown on the result page. It should be noted that this program was developed for considering the clear water condition cases. Therefore, sediment effects such as clogging of the screen due to the sedimentation may lead to some differences in the results gathered from the program and real-life application.

2.2.2. Sediment – Water Studies Related with Coanda Intakes

So far, studies that were performed under clear water conditions are discussed for Coanda type intakes. However, in real-life applications, the screens are exposed to the sediment-water mix type concentrated flows. Therefore, some researchers performed studies considering this fact. (May 2015) took a sample from northern Nicaragua to obtain a reference model for particle size distribution for using it in the experimental studies. (May 2015) also made some adjustments on this reference particle size distribution to make it appropriate for experiments. The particle size distribution of Nicaragua sample

and the adjusted particle distribution are given in Figure 24. In this experimental study, the concentration was prepared to be 25.000 mg/l. May noted that this concentration value is greater than the actual concentration value that a Coanda screen can be exposed to.

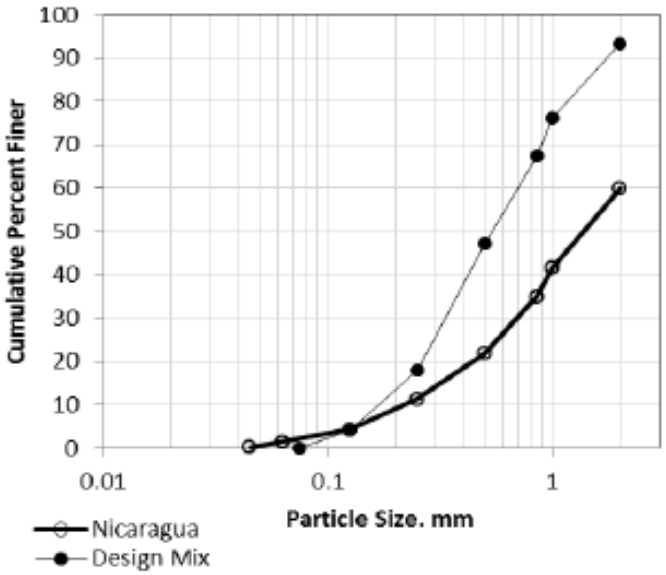

Figure 24. Particle size distributions of Nicaragua sample and design mixture (Source: May 2015)

(May 2015) collected the samples at the 2, 5, and 8 minutes. Samples were dried first and then sediment size distributions were determined with a standard sieve method. The purpose of the study was to seek the effect of clogging of the screens and its reduction effect on the screen performances. The result of the study was given in Figure 25 and the amount of the excluded sediment values are given in Table 6. Results show that the general exclusion rate is between 43% to 81%. According to data, the exclusion rate is increasing as the sediment distribution becomes coarser.

Table 6**.** Excluded sediment ratios (Source: Data were taken from May 2015)

Screen type	Total Exclusion (%)	Flow reduction (%)
1) 3/16-10-1,0	52 %	11 %
2) 3/16-10-0.5	69 %	47 %

(Cont. on the next page)

1) 3/16-10-0.3	76 %	55 %
2) 1/8-13-1.0	43 %	-4 %
3) 1/8-13-0.5	52 %	7 %
4) 1/8-13-0.3	81 %	40 %

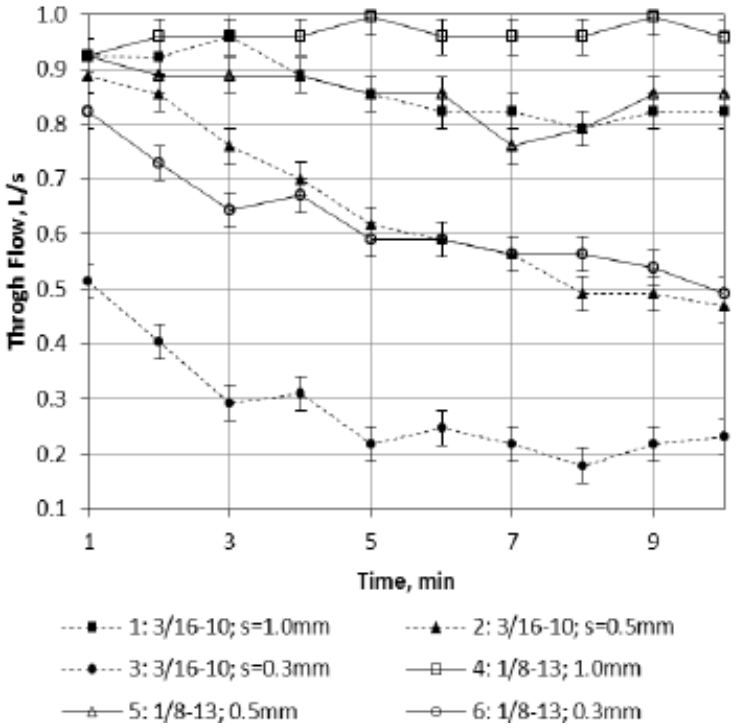

Figure 25. Through flow rate with a function of time (Source: May 2015)

(May 2015) summarized that the screens that have smaller wire spacing are good at excluding sediment. On the other hand, these screens are more susceptible to clogging therefore, the through-flow reduction can be seen more frequently.

As a part of the study of (May 2015), a field prototype was constructed to obtain realistic data from the real-life application. The screen was constructed on a small irrigation canal which has less amount of sediment concentration than the concentration used in the laboratory study. The field prototype was constructed with the same shape, size, and flow capacity with the laboratory model. The model's flow capacity was designed as being 1.26 lt/s. The screen slope was 45^0. The screen drop height and the horizontal length of the prototype were 66 cm and the screen length was 15cm x 30cm. The illustration of the field prototype is given in Figure 26.

It can be said that experiments were performed for different screen geometries and flow rates, on the other hand, these studies were performed only for 45-degree screen slope and same screen arc radius. Different slope case and screen curvature radius were not considered. In addition, there cannot be found any developed empirical equation in that work.

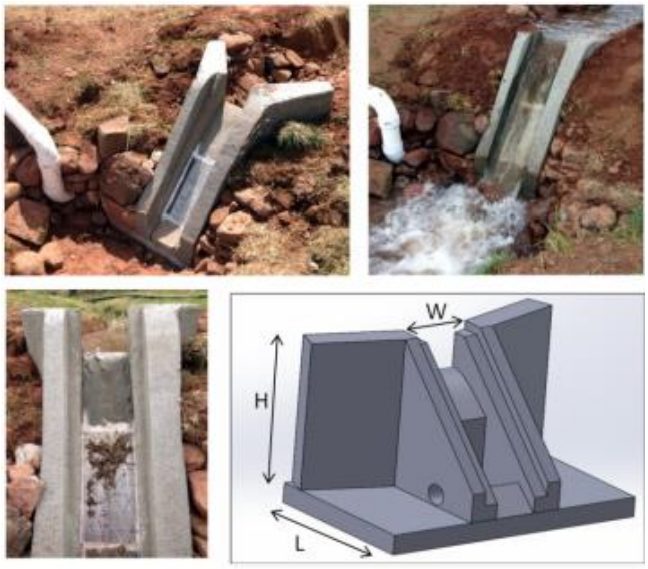

Figure 26. Field prototype of May's study (Source: May 2015)

Another study which is named as BEDUIN project was commissioned by Norwegian Water Resources and Energy Directorate to the Norwegian University of Science and Technology. (Huber 2005) worked in this project and wrote a report about works that were done in the project. The aim of the project was to investigate problems on small hydroelectric power plants. One of the main problems was the sedimentation. Because, sediment caused problems directly affect both the withdrawn water quality and mechanical devices of the power plant, it is necessary to find a solution for the better design of intake structures. Therefore, a series of experiments using Coanda intakes were performed. In these studies, three Coanda intakes that were supplied by Dulas Company were tested.

According to the report (Huber 2005), the sloth widths of the screens were 1 mm, 0,5 mm and 0,2 mm. Details of the screens are given in Figure 27. Plan view and side view of the experimental setup is given in Figure 28 and Figure 29 respectively.

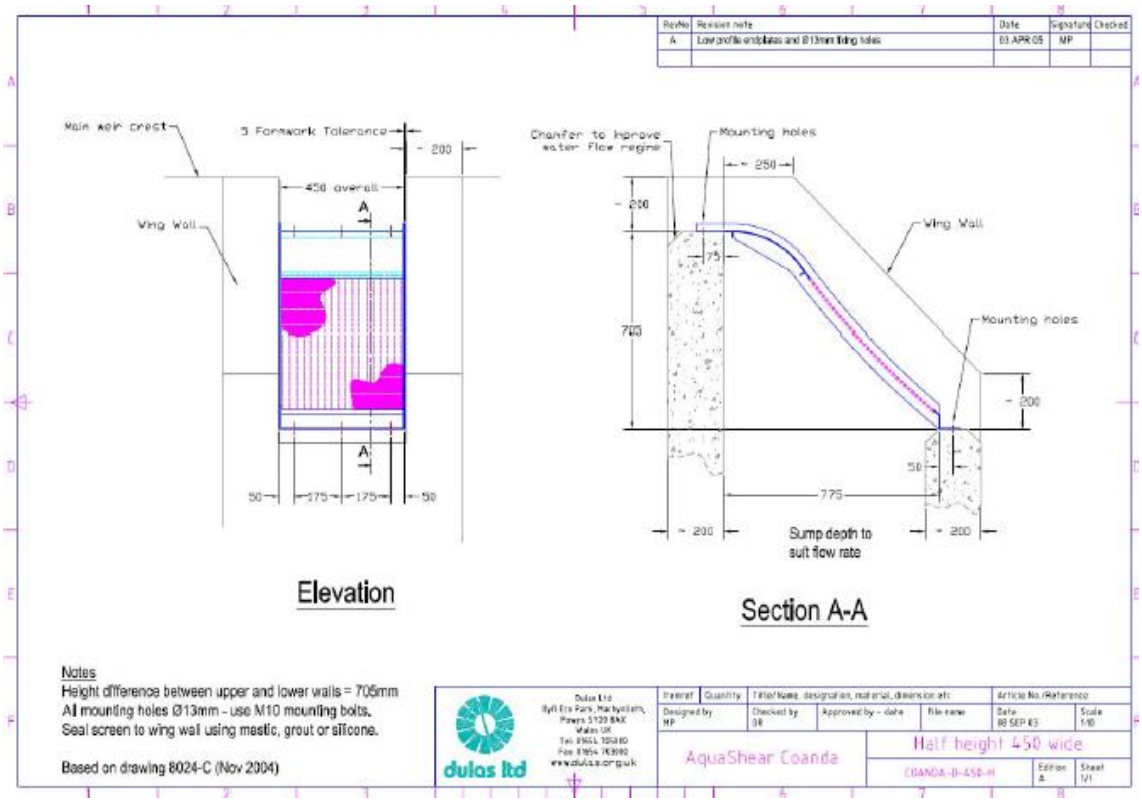

Figure 27. Coanda effect screen used in BEDUIN Project (Source: Huber 2005)

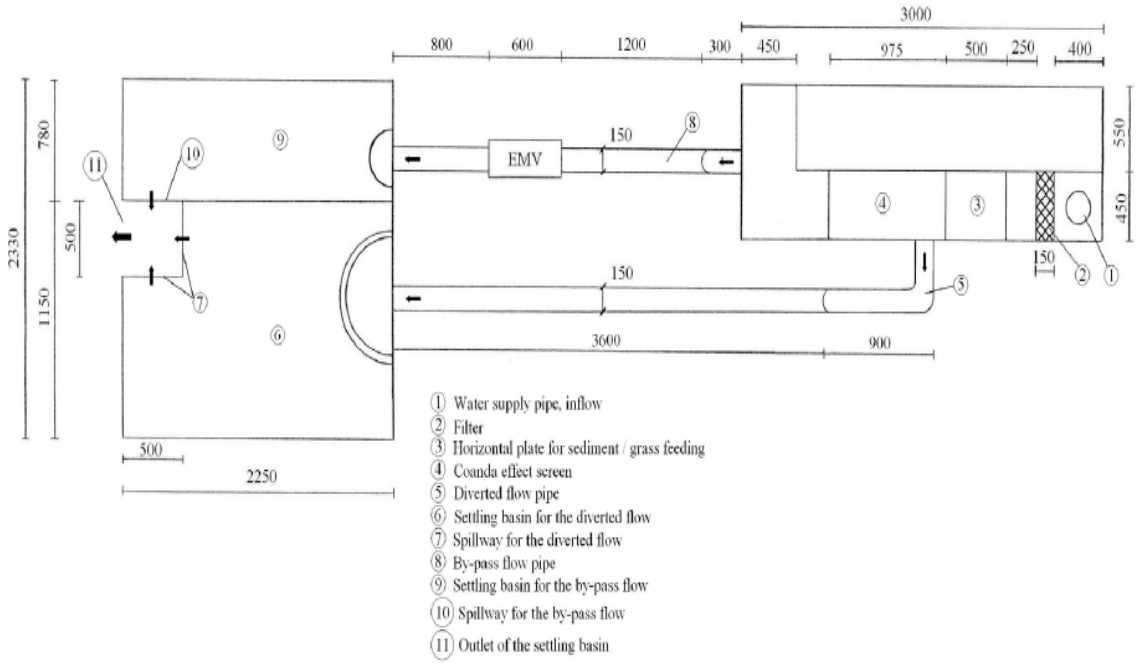

Figure 28. Plan view of the experimental setup used in BEDUIN Project (Source: Huber 2005)

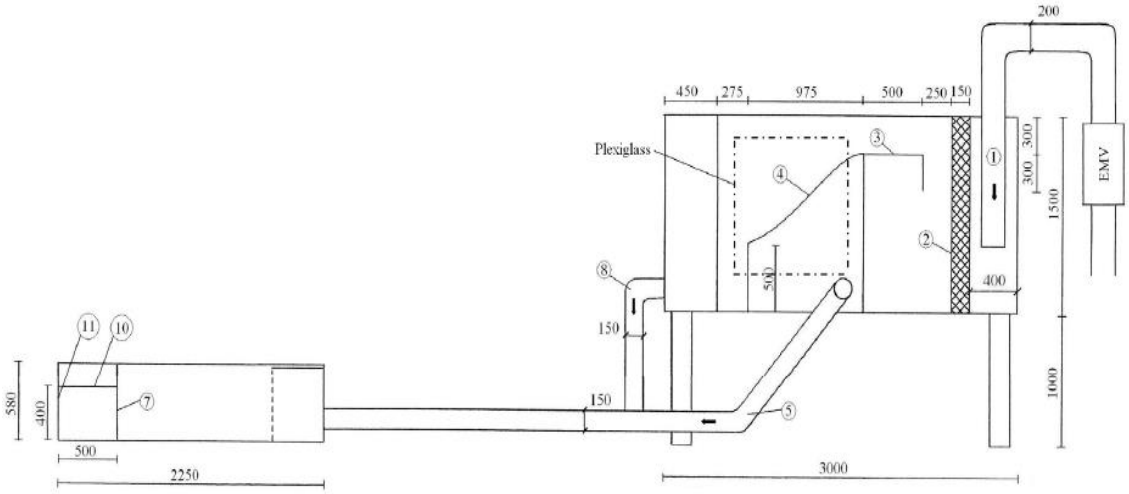

Figure 29. Side view of the experimental setup used in BEDUIN Project (Source: Huber 2005)

Sediment exclusion test was performed for two different discharge rates and three different sloth widths. In addition, three different sediment feeding method was used. (Huber 2005) proposed Table 7 that contains information about the experiments that were carried out. (Huber 2005) indicated in the report that three different sediment feeding methods were used in the experimental studies. These methods were symbolized as the Methods A, B, and C. In the case of Method A it consisted of feeding sediments with a vibrating sediment feeder. In this method, dry sediment was used. In the case of Method B, the sediments were mixed with water first then the mixture was released to the flume with a trowel. In this method, the sediment feeding process is performed while the water is running. In the case of Method C, wet sediments were laid to the upstream part of the flume before the beginning of the test and water running.

Table 7. Sediment exclusion test for BEDUIN project (Source: Huber 2005)

Test	Sloth width (mm)	Flow (lt/s)	Mass of sediment (kg)	Duration (min)	Feeding method
1mm-5 l/s-sediment	1 mm	5	20	70	A
1mm-30 l/s-sediment	1 mm	30	20	15	B
0.5 mm-5 l/s-sediment	0.5 mm	5	20	19	B
0.5 mm-30 l/s-sediment	0.5 mm	30	20	12	B
0.2 mm-5 l/s-sediment	0.2 mm	5	20	18	B
0.2 mm-30 l/s-sediment	0.2 mm	30	5	0.5	C

(Huber 2005) defined the term sediment exclusion efficiency is a percentage of the excluded sediment amount to the total sediment amount. (Huber 2005) indicated that the clogging of the screen due to sedimentation is the reason for the changes in the screen capacity. According to the results, screens that have 1 mm sloth width showed very little clogging whereas the other screens having 0.5 mm and 0.2 mm sloth widths were highly clogged. From this study, it can be shown that by decreasing the screen sloth width, the sediment exclusion efficiency is increasing. On the other hand, decreasing the sloth width increases the risk of clogging. Also, increment on the necessary screen length is increasing the withdraw water. (Huber 2005) proposed a table for the sediment exclusion efficiency. This table is given in the Table 8.

Table 8. Exclusion efficiency for the screens (Source: Huber 2005)

Exclusion efficiency definition	Test	Screen aperture (mm)	Flow (l/s)	d'<½ Size'' (%)	½ Size<d<Size (%)	Size<d (%)
1st	*1 mm – 5 l/s – sed*	1	5	1.4	16.9	89.1
1st	*1 mm – 30 l/s – sed*	1	30	1	39.7	91.4
1st	*0.5 mm – 5 l/s – sed*	0.5	5	4.1	44.2	97.6
1st	*0.5 mm – 30 l/s – sed*	0.5	30	2.8	46.9	98.5
1st	*0.2 mm – 5 l/s – sed*	0.2	5	67.4	79.2	100.8
2nd	*0.2 mm – 5 l/s – sed*	0.2	5	49.9	68	101.2
1st	*0.2 mm – 30 l/s – sed*	0.2	30	49.5	64.4	99.8

Where; d^* is the particle size in mm.

‘’For the 1 mm aperture screen, Size = 1 mm and ½ Size = 0.5 mm

For the 0.5 mm aperture screen, Size = 0.5 mm and ½ Size = 0.25 mm

For the 0.2 mm aperture screen, Size = 0.2 mm and ½ Size = 0.1 mm

It can be said that for the report of (Huber 2005), these studies were performed for different screens and discharge rates. The effect of screen types and discharge rates can be observed however, the screen slope was taken constantly during these studies. Because of this, there is a lack of information about the effect of screen slope. Addition these, there cannot be seen any numerical or empirical studies about the Coanda screens.

2.3. Aim and Motivation of the Project

So far, some information is given about the previous studies related to bottom intake structures. Although this thesis study is related to Coanda type water intake structures, many studies that were performed for Tyrolean type intakes are also given. The main reason for this is the Tyrolean type of intakes can be considered as a previous generation of the bottom type intakes and the equations that were developed for them enables to development of Coanda type intakes.

It is obvious that pioneer studies of Tyrolean type intakes were mostly performed for discovering the effects of the screen parameters and flow conditions on the withdrawn flow rates. Although majority of these studies were performed under clear water conditions, some of these studies also consider the sediment and clogging effects. On the other hand, there cannot be found any empirical or analytical formulations that give the diverted unit discharge or water capture efficiency. Because there is a lack in the literature for the formulation studies of Tyrolean type intake structures, we included a part for the formulation study of Tyrolean intakes. Therefore, a series of experimental studies were performed with Tyrolean type water intake structure and a formulation study was also performed for the Water Capture Performance. More details for this topic is given in next chapters of this study.

In the literature, it is possible to see some studies for Coanda intakes for both clear water and sediment-water mixed conditions. For example, when we consider studies of (T. L. Wahl 2001, 2003) which we mentioned in the previous part, it is clear that the studies were performed for only the clear water conditions. However, in real-life applications, these structures exposed to sediment mixed flow conditions and sediment related problems. Some of the other researchers concerned this situation and performed their studies under sediment-mixed conditions. However, these studies were performed under a constant screen inclination and a constant screen curvature radius. Therefore, we can say that there is a lack in the literature in case of determining the effect of screen inclination and the screen curvature radius on the performance of Coanda type water intake structures. In addition, there cannot be found any formulation study for the Water Capturing Performance and Sediment Release Efficiency. Although there is a computer program that was published by U.S.B.R for determining the diverted water discharge through the screen, this program is only operating under clear water condition and it does

not determine sediment concentration in the diverted water or any sediment related parameter. However, sediment concentration in withdrawn water is very important for some aspects that we mentioned before. These lacks in the literature motivated us to full fill these gaps via a series of experimental studies. The presented study focused on the Water Capturing Performance of both Tyrolean and Coanda type intakes and Sediment Release Efficiency for Coanda intakes through experimental works. Water Capture Performance and Sediment Release Efficiencies are related to parameters used in the experiments including Coanda type, rack angle, void ratio, sediment amount and flow rate based on the statistical analyses of these parameters.

In the first part of the study, experiments were performed under clear water condition and effects of the screen parameters on the Water Capturing Performance was observed. In the second part of the study, these experiments were repeated for the sediment laden flow case. In this part, we observed the effect of the screen parameters on the Sediment Release Efficiency. Using the data from the current experiments presented in this paper, the multiple linear regression analysis is utilized to predict Water Capture Performance and the Sediment Release Efficiency for Coanda and Tyrolean type intakes. After completing these analyses, three formulas were proposed. One of these formulas is proposed for the determination of the Water Capture Performance of a Tyrolean water intake structure and the others are proposed for the Water Capture Performance and Sediment Release Efficiency of a Coanda intake structure.

CHAPTER 3

HYDRAULIC MODEL EXPERIMENT

3.1. Experimental Setup

Experiments are conducted in the hydraulics laboratory of Izmir Institute of Technology in Turkey, utilizing a setup specifically designed for this study (Figure 30 and Figure 31). Two types of intake structures – Tyrolean and Coanda types are built so that the effects of intake type, incoming flow rate, sediment concentration and composition, rack angle, the void ratio on the Water Capture Performance and the Sediment Release Efficiency can be studied.

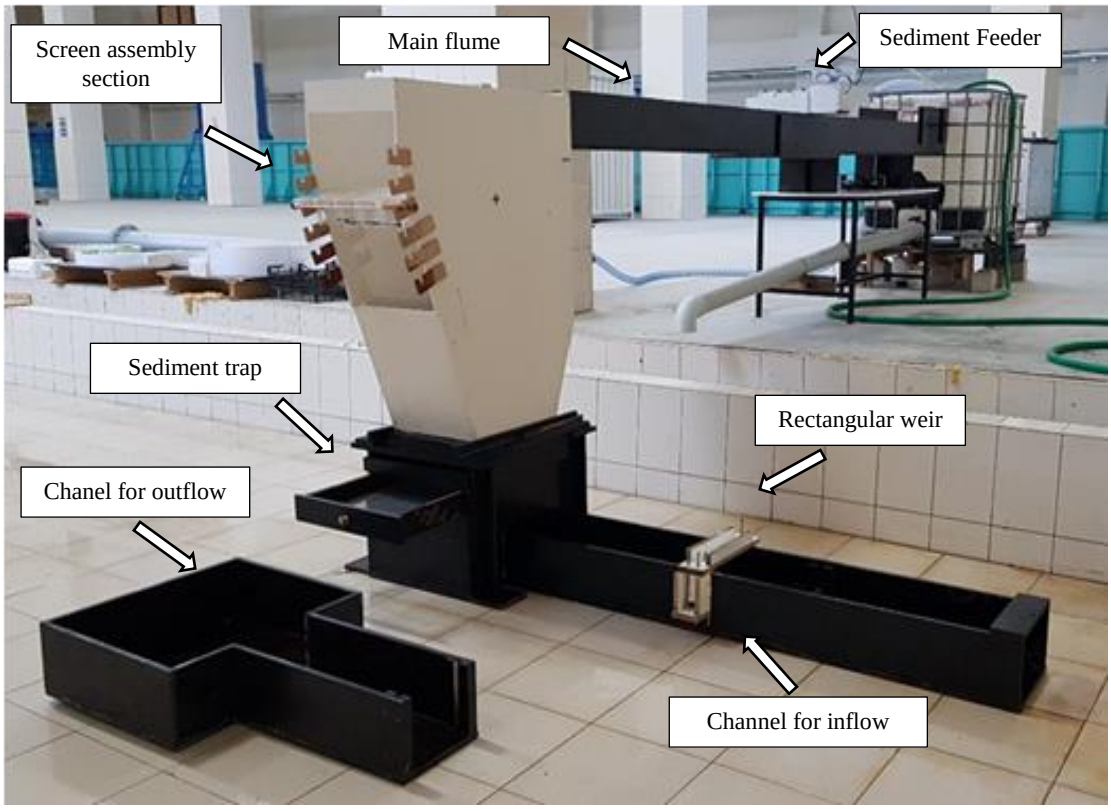

Figure 30. General view of the experimental setup

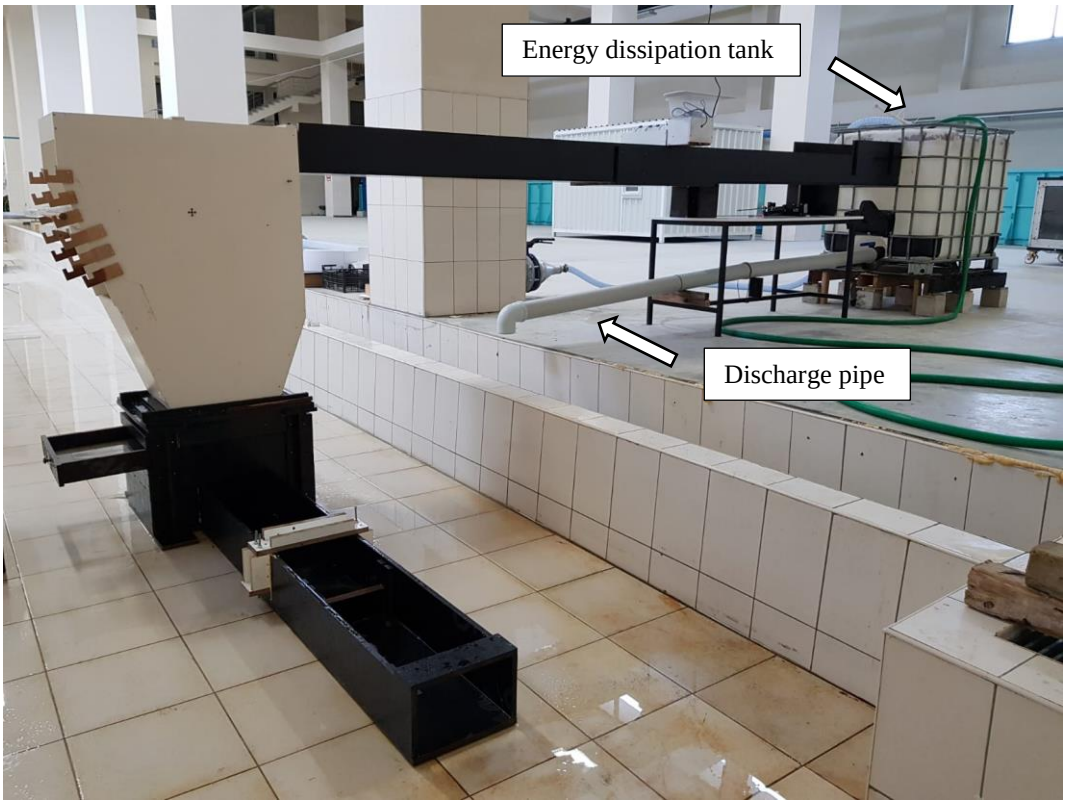

Figure 31. General view of the experimental setup – 2

The experimental setup consists of intake screens and other components such as; energy dissipation tank, main flume, sediment feeder device, intake assembly system, sediment trapper, inflow flume, outflow flume, and the discharge pipe.

Six different Coanda intakes and one Tyrolean intake were produced for the experimental studies. As we discussed in the literature review part of this thesis study, there is not any restriction for the determination of the screen curvature radius. On the other hand, some manufacturers produced their products with having 3 m of screen curvature radius as we discussed in previous sections. In addition, the best performance was obtained when the curvature radius is approximately 1.5 m as can be seen in Figure 21. Referencing this graph taken from the (T. L. Wahl 2003), we decided to produce intake structures close to this value. The screen radiuses of the intakes were determined as 800 mm, 1200 mm, and 1600 mm for Coanda types. All of the Coanda screens have 60 cm net screen length and the total length of the screens becomes 100 cm with assembling parts. When the screen length is constant, with increasing value of curvature radius, screens become flatter. This situation can be described with a sagging distance parameter. The illustration for the sagging distance can be seen in Figure 32.

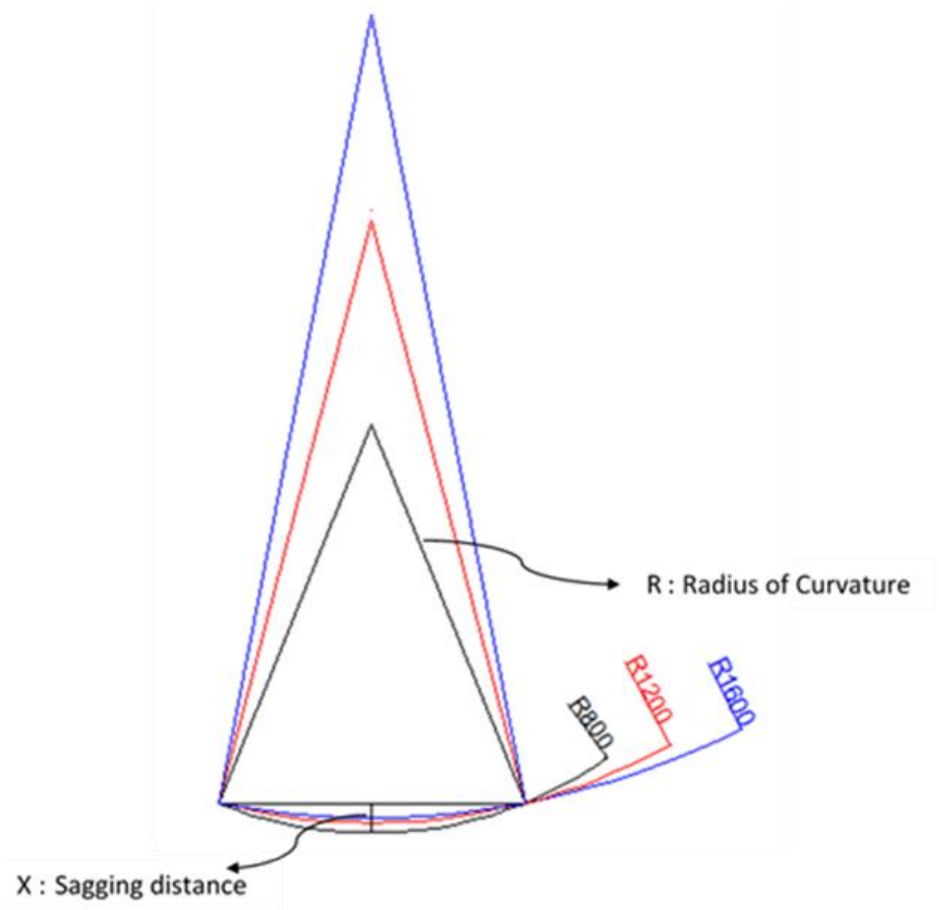

Figure 32. Sagging distances for various curvature Radius values

Screen parameters such as the total and net screen lengths, the width of the screen, void ratios, screen curvature radius and etc. are given below as Table 9.

Table 9. Details of the screens

Screen model	Screen Width (cm)	Screen net Length (cm)	Screen total Length (cm)	Radius of Curvature (cm)	Void Ratio
Tyrolean Type	40	60	100	0	0.046
Coanda R800 (1)	40	60	100	80	0.048
Coanda R800 (2)	40	60	100	80	0.096
Coanda R800 (3)	40	60	100	80	0.144
Coanda R1200	40	60	100	120	0.048
Coanda R1600 (1)	40	60	100	160	0.048
Coanda R1600 (2)	40	60	100	160	0.096

Plan drawing and the production of the intake structures and all of the other components of the experimental model were made by ourselves and then placed in the Hydraulic Laboratory of the Izmir Institute of Technology. The production step of a one intake structure is described below for an example. The manufacturing steps of the other screens are similar.

3.1.1. Manufacturing Steps of the Intake Structures

It will be better to give information about the materials used in the model before proceeding to the production stages. In the case of the production of intake screens, transparent plexiglass is used. For the outer side parts and the middle parts, which is forming the curvature structure and where the screen T-bars will be placed, are used with 5 mm plexiglass. T – shape bars are produced with 3 mm plexiglass material. The assembly of the pieces and parts are glued with a special glue that is produced for the using in plexiglass works. Also, lid part that can be described as a cover that prevents the incoming water from spilling out is also produced with 3 mm plexiglass material. The illustration of the lid will be given further.

For the assembly phase of the T – bars, a small T – shaped formwork is produced to obtain perfect shape T – bars. A photo of the production of a T – shape bar is given in Figure 33 and the drawing of T – shape formwork is given in Figure 34.

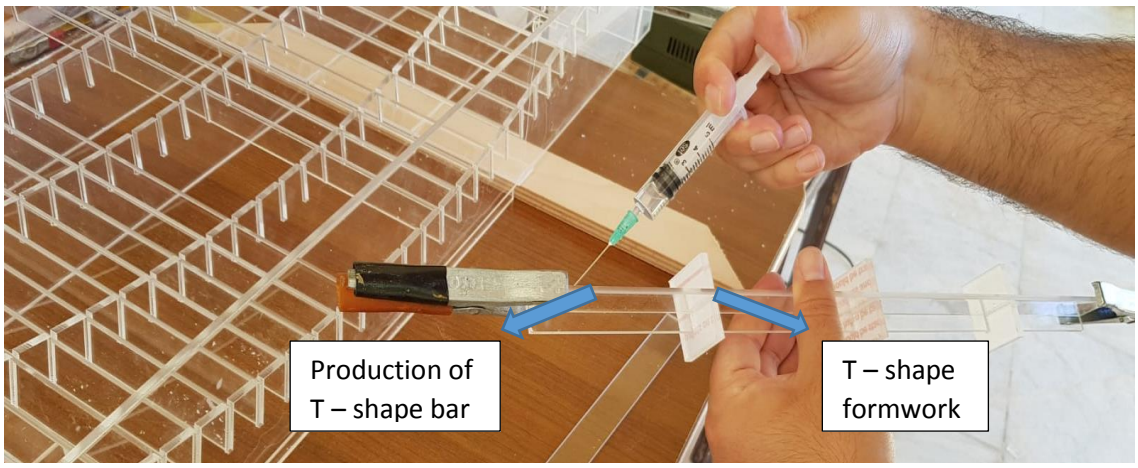

Figure 33. Assembly of a T - shape bar and the T - shape formworks

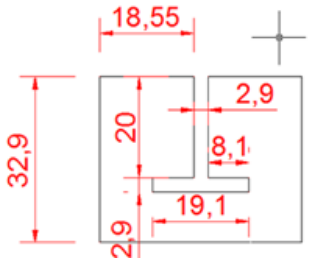

Figure 34. Drawing of the T - shape formwork

1st Step

As a first step of the manufacturing processes, a wooden frame is constructed for making easier to assemble the parts of the intake structure (Figure 35). Constructing the frame structure is also important for obtaining the correct size model. A chrome pin which will be also used in fasten the intake structure to the model body is used for collimating the parts of the screen.

Figure 35. Wooden frame for constructing intakes

2nd Step

As a second step, outer side parts are placed and collimate. Then, the middle parts on which the screen T bars are to be placed are assembled on the appropriate locations in the model (Figure 36). These middle parts will also give a curved shape to the Coanda type intake models.

Figure 36. Assembly of middle parts to the Coanda screen model

3rd Step

After finishing the installation of the main skeleton of the intake structure, the T-shape bars are fixed in their positions on the middle curved parts of the model. These steps can be seen in Figure 37 and Figure 38.

Figure 37. Fixing the T-shape bars in their positions on the model

Figure 38. Fixing last T-shape bar on its position

4th Step

After completing the placement of the T-shape bars on to the model, a lid part can be montage to the intake structure. It is better to fixing the intake structure to the body part of the experimental model before assemble the lid part to measure the location where the screen will be drilled and the lid will be fixed. When the measuring is performed and the lid part is assembled to the intake structure it can be fixed again to the body part and checked whether it works or not. The image of the intake structure which is fixed in the main body with lid part can be seen in Figure 39.

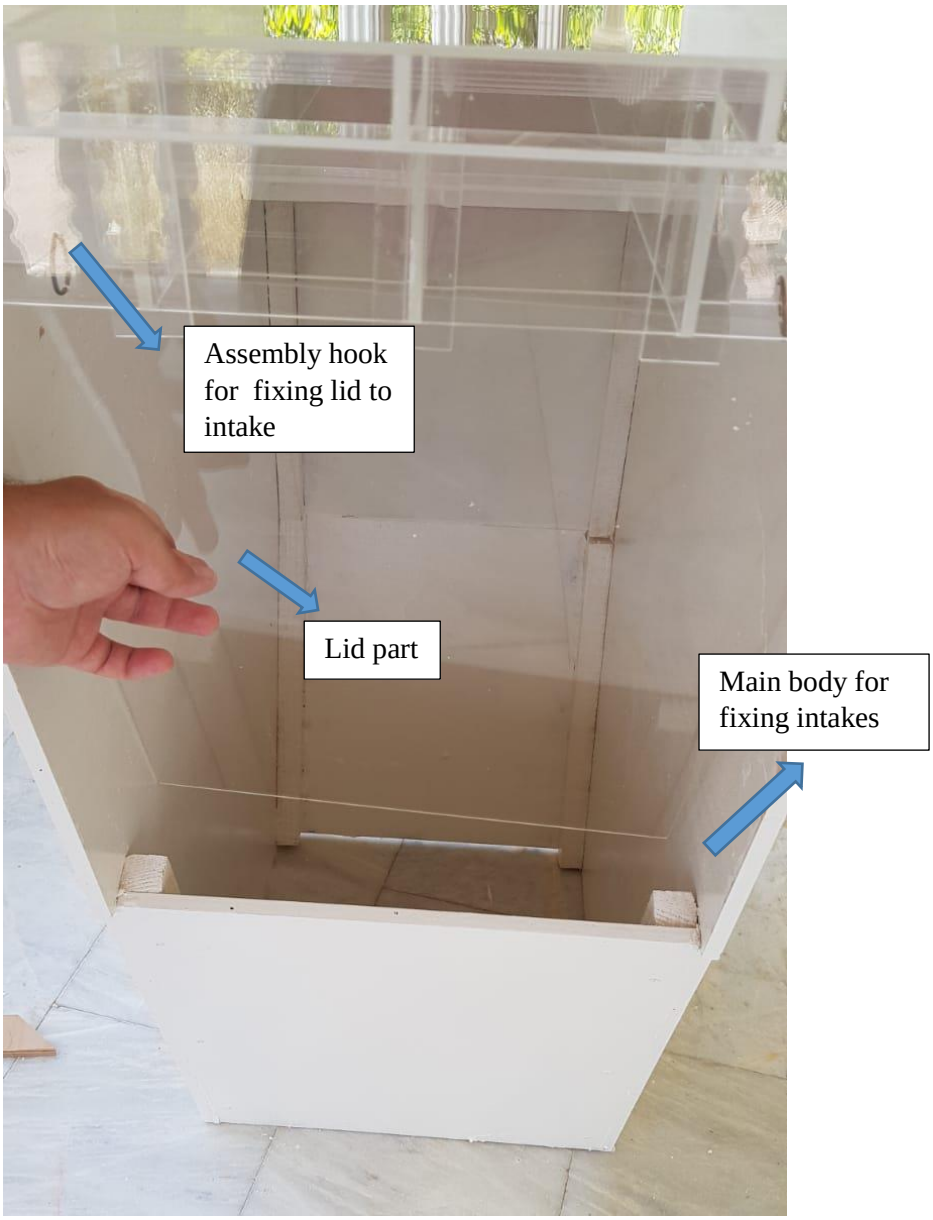

Figure 39. Lid part of the intake structure

If all the necessary parts are montaged to their positions and all the checks are performed, the intake screen is ready for use in the experimental studies. Example of a completed Coanda and Tyrolean intakes are given in Figure 40 and Figure 41 respectively.

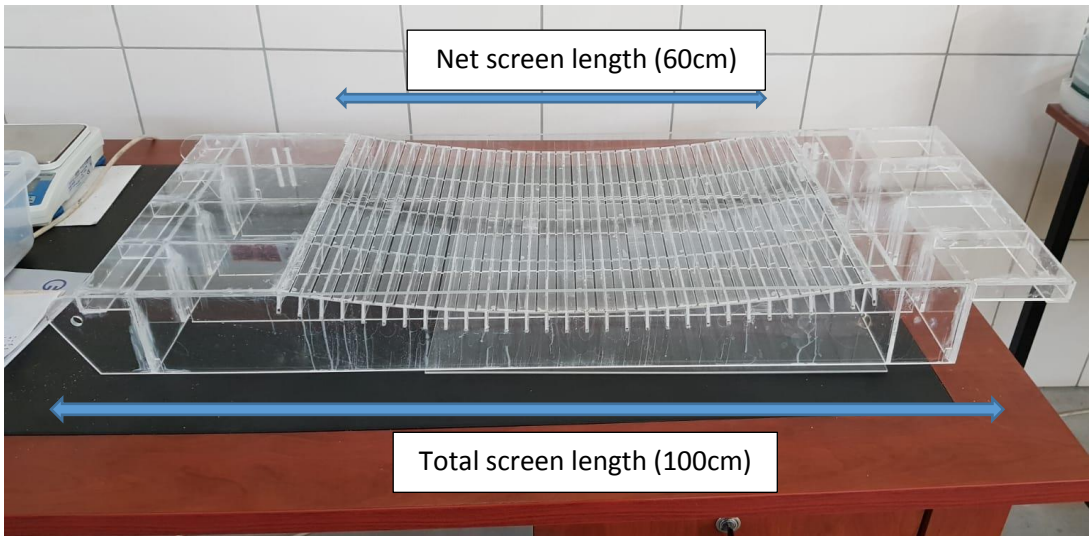

Figure 40. Example of a Coanda intake that is used in the experiments

Figure 41. Example of the Tyrolean intake that is used in the experiments

The net length describes the effective screen length where the incoming flow is diverting to the collecting channel. The total length is obtained after adding solid rectangular two parts to the head and toe of the screens. The reason for adding one of these parts to the head of the screen is preventing any jump over the T – shape bars and

reduction of the effective screen length. This can be prevented by using an accelerator plate, on the other hand, there are 3 different Coanda intakes which have different screen curvature and the experiments were conducted for 6 different screen inclination case. In addition to this, 3 different flow rates were used in these experiments. Because the shape of the accelerator plates depends on the screen curvature and shape, incoming flow rate and screen inclination, it is more economical and practical to use this solid part. Under these conditions, there should be (3 x 6 x 3 = 54) 54 different accelerator plates if this extension part is not used. The other additional part is also used in the toe of the intake to transmit overflow to the downstream part.

3.1.2. Manufacturing Steps and the Information about Flumes

In order to use in the experiment, 3 different flumes have been constructed. One of them is the main flume which carries the incoming flow from the tank. The main flume has 40 cm width, 30 cm height, and 5 m length. The main flume is designed to consist of two parts because of its length. The design drawing of the main flume is given in Figure 42 and the photo which is taken during the construction of the main flume is given in Figure 43. All of the flumes are produced using high quality plywood, which is durable to the effect of water, and then they are painted with a synthetic paint to obtain extra protection against the effect of water.

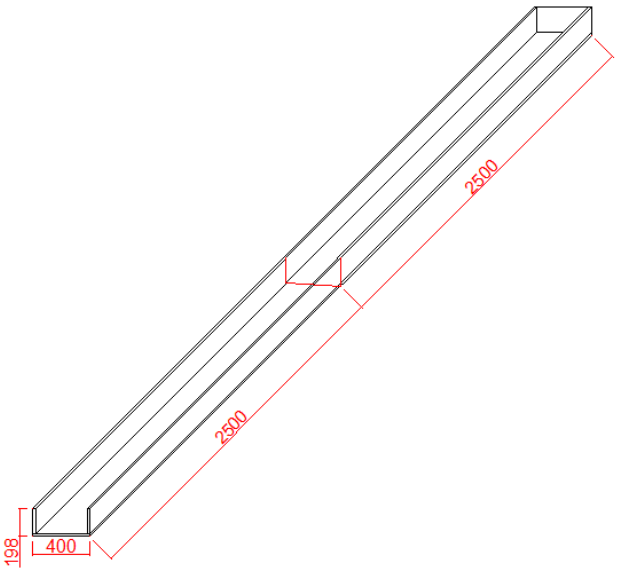

Figure 42. Design Drawing of the main flume

Figure 43. Photo of the main flume taken during its construction process

Another flume was constructed for routing the diverted water and measure the discharge rate of this flow. The same materials were used for this flume as used in the other flumes. This flume consists of two different parts, one of these parts is sediment trapper and the other part is the channel part where the rectangular weir is located on it for measuring the discharge rate. The first part sits on the second part and they together form the complete flume. The plan drawing of the diverted water flume is given in Figure 44. Sediment trapper consists of a sliding drawer and a frame. There are a fine mesh and cheesecloth on the drawer. Diverted sediment are hold using this drawer. The photo of the sediment trapper and complete flume can be seen in Figures 45 and Figure 46.

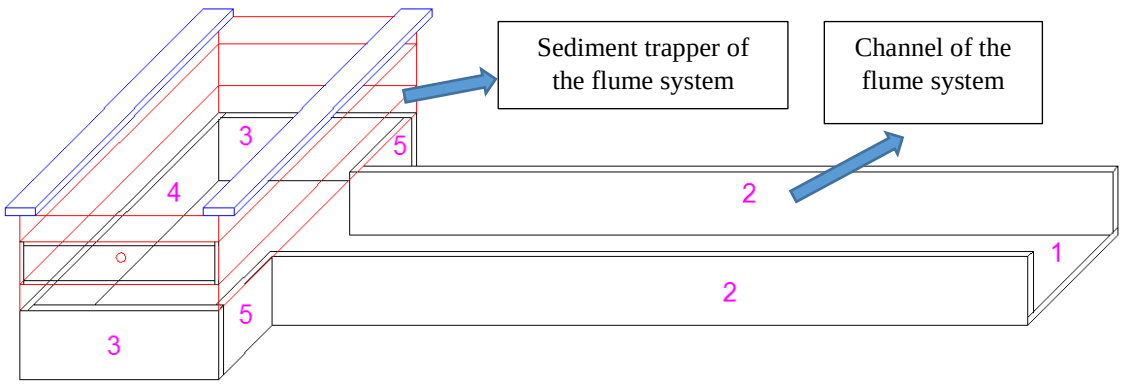

Figure 44. Plan drawing of the diverted water flume

Figure 45. Sediment Trapper (Sliding drawer and its frame)

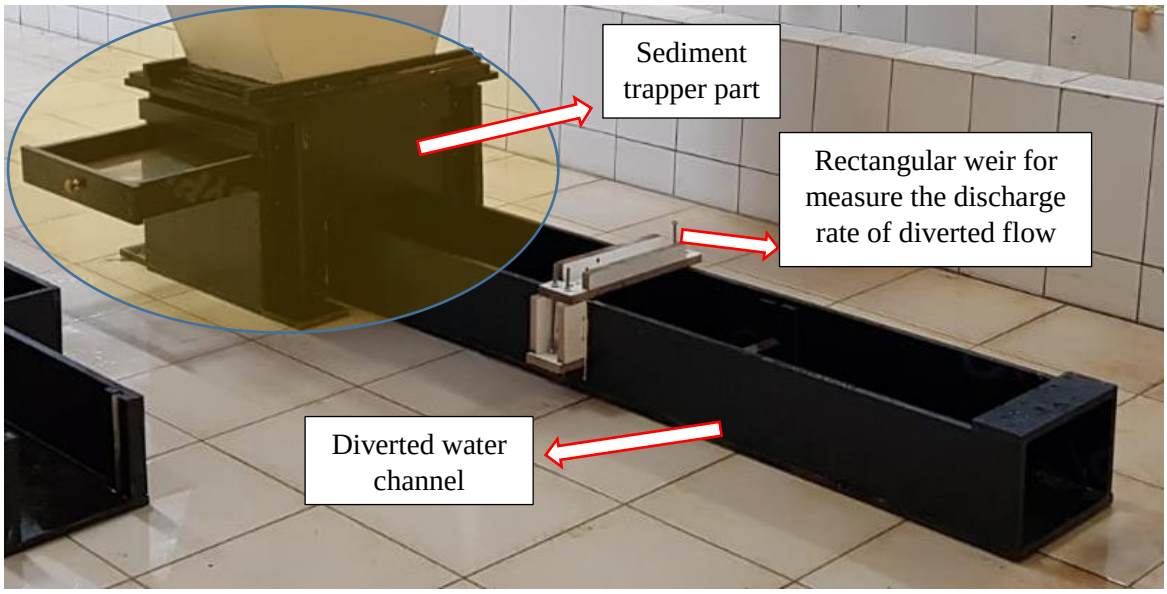

Figure 46. Complete diverted water flume

The last flume is constructed for use to route the downstream flow which can be described as the flow which is not diverted by the intake structure and passes through the downstream part. Also, a cheesecloth is placed on the flume for trapping sediment which cannot be passed through between the screen bars. The photo of the flume is shown in Figure 47.

Figure 47. Flume for routing the downstream flow

3.1.3. Information for the Intake Assembly Body

Another part of the experimental setup is the intake assemble part which's an unpainted photo is given in Figure 48. This part is produced by marine-plywood which is highly durable for the harmful effects of the water. Additionally, it is painted with synthetic paint for obtaining maximum protection.

Figure 48. Intake assembly frame

This part sits on the sediment trapper part and the Coanda and Tyrolean intakes are fixing to this part. Also, wood sockets mounted on the two sides of the intake walls served the purpose of eliminating the human error when varying rack angle from 0 to 30 degrees at 5 degrees incremental. The photo of the painted and final version of the intake assembly part is given in Figure 49.

Figure 49. Intake assembly part

3.1.4. Other Parts of the Experimental Setup

Sediment feeder is another important part of the experiment system. It is specifically designed for this study. The sediment feeding system consists of a geared DC electric motor, receptacle, and wooden frame. This DC motor capable of turning 30 revolutions per minute. The sediment discharge rate can be adjustable by using caps located on the receptacle. The photo of the sediment feeder is given in Figure 50.

Figure 50. Sediment feeder device

Another part of the experimental system is the energy dissipation tank. This tank was bought for use in the experiments. It has 1-ton volume and during the experiments, water pumped from the storage tank is directed into this tank attached to the setup to dissipate excess energy and water is let into the channel through a weir. Two different pumps; submersible pump having a discharge capacity of 4 l/s (constant head) for low discharge experiments and the main pump in the laboratory having a discharge capacity of 120 l/s (having adjustable efficiency) are used in the experiments. The water left in the tank is discharged through the drain pipe. The images of the tank and the discharge pipe are given in Figure 51 and Figure 52 respectively.

Figure 51. Image of energy dissipation tank

Figure 52. Image of discharge pipe

3.2. Conducting Experiments

The Water Capture Performance (WCP) and the Sediment Release Efficiency (SRE) of the two types of intakes are evaluated through experiments. The angle of rack inclination, θ was selected as 5°, 10°, 15°, 20°, 25°, and 30° in the experiments. In the case of obtaining WCP, 3 different incoming discharge rates that are 2.4 l/s, 5.56 l/t, and 7.96 l/s were used. During the experiments, 3 different Coanda screens, which have different screen curvature radius, were used. The spacing between the bars of the racks is selected as 1 mm for all type screens, 2 mm for both R1600 and R800 type screens, and 3 mm is for only R800 screen, which resulted in void ratios of 0.046, 0.092, and 0.138 respectively. Obtained results were plotted to see the effects of screen curvature, rack inclination, void ratio, and the incoming flow on WCP. A vertical point gauge is used to measure head over sharp-crested weir installed at the outlet for diverted discharge measurement. The measuring head is then converted to flow rate via the weir equation given as Equation 3.1.

$$Q=C\frac{2}{3}b\sqrt{2g}\,H^{\frac{3}{2}} \tag{3.1}$$

Where; b= crest width, H= weir head, g= gravitational acceleration, and C= discharge coefficient. The discharge coefficient can be defined as Equation 3.2.

$$C=0.598+0.0897\frac{H}{P_w} \tag{3.2}$$

Where H= weir head and P_w = water height

Than multiple linear regression analysis was utilized to obtain a relation between the dependent parameter WCP and the independent parameters. In the case of Tyrolean intake, only one screen is used. Because this presented study is related to the Coanda intake structures, furthermore, no other Tyrolean intakes were produced. Using selected data from other studies (Yılmaz 2010) and (Righetti and Lanzoni 2008) and the data gathered from our Tyrolean intake structure, multiple linear regression analysis was utilized to obtain a relation for the WCP of Tyrolean intake structure. A summary chart of the experimental studies that were performed for determining the WCP is given in Table 10.

Table 10. Experiments performed for WCP and screen characteristics

Parameters	Description	Coanda Screen Types					
		R800-1	R800-2	R800-3	R1200	R1600-1	R1600-2
θ (degree)	Screen inclination	5-10-15 20-25-30	5-10-15 20-25-30	5-10-15 20-25-30	5-10-15 20-25-30	5-10-15 20-25-30	5-10-15 20-25-30
R (mm)	Curvature radius	800	800	800	1200	1600	1600
x (mm)	Sagging distance	63.2	63.2	63.2	38.4	24.96	24.96
x / R	Screen characteristic	0.079	0.079	0.079	0.032	0.0156	0.0156
w (mm)	Width of the screen	40	40	40	40	40	40
L total (mm)	Total screen length	100	100	100	100	100	100
L net (mm)	Net screen length	60	60	60	60	60	60
e (mm)	Gaps between racks	1	2	3	1	1	2
Qin (l/s)	Incoming flow	2.4-5.56-7.96	2.4-5.56-7.96	2.4-5.56-7.96	2.4-5.56-7.96	2.4-5.56-7.96	2.4-5.56-7.96

In case of obtaining a relation for SRE, the same Coanda screens were used. Again the angle of rack inclination was selected as 5°, 10°, 15°, 20°, 25°, and 30° in the

experiments and the incoming flow rates were selected as 2.4 l/s, 5.56 l/s, and 7.96 l/s. The sediment amount and composition are varied to investigate different parameters. At the beginning of the study, only a uniform sediment sample whose diameter is between 0.71 mm – 1 mm was used. In later stages, 4 different sediment compositions were prepared to investigate the effect of size distribution on the SRE. Sediment composition groups and details are given in Table 11, Table 12, Table 13 and Table 14 and grading curves are given as Figure 53, Figure 54, Figure 55, and Figure 56. Detailed explanations and information will be given in Chapter – 4.

Table 11. Sediment composition - 1

Screen No	Retained sediment (gr)	Retained sediment (%)	Cumulative retained (%)	Passing (%)
2	0	0	0	100
1,7	65	9	9	91
1	200	29	38	62
0,71	300	43	81	19
0,5	130	19	100	0

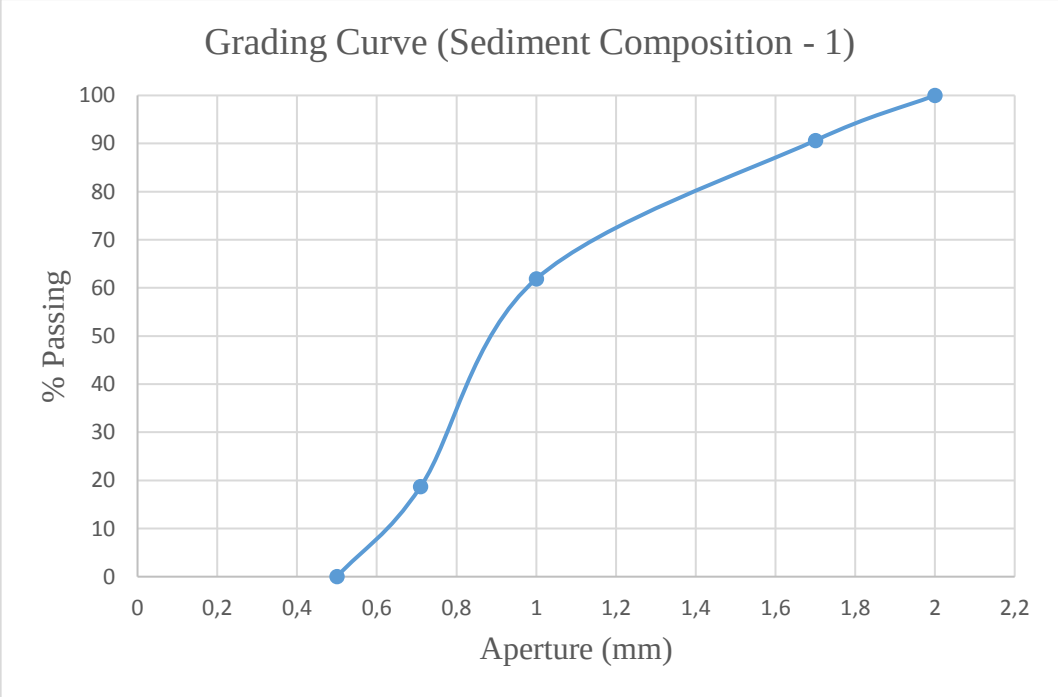

Figure 53. Grading curve for sediment composition – 1

Table 12. Sediment composition - 2

Screen No	Retained sediment (gr)	Retained sediment (%)	Cumulative retained (%)	Passing (%)
2	0	0	0	100
1,7	200	25	25	75
1	200	25	50	50
0,71	200	25	75	25
0,5	200	25	100	0

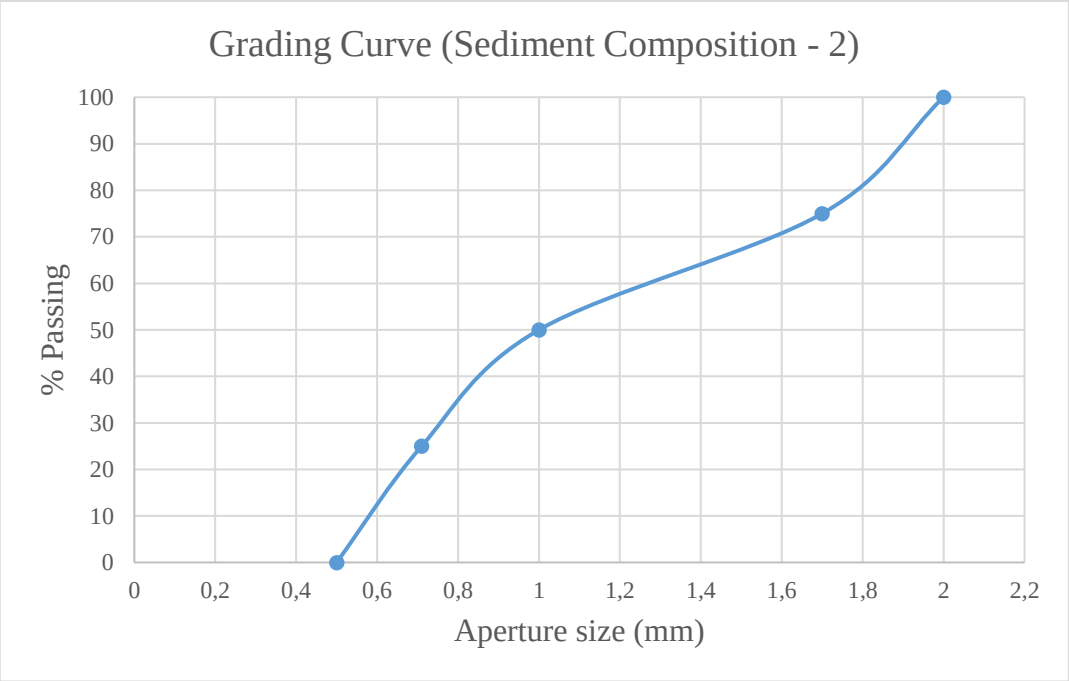

Figure 54. Grading curve for sediment composition – 2

Table 13. Sediment composition - 3

Screen No	Retained sediment (gr)	Retained sediment (%)	Cumulative retained (%)	Passing (%)
2	0	0	0	100
1,7	100	12,5	13	88
1	100	12,5	25	75
0,71	300	37,5	63	38
0,5	300	37,5	100	0

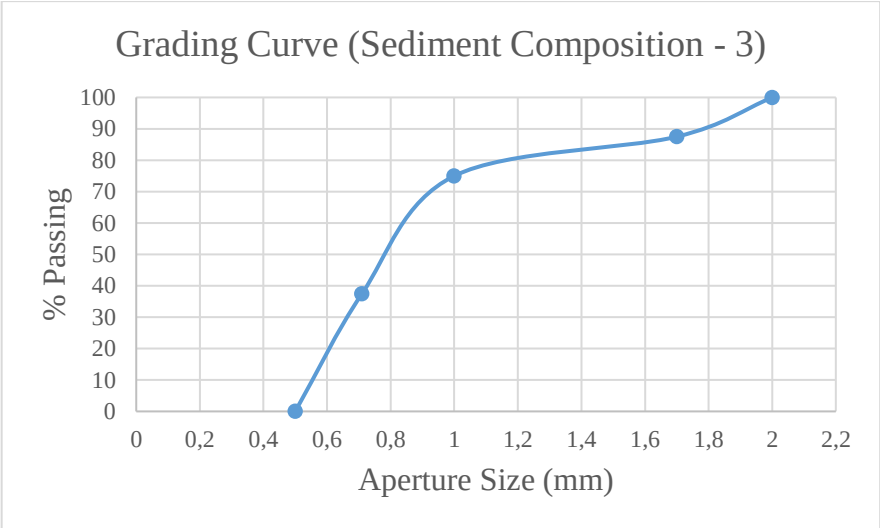

Figure 55. Grading curve for sediment composition – 3

Table 14. Sediment composition - 4

Screen No	Retained sediment (gr)	Retained sediment (%)	Cumulative retained (%)	Passing (%)
2	0	0	0	100
1,7	100	12,5	13	88
1	100	12,5	25	75
0,71	200	25	63	38
0,5	400	50	100	0

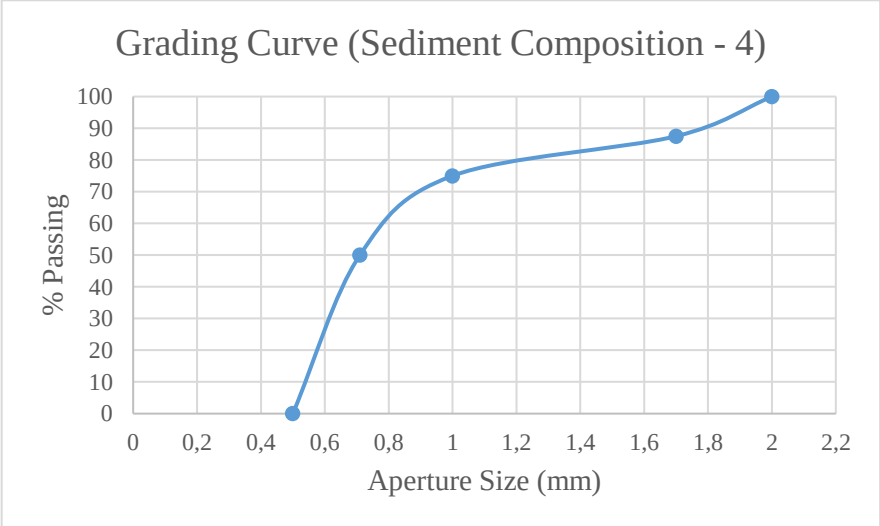

Figure 56. Grading curve (Sediment Composition - 4)

In sediment composition – 1, sediment ratios in the mixture were chosen randomly and a total of 695 gr sediment was used. In the case of sediment compositions 2, 3, and 4 total of 800 gr sediment were used in each experiment. In the second composition, 50% of the sediment is designed to pass through the gap between the screen bars. In other words, 50% of the sediment has the diameter sizes which is less than the gaps in between the screen racks. In the third composition, the ratio of the sediment which is passed through the screen is changed and increased from 50% to 75% to see the effect of fineness of the mixture on the SRE. In the fort composition, the ratio of the sediment whose diameters are smaller than the bar opening stayed 75% on the other hand, the distribution of sediment groups which are (0.5-0.71) and (0.71-1) were changed. The experiments that have been conducted for the sediment related studies are summarized in Table 15.

Table 15. Summary of sediment related experiments

Sediment Compositions	**Screen Types**					
	R800(1)	**R800(2)**	**R800(3)**	**R1200**	**R1600(1)**	**R1600(2)**
Uniform Sediment	done	done	done	done	done	done
Composition – 1	done	x	x	x	done	x
Composition – 2	done	x	x	x	x	x
Composition – 3	done	x	x	x	x	x
Composition – 4	done	x	x	x	x	x

Experiments using uniform sediment distribution were performed for all types of intake structures. Results will be given in next chapter in details. It is necessary to clarify why sediment composition experiments were not done by using all types of intake structures. We can say very briefly that the best performances about the SRE were obtained from the R800(1) and R1600(1) type intakes from the uniform sediment experiments. Therefore, due to the time limitation, experiments using sediment composition – 1 was performed for only R800(1) and R1600(1) type intake structures. From these experiments, the R800(1) type intake structure showed the best performance in the case of SRE. Therefore, other sediment composition experiments were performed using the R800(1) type Coanda intake structure. However, for future studies, it would be

better to expand the experiment area to include the other Coanda screens. The statistical analysis for the SRE was performed based on the uniform sediment experiments. The reason for this and more information will be given in Chapter – 4.

CHAPTER 4

RESULTS OF EXPERIMENTS

4.1. Experimental Results

Under this caption, we will discuss the results gathered from the experimental studies and we will deal with the effects of the screen and flow conditions on the WCP and SRE. We divide this section into two parts as the results gathering from the clear water experiments and the results gathering from the sediment-waterer experiments. First, we start by examining the results obtained from the clear water tests. After then we discuss the sediment-water studies.

4.1.1. Results Obtained from the Clear Water Tests

4.1.1.1. Effects of Intake Type and Screen Inclination

As described earlier, three different Coanda intake designs all having the same dimensions are used and their results are compared in the experiments. The angle of rack inclination, θ is selected as 5, 10, 15, 20, 25, and 30 degrees in the experiments. A vertical point gauge is used to measure head over sharp-crested weir installed at the outlet for diverted discharge measurement. The measuring head is then converted to flow rate via the weir equation. The results show that the diverted discharge rate and the WCE are decreasing with increasing the screen inclination. Figure 57, Figure 58, and Figure 59 show the effect of screen inclination on the WCP of the Coanda screens at the incoming discharge rates of 2.4 l/s, 5.56 l/s and 7.96 l/s respectively. According to the results, the R1200 Coanda type intake shows the best performance of the WCP.

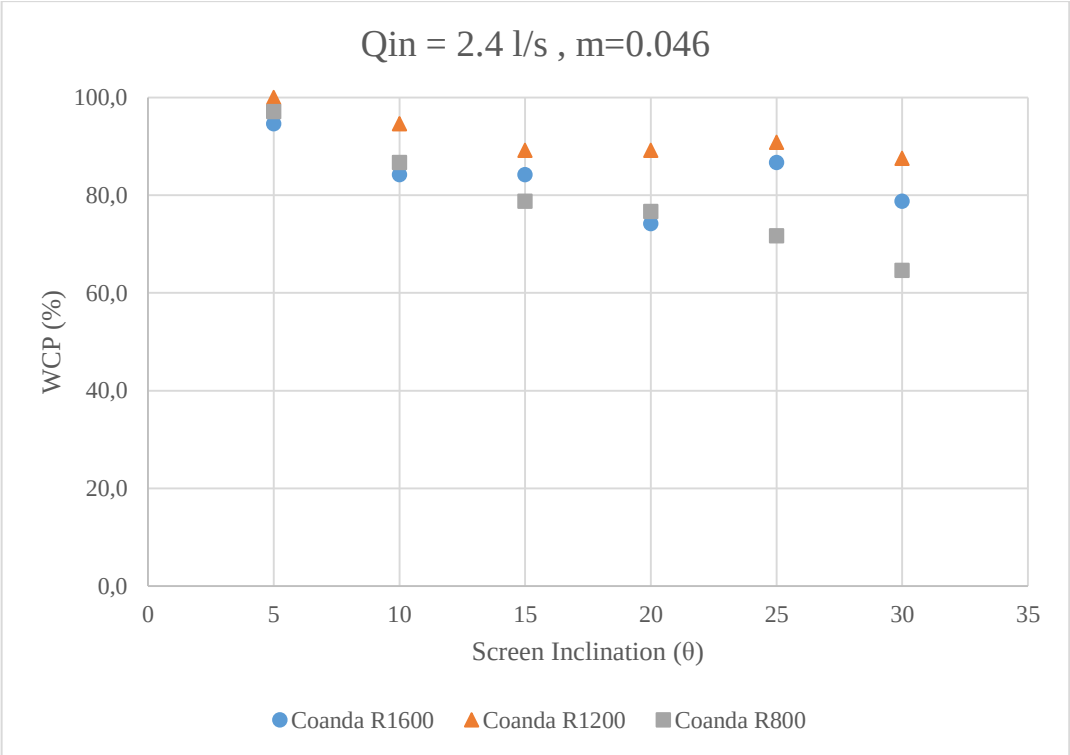

Figure 57. Effect of screen type and inclination on the WCP in case of Q=2.4 l/s

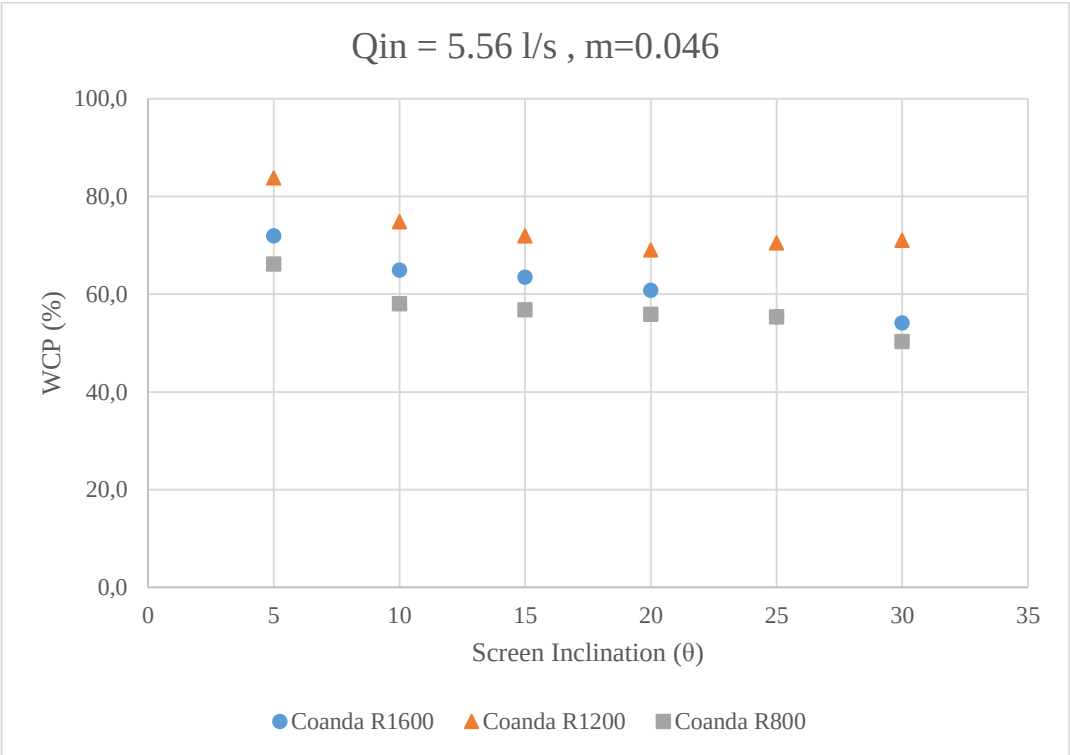

Figure 58. Effect of screen type and inclination on the WCP in case of Q=5.56 l/s

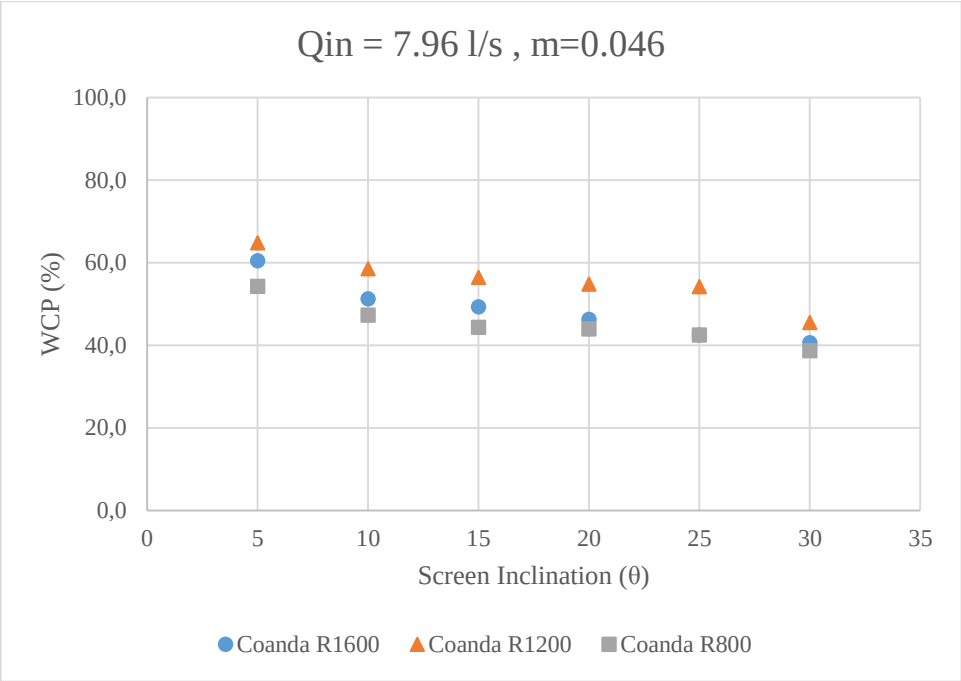

Figure 59. Effect of screen type and inclination on the WCP in case of Q=7.96 l/s

As can be seen in the figures, the Coanda screen which has the 1200 mm screen curvature radius shows the best performance for all discharge rates. In addition, R800 and R1600 type Coanda intakes also show similar performances. Therefore, it can be said that either increasing or decreasing the screen curvature from a point, it affects the performance of the screens in case of WCP in a negative manner. It is also important to point out that in these experimental studies, the effect of the wire tilt angle is not considered. Therefore, the effect of the wire tilt angle can be a topic for another study. Summary of the results of WCP is given in Table 16, Table 17, and Table 18.

Table 16. Results of WCP in case of Q=2.4 l/s

Screen Inclination (θ)	Screen Types and WCP performances %		
	R800(1)	R1200(1)	R1600(1)
5	97.1	100	94.6
10	86.7	94.6	84.2
15	78.8	89.2	84.2
20	76.7	89.2	74.2
25	71.7	90.8	86.7
30	64.6	87.5	78.8

Table 17. Results of WCP in case of Q=5.56 l/s

Screen Inclination (θ)	Screen Types and WCP performances %		
	R800(1)	R1200(1)	R1600(1)
5	66.2	83.8	71.9
10	58.1	74.8	64.9
15	56.8	71.9	63.5
20	55.9	69.1	60.8
25	55.4	70.5	55.4
30	50.4	71.0	54.1

Table 18. Results of WCP in case of Q=7.96 l/s

Screen Inclination (θ)	Screen Types and WCP performances %		
	R800(1)	R1200(1)	R1600(1)
5	54.3	64.8	60.4
10	47.2	58.5	51.3
15	44.3	56.4	49.2
20	44.0	54.8	46.2
25	42.5	54.1	42.5
30	38.7	45.5	40.6

4.1.1.2. Effects of Flow Rate

One of the other parameters that we studied is the incoming flow rate and its effects on the WCP. In the previous part, we discussed the effect of screen types and the screen inclination on the WCP. As can be seen in both Figures 57, 58, and 59 and also Tables 18, 19, and 20 the WCP is decreasing with the increasing the incoming flow rate. This is a very important point that must be clarified. Decreasing on the Water Capturing Performance with increasing the incoming flow rate is not meaning that the diverted discharge which is obtained from the 2.4 l/s is higher than the diverted discharges which are obtained from the incoming flow rates of 5.56 l/s or 7.96 l/s. When we remember the definition of the WCP it is the ratio of diverted discharge to total discharge thus WCP defines how much percent water is diverted from the main flow. Table 19 clearly defines the relation between WCP and diverted discharge.

The question of why the WCP is decreasing with the increasing of the incoming flow rate can become in mind. It is important to remind that these experimental studies were performed for a fixed screen length of 60 cm. This situation can be the answer to the question. As we discussed in the literature review part, the diverted water is proportional to the screen length. Because experiments of this study performed under a constant screen length, the capacity of the screen is limited. However, diverted flow can be also increased by increasing the void ratio of the screen. This situation will be discussed in previous parts.

Table 19. Relation of the WCP and diverted water flow in case of R1200 type intake

R1200, e= 1mm Type Coanda Intake						
Screen Inclination	**Q=2.4 l/s**		**Q=5.56 l/s**		**Q=7.96 l/s**	
	WCP (%)	**Diverted Water (l/s)**	**WCP (%)**	**Diverted Water (l/s)**	**WCP (%)**	**Diverted Water (l/s)**
5	100	2.4	83.8	4.66	64.8	5.16
10	94.6	2.27	74.8	4.16	58.5	4.66
15	89.2	2.14	71.9	4	56.4	4.49
20	89.2	2.14	69.1	3.84	54.8	4.36
25	90.8	2.18	70.5	3.92	54.1	4.31
30	87.5	2.1	71.0	3.95	45.5	3.62

As is seen in Table 19, WCP is decreasing with increasing the screen inclination for all the incoming flow cases. Similarly, the WCP and the diverted water discharges are also decreasing with increasing the inclination. Let's consider the 5^{o} screen inclination and look for the diverted water discharges and the WCP ratios for all the incoming flow cases. When the incoming flow is 2.4 l/s all of the incoming flow is diverted so the WCP is obtained as 100%. In case of the incoming flows 5.56 l/s and 7.96 l/s the diverted flows are 4.66 l/s and 5.16 l/s and also, the WCP ratios are 83.8% and 64.8% respectively. Although the WCP values decreasing with the increasing of the incoming flow rate the diverted water discharges increasing. Hence, it can be summarized that if the screen length is constant the WCP is decreasing with increasing the screen inclination although the diverted water discharge is increasing. The meaning of the WCP and diverted water discharge can be understood more clearly by examining Figure 60 and Figure 61.

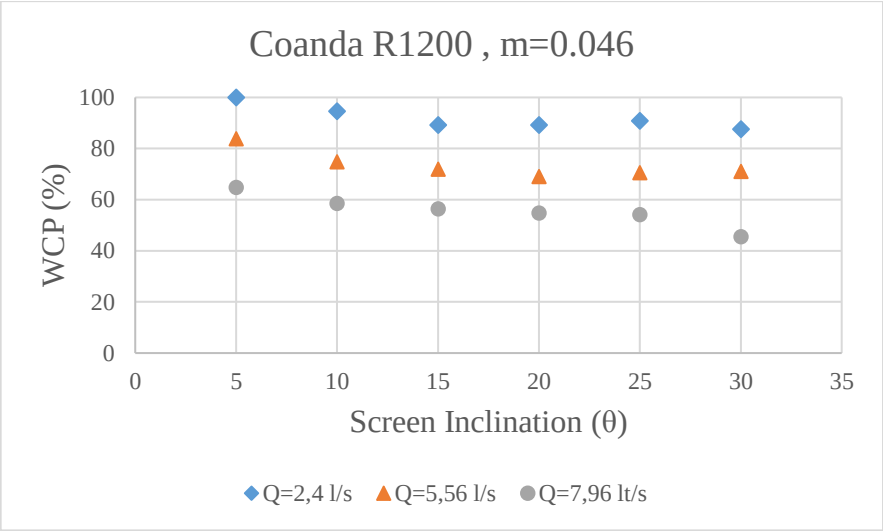

Figure 60. WCP vs screen inclination graph in case of R1200, m= 0.046 Coanda intake

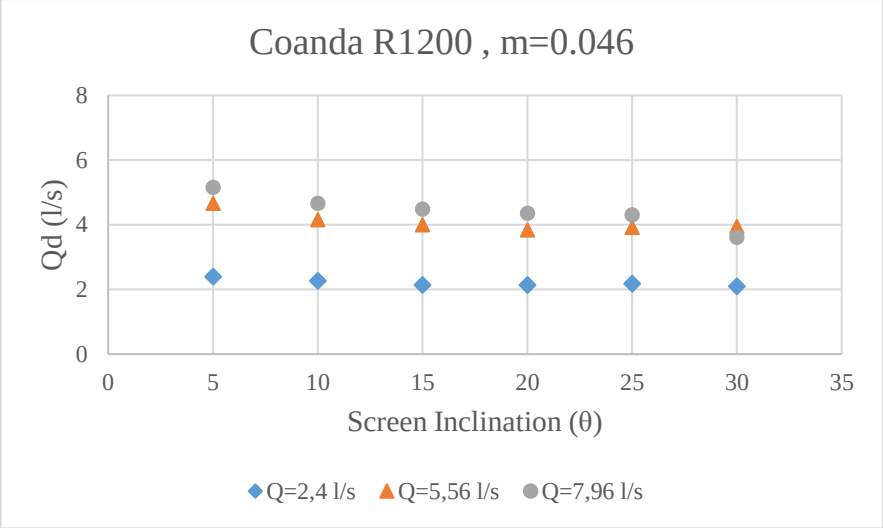

Figure 61. Relation of the diverted discharge and screen inclination in case of R1200, m=0.046 type Coanda intake

4.1.1.3. Effects of Bar Spacing

For the investigation of the effect of void ratio on water capture performance, 3 different Coanda type intakes having a curvature radius of R=80 cm with different bar spacings are manufactured and used in the experiments. Various flow rates are passed

through three different racks having bar spacings of e= 1, 2 and 3 mm corresponding to void ratios of m=0.046, 0.092, 0.138 respectively. The effects of the void ratio on the WCP and diverted discharge are given in Figure 62, Figure 63, and Figure 64 for the case of incoming flow rates of 2.4 l/s, 5.56 l/s, and 7.96 l/s respectively.

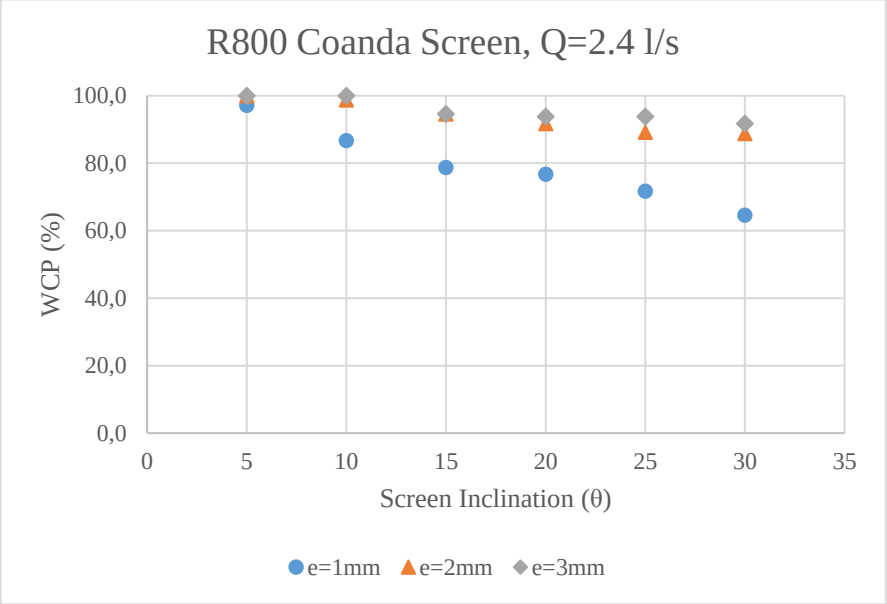

Figure 62. Effects of different void ratios on the WCP in case of Q=2.4 l/s

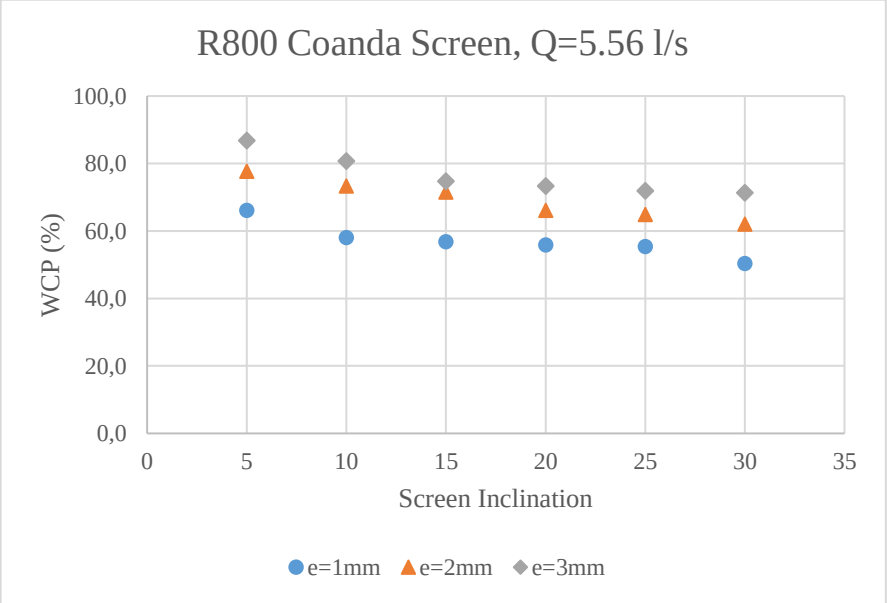

Figure 63. Effects of different void ratios on the WCP in case of Q=5.56 l/s

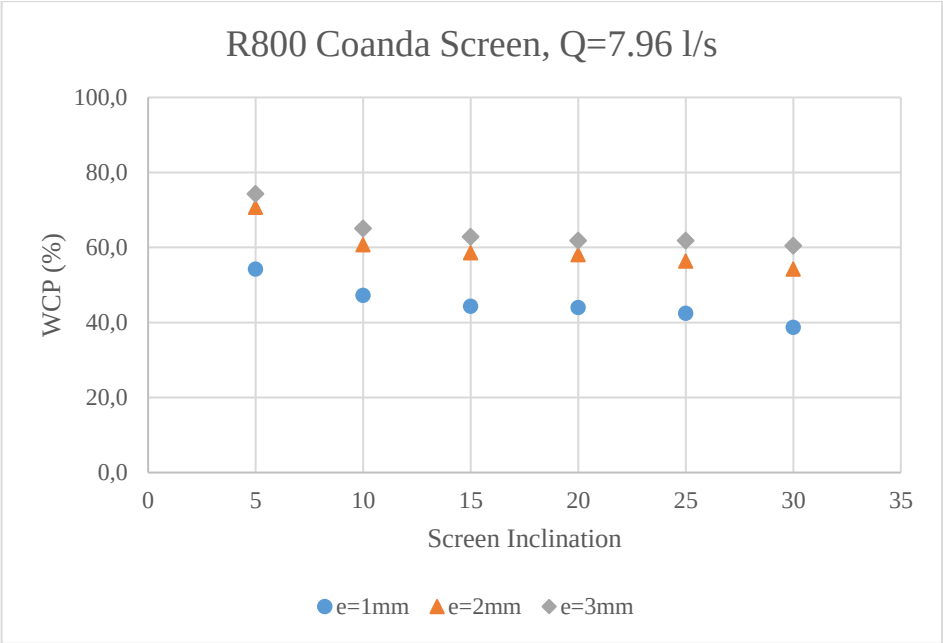

Figure 64. Effects of different void ratios on the WCP in case of Q=7.96 l/s

As it is seen in the figures given above, the WCP is increasing with, increasing the void ratio for all the inflow cases. In the case of the incoming flow of 2.4 l/s, the WCP performances of the screens that have 2 mm and 3 mm spacings show very close performances due to the relatively small incoming flow rate. On the other hand, in the case of 5.56 l/s and 7.96 l/s incoming flow cases, the Coanda screen that has 3 mm spacing in between its bars shows better performances on the WCP. Summarized results can be found in Tables (20, 21, and 22).

Table 20. Effects of void ratio on the WCP in case of Q=2.4 l/s

Effects of void ratio on WCP for R800 Coanda Screens in case of Q=2.4 l/s						
Screen Inclination (θ)	**e = 1 mm**		**e = 2 mm**		**e = 3 mm**	
	m = 0.048		**m = 0.096**		**m = 0.144**	
	WCP (%)	**Q_d (l/s)**	**WCP (%)**	**Q_d (l/s)**	**WCP (%)**	**Q_d (l/s)**
5	97.1	2.33	100.0	2.4	100.0	2.4
10	86.7	2.08	98.8	2.37	100.0	2.4
15	78.8	1.89	94.6	2.27	94.6	2.27
20	76.7	1.84	91.7	2.2	93.8	2.25
25	71.7	1.72	89.2	2.14	93.8	2.25
30	64.6	1.55	88.8	2.13	91.7	2.2

Table 21. Effects of void ratio on the WCP in case of Q=5.56 l/s

Effects of void ratio on WCP for R800 Coanda Screens in case of Q=5.56 l/s						
Screen Inclination (θ)	**e = 1 mm**		**e = 2 mm**		**e = 3 mm**	
	m = 0.048		**m = 0.096**		**m = 0.144**	
	WCP (%)	**Q_d (l/s)**	**WCP (%)**	**Q_d (l/s)**	**WCP (%)**	**Q_d (l/s)**
5	66.2	3.68	77.7	4.32	86.9	4.83
10	58.1	3.23	73.4	4.08	80.8	4.49
15	56.8	3.16	71.6	3.98	74.8	4.16
20	55.9	3.11	66.2	3.68	73.4	4.08
25	55.4	3.08	64.9	3.61	71.9	4
30	50.4	2.8	62.1	3.45	71.4	3.97

Table 22. Effects of void ratio on the WCP in case of Q=7.96 l/s

Effects of void ratio on WCP for R800 Coanda Screens in case of Q=7.96 l/s						
Screen Inclination (θ)	**e = 1 mm**		**e = 2 mm**		**e = 3 mm**	
	m = 0.048		**m = 0.096**		**m = 0.144**	
	WCP (%)	**Q_d (l/s)**	**WCP (%)**	**Q_d (l/s)**	**WCP (%)**	**Q_d (l/s)**
5	54.3	4.32	70.7	5.63	74.2	5.91
10	47.2	3.76	60.7	4.83	65.1	5.18
15	44.3	3.53	58.5	4.66	62.8	5
20	44.0	3.5	58.0	4.62	61.8	4.92
25	42.5	3.38	56.4	4.49	61.8	4.92
30	38.7	3.08	54.3	4.32	60.4	4.81

4.1.1.4. Results for Tyrolean Type Intake

As it was described earlier a Tyrolean type intake was produced for using it some experiments to obtain results for comparing the Coanda effect screens. Although the properties of the Tyrolean type intake are given in Chapter – 3, it is useful to remind that the properties of the Tyrolean type intake one more time. The intake has 60 cm screen length and 40 cm width which is the same as the Coanda type intakes. It has 1 mm bar spacing which is corresponding to a void ratio of 0.046 which is closely similar to the Coanda intake structures which have a 1 mm bar spacing and void ratio of 0.048. Hence,

results gathered from the Tyrolean intake and the Coanda intakes which have the same void ratios with the Tyrolean type can be compared with each other in some cases. The WCP performances of the Tyrolean intake for different flow rates and its changes with the screen inclination are given in Figure 65 and diverted water discharges are given in Figure 66.

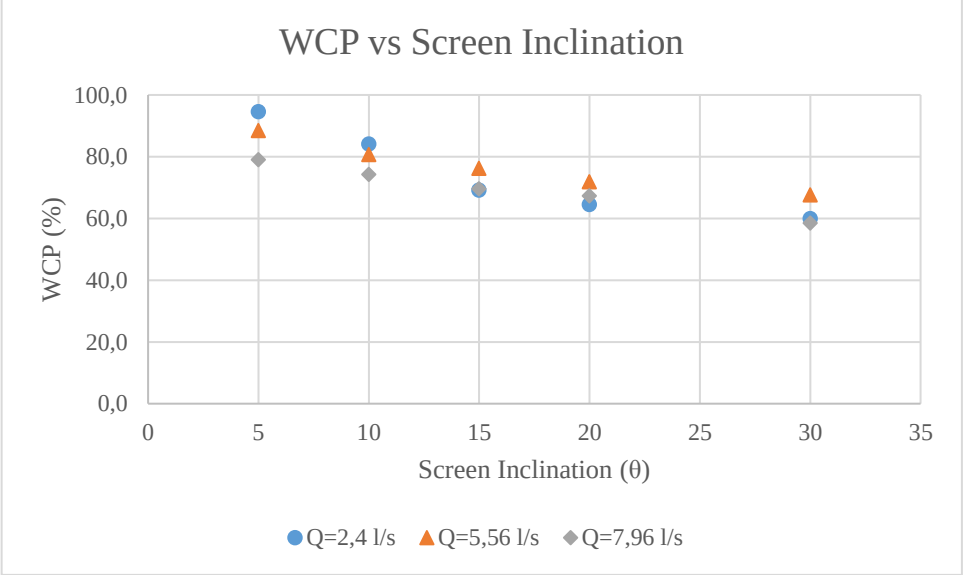

Figure 65. Effect of screen inclination on the WCP for Tyrolean intake

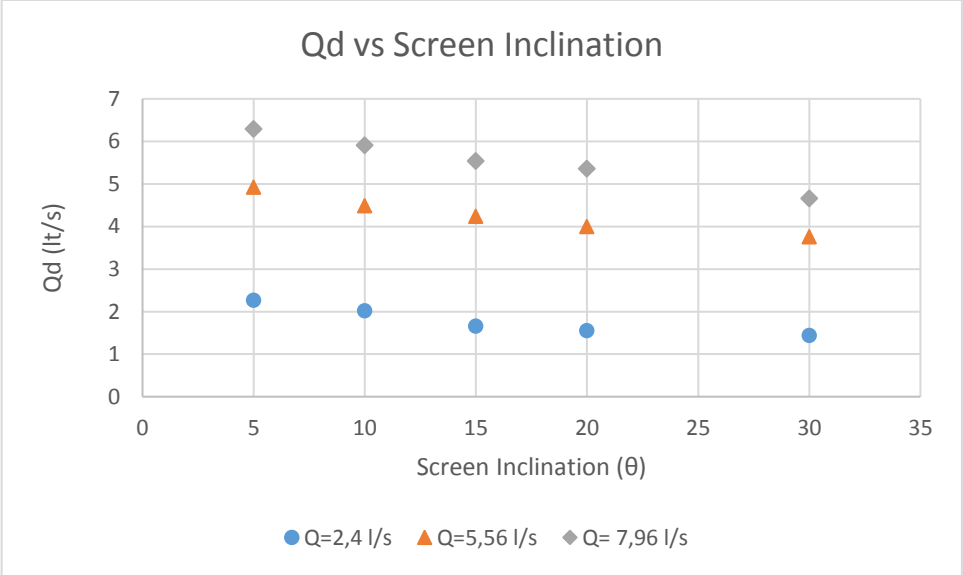

Figure 66. Effect of screen inclination on the diverted discharge for Tyrolean intake

In case of comparison of the Tyrolean intake and the R1200(1) type Coanda intake structures are used. It is clearly seen that the Coanda screen shows better performance, especially in the higher screen inclinations in case of diverted discharge rate where the inflow is 2.4 l/s. (Figure 67).

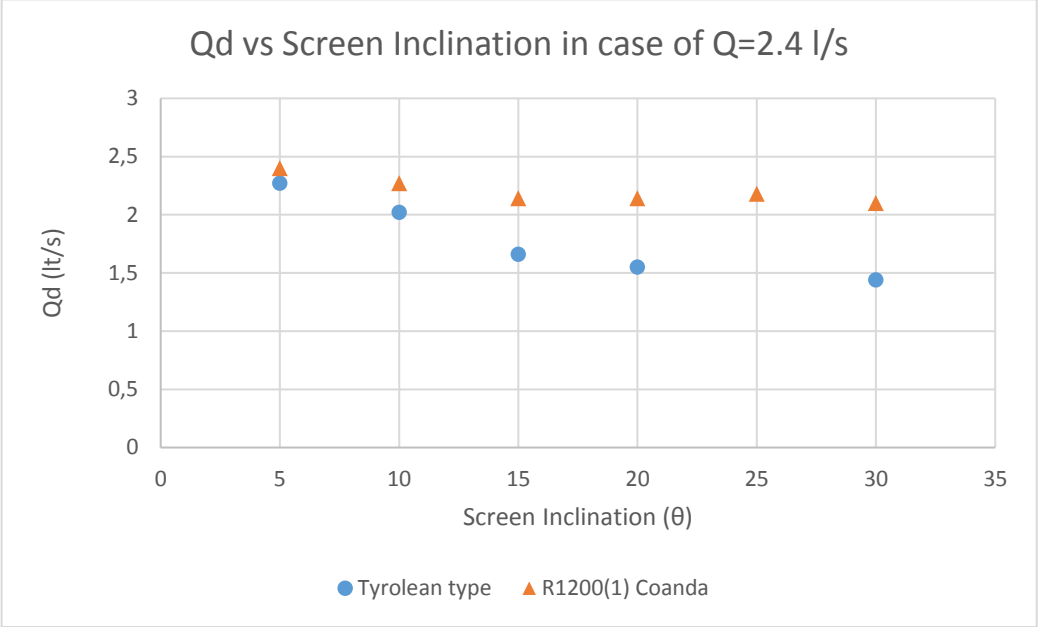

Figure 67. Comparison of the Tyrolean intake and the R1200(1) type Coanda intake in case of Q=2.4 l/s

On the other hand, when the incoming flow rate increased from 2.4 l/s to 5.56 l/s, both of two structures show similar performances. The summary of the results which were obtained from the Tyrolean type intake is given in Table 23.

Table 23. WCP performance of the Tyrolean type intake

Screen Inclination	Q_{in}=2.4 l/s		Q_{in}=5.56 l/s		Q_{in}=7.96 l/s	
	WCE %	Q_d (l/s)	WCE %	Q_d (l/s)	WCE %	Q_d (l/s)
5	94.6	2.27	88.5	4.92	79.0	6.29
10	84.2	2.02	80.8	4.49	74.2	5.91
15	69.2	1.66	76.3	4.24	69.6	5.54
20	64.6	1.55	71.9	4	67.3	5.36
30	60.0	1.44	67.6	3.76	58.5	4.66

4.1.2. Results Obtained from Sediment Related Studies

Sediment related studies can be classified as two parts such as the results which are gathered from the uniform sediment studies and the results which are gathered from the sediment composition studies. In the sub-chapters of this part, both categories will be analyzed in order to examine the effects of screen type (screen curvature radius), screen inclination, incoming flow rate, and void ratio on the Sediment Release Efficiency (SRE) and Sediment Release Efficiency base on concentration (SRE_C). First, we will start analyzing the results obtained from uniform sediment distribution. After than sediment composition studies and their results will be investigated.

4.1.2.1. Results Obtained from Uniform Sediment Distribution Studies in Case of Same Incoming Concentration

4.1.2.1.1. Effects of Intake Type and Screen Inclination

In the uniform sediment studies, the sediment diameters range in between 0.71 mm to 1 mm and the d_{50} of the sediment defined as 0.85 mm. Experiments were performed for 0^o, 5^o, 10^o, 15^o, 20^o, 25^o, and 30^o screen inclinations. Experiments were repeated for three different incoming flow cases of 2.4 l/s, 5.56 l/s, and 7.96 l/s. All of the intake structures were used during the experiments.

During the experiments, 300 g, 695 g, and 995 g sediment amounts were fed into the main channel corresponding to 2.4 l/s, 5.56 l/s and 7.96 l/s respectively. The sediment amounts used in the experiments were adjusted to create an equal concentration of all flow rates. We can explain this situation with examples. The sediment feeding process takes 30 seconds for all sediment amount cases. In the case of the 2.4 l/s incoming flow, 300 g sediment was used so, the sediment amount that passes in the main channel in a second is defined as 300 g / 30 s = 10 g/s. The unit discharge that passes through the main channel is 2.4 l/s and so the concentration can be defined as 10 (g/s) / 2.4 (l/s) = 4.17 g/l.

A similar manner in the case of the main channel flow of 5.56 l/s, 695 g sediment was fed into the system. The sediment amount that passes through the main channel in one second is 695 g / 30 s = 23.17 g/s and the concentration can be defined as 23.17 (g/s) / 5.56 (l/s) = 4.17 g/l. These calculations also valid for the incoming flow of 7.96 l/s and the concentration is the same as the other flow cases.

Sediment Release Efficiency indicates that how much percent of the sediment is excluded from the intake structure. SRE can be also explained with an example. Think that we are working with the R1200(1) type Coanda intake structure at 20^{o} screen inclination and under the incoming flow of 5.56 l/s. At that conditions, the sediment amount which is diverted by the intake is 237.7 g where the total sediment amount which is fed into the main channel is 695 g. The ratio of capturing sediment can be found as Sd/Sin which is equal to 237.7/695 and result is 34%. Because the SRE is the ratio of the excluded sediment so, SRE can be found as 100% - 34% which is equal to 66%.

The effect of the screen types and screen inclination on the SRE and concentration of the diverted water will be explained in this part. Results that are obtained from the incoming flow rate of 5.56 l/s are given in Figure 68 and Figure 69.

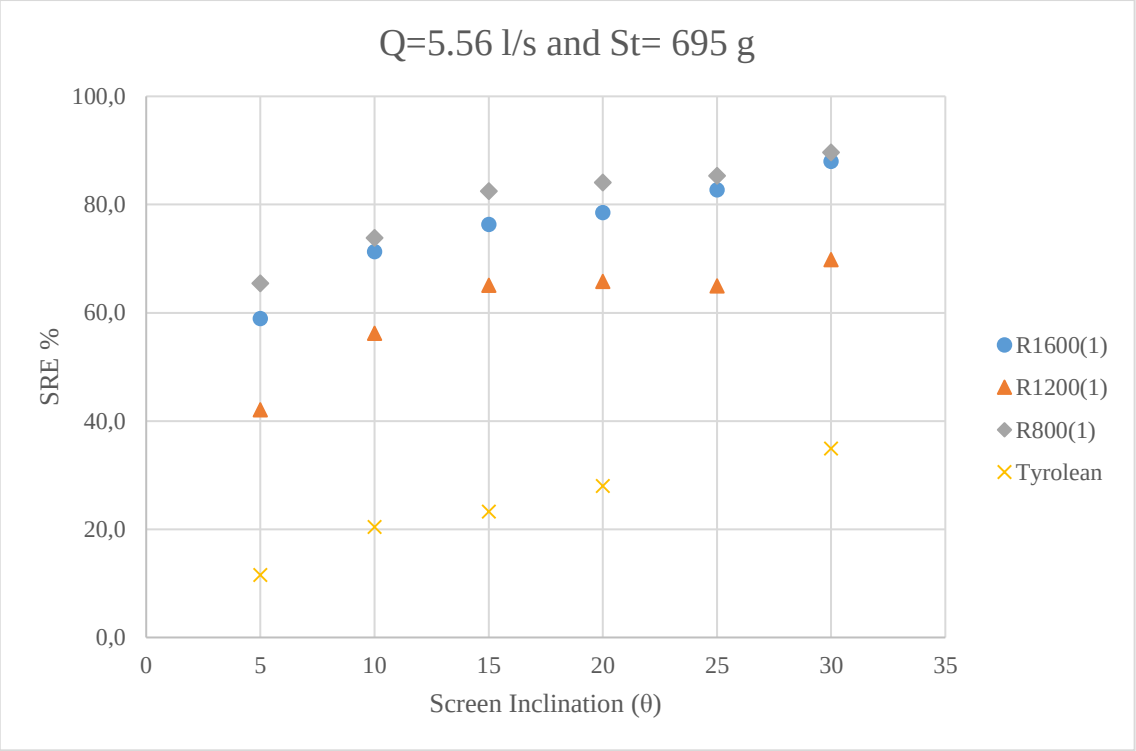

Figure 68. Effect of screen type and inclination on the SRE in case of Qin = 5.56 l/s and St=695 g

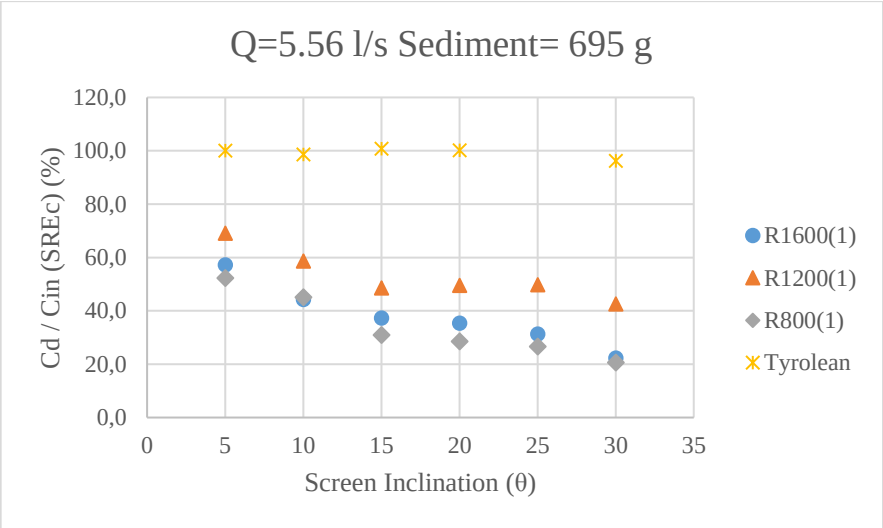

Figure 69. Effect of screen type and inclination on the dimensionless concentration value SRE_C in the case of Qin=5.56 l/s and St= 695 g

When we look for Figure 68, it is clearly seen that the Tyrolean type intake shows the poorest performance for the sediment exclusion. R1200(1) also shows slightly low performance for the SRE unlike with the case of WCP. The results show that R800(1) and R1600(1) type intakes performed similarly. This is also valid for the sediment concentration of the diverted water. In Figure 69, it is seen that the sediment concentration of the diverted water is approximately equal to 20% of the incoming sediment concentration at 30^o screen inclination.

Screen inclination affects all the types of intake structures in the same way. Increasing the value of the screen inclination increases the sediment exclusion performances namely increases the SRE. R1600(1) and R800(1) types of Coanda intake structures exclude nearly 90% of the incoming sediment at 30^o screen inclination.

4.1.2.1.2. Effect of Flow Rate

One of the important parameters which are effective on the screen performances is the incoming flow rate. As we discussed in the part of clear water experiments increasing the incoming flow rate also increases the diverted water discharge. Now, we will deal with the effects of the incoming flow rate on the sediment related parameters

such as Sediment Release Efficiency (SRE) and the dimensionless concentration values (SRE_C). Relations between the SRE and flow rates for different intakes are given in Figures 70, 71, and 72.

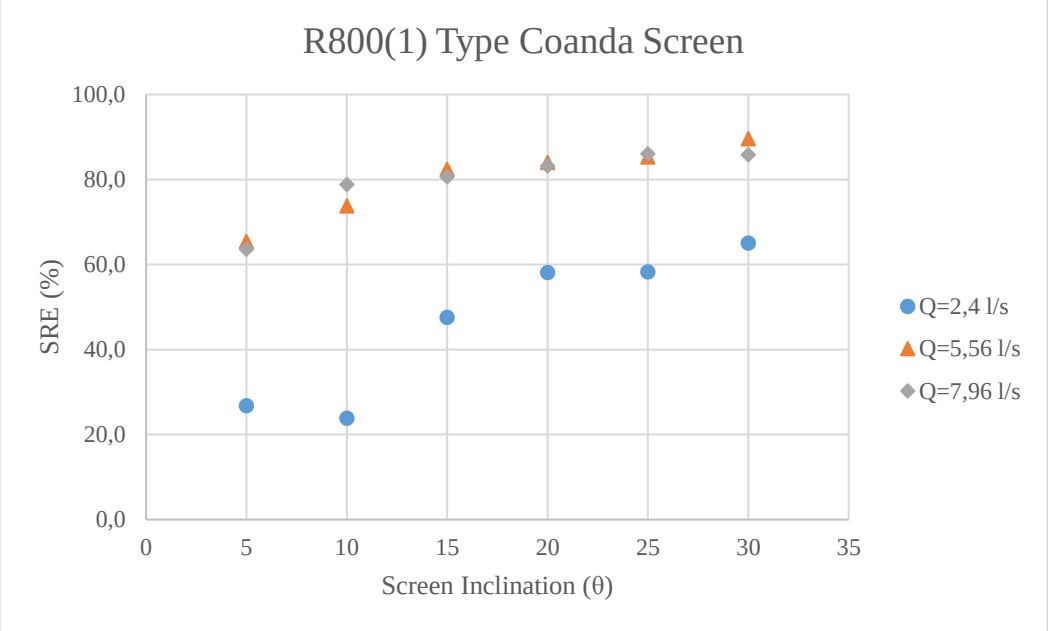

Figure 70. Effect of flow rate on the SRE for R800(1) Coanda intake

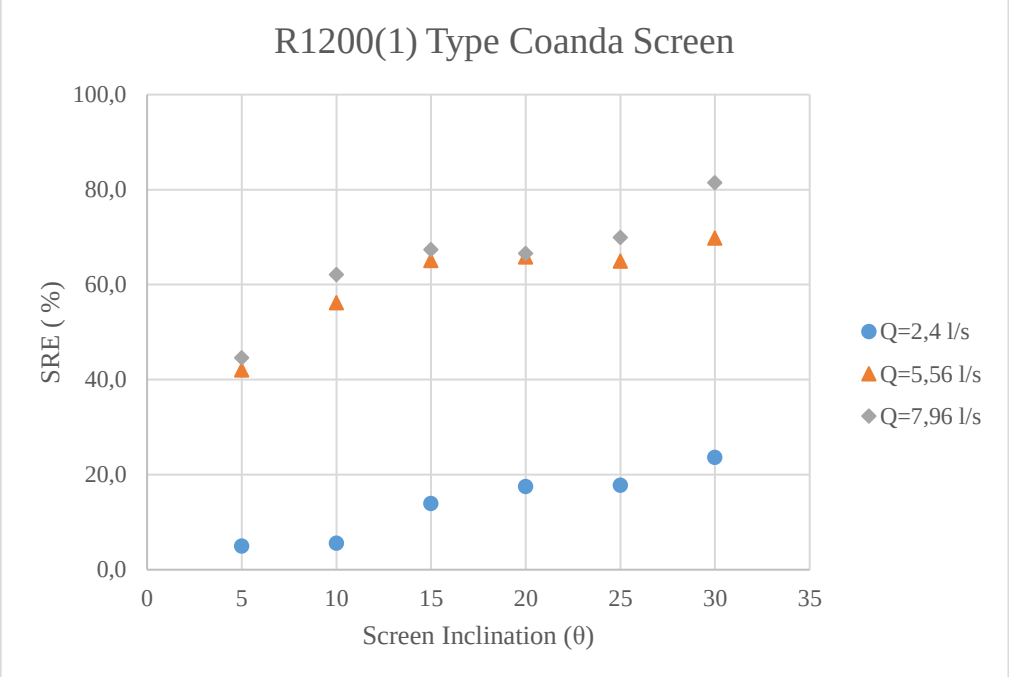

Figure 71. Effect of flow rate on the SRE for R1200(1) Coanda intake

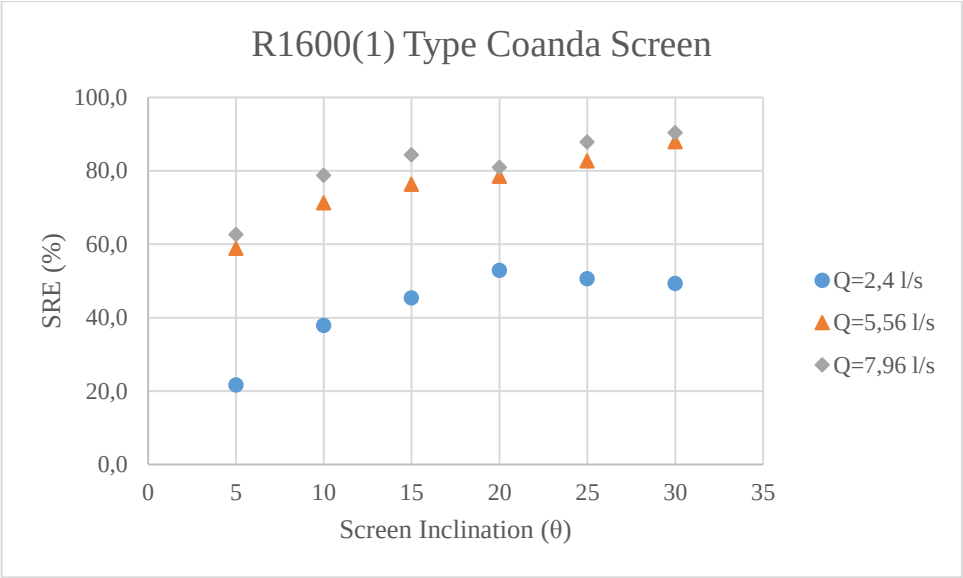

Figure 72. Effect of flow rate on the SRE for R1600(1) Coanda intake

As it is seen from the figures given above, Sediment Release Efficiencies of the intake structures increase with increasing the incoming flow rate. According to the results, intake structures show better performances at the high flow rates in the case of SRE. Similarly, the SREc (C_d /C_{in}), where C_d is the diverted flow concentration and C_{in} is main channel concentration respectively, values are also decreasing with increasing the incoming flow rate. An example of this is given in Figure 73 for the R800(1) Coanda intake structure. Summary of the results are given in Table 24.

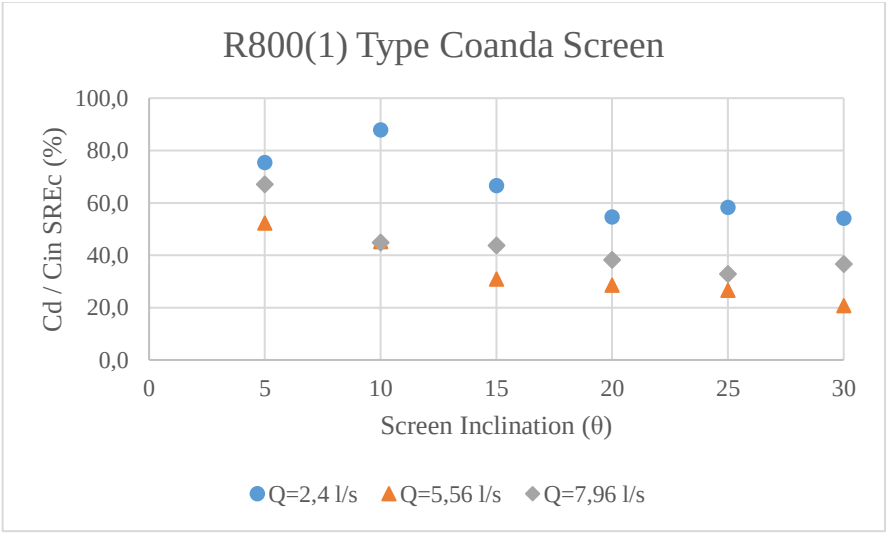

Figure 73. Effect of flow rate on Cd/Cin (SREc) for R800(1) Coanda intake

Table 24. Summary of the results

	Inclination	Q_d (l/s)	S_d (g)	SREc (%)	SRE (%)
R1600, e=1mm, Q_{in}=2.4 l/s and S_{in}=300g	5	2.27	235.0	82.8	21.7
	10	2.02	186.5	73.9	37.8
	15	2.02	164.0	65.0	45.3
	20	1.78	141.5	63.6	52.8
	25	2.08	148.3	57.0	50.6
	30	1.89	152.1	64.4	49.3
	Inclination	**Q_d (l/s)**	**S_d (g)**	**SREc (%)**	**SRE (%)**
R1600, e=1mm, Q_{in}=5.56l/s and S_{in}=695g	5	4	285.7	57.1	58.9
	10	3.61	199.5	44.2	71.3
	15	3.53	164.6	37.3	76.3
	20	3.38	149.5	35.4	78.5
	25	3.08	120.3	31.2	82.7
	30	3.01	83.8	22.3	87.9
	Inclination	**Q_d (l/s)**	**S_d (g)**	**SREc (%)**	**SRE (%)**
R1600, e=1mm, Q_{in}=7.96l/s and S_{in}=995g	5	4.81	371.7	61.8	62.6
	10	4.08	211.0	41.4	78.8
	15	3.92	155.2	31.7	84.4
	20	3.68	189.1	41.1	81.0
	25	3.38	120.5	28.5	87.9
	30	3.23	95.9	23.8	90.4

	Inclination	Q_d (l/s)	S_d (g)	SREc(%)	SRE (%)
R1200, e=1mm, Q_{in}=2.4 l/s and S_{in}=300g	5	2.40	285.2	95.1	5.0
	10	2.27	283.2	99.8	5.6
	15	2.14	258.1	96.5	14.0
	20	2.14	247.5	92.5	17.5
	25	2.18	246.7	90.5	17.8
	30	2.10	229.0	87.2	23.7
	Inclination	**Q_d (l/s)**	**S_d (g)**	**SREc (%)**	**SRE (%)**
R1200, e=1mm, Q_{in}=5.56l/s and S_{in}=695g	5	4.66	402.6	69.1	42.1
	10	4.16	304.6	58.6	56.2
	15	4.00	242.8	48.6	65.1
	20	3.84	237.7	49.5	65.8
	25	3.92	243.6	49.7	64.9
	30	3.95	209.9	42.5	69.8
R1200, e=1mm, Q_{in}=7.96l/s and S_{in}=995g	**Inclination**	**Q_d (l/s)**	**S_d (g)**	**SREc (%)**	**SRE (%)**
	5	5.16	551	85.4	44.6
	10	4.66	377.2	64.8	62.1
	15	4.49	324.6	57.8	67.4

(Cont. on the next page)

	20	4.36	332.8	61.1	66.6
	25	4.31	299.14	55.5	69.9
	30	3.62	184.5	40.8	81.5
R800, e=1mm, Q_{in}=2.4 l/s and S_{in}=300g	**Inclination**	**Q_d (l/s)**	**S_d (g)**	**SREc (%)**	**SRE (%)**
	5	2.33	219.6	75.4	26.8
	10	2.08	228.3	87.8	23.9
	15	1.89	157.3	66.6	47.6
	20	1.84	125.6	54.6	58.1
	25	1.72	125.2	58.2	58.3
	30	1.55	104.7	54.0	65.1
R800, e=1mm, Q_{in}=5.56l/s and S_{in}=695g	**Inclination**	**Q_d (l/s)**	**S_d (g)**	**SREc (%)**	**SRE (%)**
	5	3.68	240.2	52.2	65.4
	10	3.23	182.1	45.1	73.8
	15	3.16	121.9	30.9	82.5
	20	3.11	110.84	28.5	84.1
	25	3.08	102.2	26.5	85.3
	30	2.80	72.2	20.6	89.6
R800, e=1mm, Q_{in}=7.96l/s and S_{in}=995g	**Inclination**	**Q_d (l/s)**	**S_d (g)**	**SREc (%)**	**SRE (%)**
	5	4.32	361.7	67.0	63.7
	10	3.76	210.6	44.8	78.8
	15	3.53	192.8	43.7	80.6
	20	3.50	167.0	38.2	83.2
	25	3.38	138.6	32.8	86.1
	30	3.08	141.0	36.6	85.8

4.1.2.1.3. Effect of Bar Spacing

For the investigation of the effect of void ratio on sediment release efficiency, 3 different Coanda type intakes having a curvature radius of R=800 mm with different bar spacing and 2 different Coanda type intakes having a curvature radius of R=1600 mm with different bar spacing were manufactured and used in the experiments. Examples for a relation between the SRE and void ratio of the R800 and R1600 type Coanda intakes are given in Figure 74.

Results show that the void ratio directly affects the SRE performance of the screens. Unlike with the case of WCP, the SRE decreasing with increasing the void ratio. It is also important to remember that in these studies the used sediment diameters ranges in between 0.71 and 1 mm which is equal and smaller than the bar spacing of 1 mm and smaller than 2 mm, and 3 mm bar spacing.

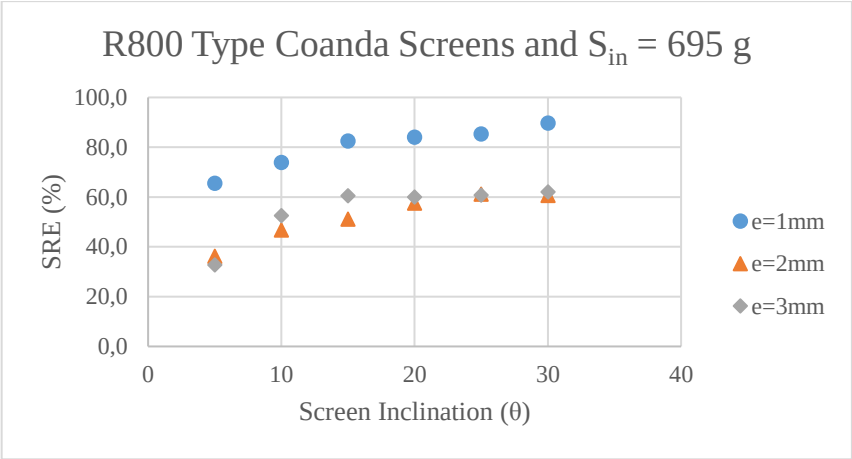

Figure 74. Effect of void ratio on SRE for R800 type Coanda intakes

1 mm bar spacing allows excluding 89.6% of total sediment while the 2 mm and 3 mm bar spacings allow excluding approximately 60% of total sediment at 30^{o} screen inclination case. In the worst case, the screen which has 1 mm bar spacing excludes 65% of the total sediment while the other screens which have 2 mm and 3 mm bar spacings could only exclude 36.2% and 32.7% of total sediment. The Figure shows that the SRE performances of the screens that have 2 mm and 3 mm bar spacing are close to each other. The reason for this is the sediment diameter that was used in the experiments, Because, the sediment diameter is between the 0.71 mm – 1 mm, there is a significant difference between the performance of the screens that has 1 mm bar spacing and the others.

One of the other important topic that must be clarified is relation between the bar spacing and the void ratio. As it was mentioned before the void ratio (m) is the ratio of the total opening of the screen to the total area of the screen, so there is a directly relation between the bar opening and the void ratio. We can use the void ratio instead of bar spacing in Figure 74, but it is important to remind that changing the bar spacing is not the only way to change the void ratio. The void ratio can be changed also changing the width of the sloths and on account of the number of sloths (bars) that is used in the screen. In our models, the number of the sloths remained constant for all the screens which have 1 mm, 2 mm, and 3 mm. Therefore, only the sloth widths were changed to obtain different bar openings instead of changing the number of sloths with remained constant as the 1 mm spacing. Because of this we plot the Figure 74 by considering the bar spacing instead of void ratio. Summary of the results related with the bar spacing and void ratio are given in Table 25.

Table 25. Summerized results related with bar spacing and void ratio

	Inclination	Q_d (l/s)	S_d (g)	SREc (%)	SRE (%)
R800, e=1mm, Q_{in}=2.4 l/s and S_{in}=300g	5	2.33	219.6	75.4	26.8
	10	2.08	228.3	87.8	23.9
	15	1.89	157.3	66.6	47.6
	20	1.84	125.6	54.6	58.1
	25	1.72	125.2	58.2	58.3
	30	1.55	104.7	54.0	65.1
R800, e=2mm, Q_{in}=2.4 l/s and S_{in}=300g	**Inclination**	**Q_d (l/s)**	**S_d (g)**	**SREc (%)**	**SRE (%)**
	5	2.4	295.6	98.5	1.5
	10	2.37	289.2	97.6	3.6
	15	2.27	284.0	100.1	5.3
	20	2.2	271.4	98.7	9.5
	25	2.14	254.8	95.3	15.1
	30	2.13	239.0	89.8	20.3
R800, e=3mm, Q_{in}=2.4 l/s and S_{in}=300g	**Inclination**	**Q_d (l/s)**	**S_d (g)**	**SREc (%)**	**SRE (%)**
	5	2.40	286.4	95.5	4.5
	10	2.40	299.0	99.7	0.3
	15	2.27	292.4	103.0	2.5
	20	2.25	269.3	95.8	10.2
	25	2.25	261.3	92.9	12.9
	30	2.20	241.7	87.9	19.4
R800, e=1mm, Q_{in}=5.56 l/s and S_{in}=695g	**Inclination**	**Q_d (l/s)**	**S_d (g)**	**SREc (%)**	**SRE (%)**
	5	3.68	240.2	52.2	65.4
	10	3.23	182.1	45.1	73.8
	15	3.16	121.9	30.9	82.5
	20	3.11	110.8	28.5	84.1
	25	3.08	102.2	26.5	85.3
	30	2.8	72.2	20.6	89.6
R800, e=2mm, Q_{in}=5.56 l/s and S_{in}=695g	**Inclination**	**Q_d (l/s)**	**S_d (g)**	**SREc (%)**	**SRE (%)**
	5	4.32	443.7	82.2	36.2
	10	4.08	369.8	72.5	46.8
	15	3.98	339.95	68.3	51.1
	20	3.68	295.2	64.2	57.5
	25	3.61	270.0	59.8	61.2
	30	3.45	274.0	63.5	60.6
R800, e=3mm, Q_{in}=5.56 l/s and S_{in}=695g	**Inclination**	**Q_d (l/s)**	**S_d (g)**	**SREc (%)**	**SRE (%)**
	5	4.83	468.0	77.5	32.7
	10	4.49	330.1	58.8	52.5
	15	4.16	275.0	52.9	60.4
	20	4.08	278.0	54.5	60.0
	25	4.00	272.5	54.5	60.8
	30	3.97	264.2	53.2	62.0

(Cont. on the next page)

	Inclination	Q_d (l/s)	S_d (g)	SREc (%)	SRE (%)
R800, e=1mm, Q_{in}=7.96 l/s and S_{in}=995g	5	4.32	361.7	67.0	63.7
	10	3.76	210.6	44.8	78.8
	15	3.53	192.8	43.7	80.6
	20	3.50	167.0	38.2	83.2
	25	3.38	138.6	32.8	86.1
	30	3.08	141.0	36.6	85.8
R800, e=2mm, Q_{in}=7.96 l/s and S_{in}=995g	**Inclination**	**Q_d (l/s)**	**S_d (g)**	**SREc (%)**	**SRE (%)**
	5	5.63	565.0	80.3	43.2
	10	4.83	460.2	76.2	53.8
	15	4.66	382.9	65.7	61.5
	20	4.62	356.0	61.6	64.2
	25	4.49	346.2	61.7	65.2
	30	4.32	372.3	68.9	62.6
R800, e=3mm, Q_{in}=7.96 l/s and S_{in}=995g	**Inclination**	**Q_d (l/s)**	**S_d (g)**	**SREc (%)**	**SRE (%)**
	5	5.91	569.2	77.0	42.8
	10	5.18	407.0	62.9	59.1
	15	5.00	330.5	52.9	66.8
	20	4.92	386.3	62.8	61.2
	25	4.92	354.9	57.7	64.3
	30	4.81	299.9	49.9	69.9
R1600, e=1mm, Q_{in}=2.4 l/s and S_{in}=300g	**Inclination**	**Q_d (l/s)**	**S_d (g)**	**SREc (%)**	**SRE (%)**
	5	2.27	235.0	82.8	21.7
	10	2.02	186.5	73.9	37.8
	15	2.02	164.0	65.0	45.3
	20	1.78	141.5	63.6	52.8
	25	2.08	148.3	57.0	50.6
	30	1.89	152.1	64.4	49.3
R1600, e=2mm, Q_{in}=2.4 l/s and S_{in}=300g	**Inclination**	**Q_d (l/s)**	**S_d (g)**	**SREc (%)**	**SRE (%)**
	5	2.40	288.9	96.3	3.7
	10	2.27	285.4	100.6	4.9
	15	2.14	251.2	93.9	16.3
	20	2.14	231.8	86.7	22.7
	25	2.11	223.0	84.5	25.7
	30	2.10	208.3	79.4	30.6
R1600, e=1mm, Q_{in}=5.56 l/s and S_{in}=695g	**Inclination**	**Q_d (l/s)**	**S_d (g)**	**SREc (%)**	**SRE (%)**
	5	4.00	285.7	57.1	58.9
	10	3.61	199.5	44.2	71.3
	15	3.53	164.6	37.3	76.3
	20	3.38	149.5	35.4	78.5
	25	3.08	120.3	31.2	82.7
	30	3.01	83.8	22.3	87.9

(Cont. on the next page)

	Inclination	Q_d (l/s)	S_d (g)	SREc (%)	SRE (%)
R1600, e=2 mm, Q_{in}=5.56 l/s and S_{in}=695g	5	4.08	328.7	64.5	52.7
	10	3.68	235,8	51.3	66.1
	15	3.53	193.1	43.8	72.2
	20	3.45	182.0	42.2	73.8
	25	3.42	174.7	40.9	74.9
	30	3.38	163.4	38.7	76.5
	Inclination	**Q_d (l/s)**	**S_d (g)**	**SREc (%)**	**SRE (%)**
R1600, e=1 mm, Q_{in}=7.96 l/s and S_{in}=995g	5	4.81	371.7	61.8	62.6
	10	4.08	211.0	41.4	78.8
	15	3.92	155.2	31.7	84.4
	20	3.68	189.1	41.1	81.0
	25	3.38	120.5	28.5	87.9
	30	3.23	95.9	23.8	90.4
	Inclination	**Q_d (l/s)**	**S_d (g)**	**SREc (%)**	**SRE (%)**
R1600, e=2 mm, Q_{in}=7.96 l/s and S_{in}=995g	5	4.83	456.9	75.7	54.1
	10	4.24	292.6	55.2	70.6
	15	4.08	237.7	46.6	76.1
	20	4.08	264.7	51.9	73.4
	25	4.0	235.16	47.0	76.4
	30	3.98	196.0	39.4	80.3

4.1.2.1.4. Results for Tyrolean Type Intake

In sediment related studies only one Tyrolean type intake which has 1 mm bar spacing was used. Experiments were performed under the incoming flow of 2.4 l/s and 5.56 l/s. According to the results, the SRE performance of the Tyrolean intake increases with increasing the screen inclination. The graph that is given in Figure 75 shows that the relation between the screen inclination, flow rate, and SRE performance. Maximum SRE performance was obtained at 30^o screen inclination. However, when we compare the results with the Coanda intakes, it is clearly seen that Tyrolean intake shows the worst performance among them as can be seen in Figure 76. According to Figure 75, changing the incoming flow rate does not affect the SRE performance directly. When we looked for the concentration case, concentration on the diverted flow is very close to the incoming flow concentration or greater than that value. The relation between the dimensionless concentration value SRE_C for Tyrolean intake is given in Figure 77.

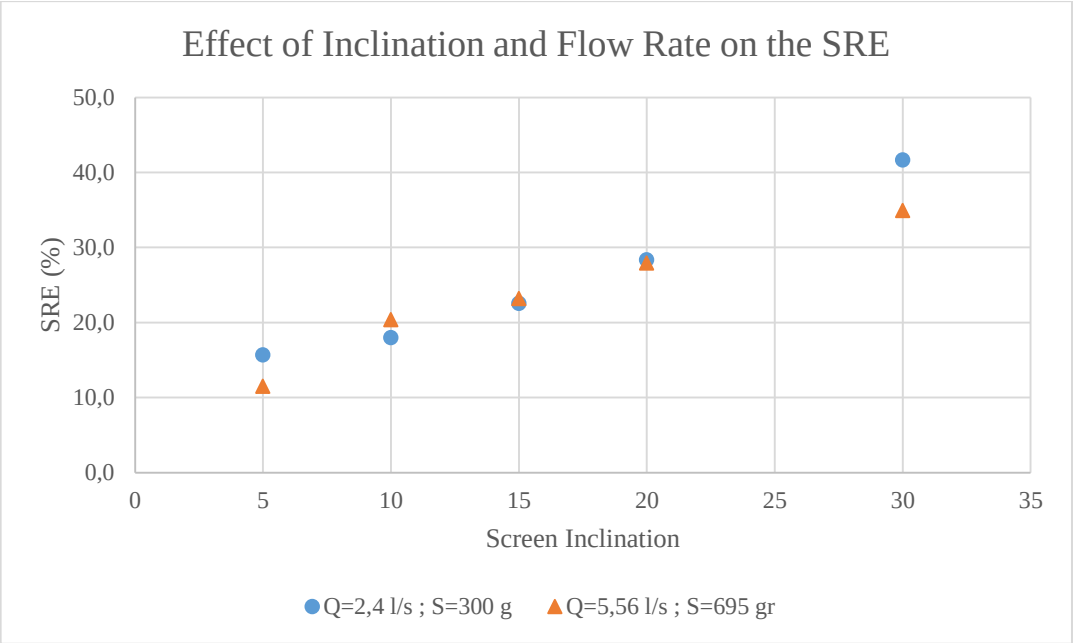

Figure 75. SRE performance of Tyrolean intake based on screen inclination and flow rate

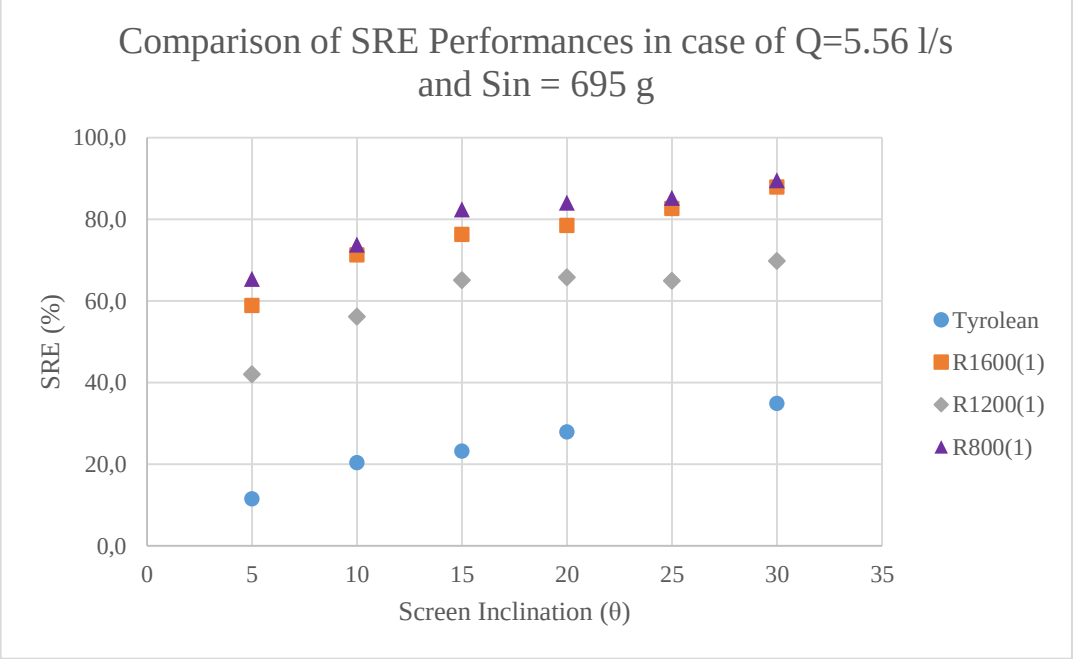

Figure 76. Comparison of SRE performances of Tyrolean and Coanda Type Intakes

All the results that were gathered from the Tyrolean intake experiments are summarized in Table 26.

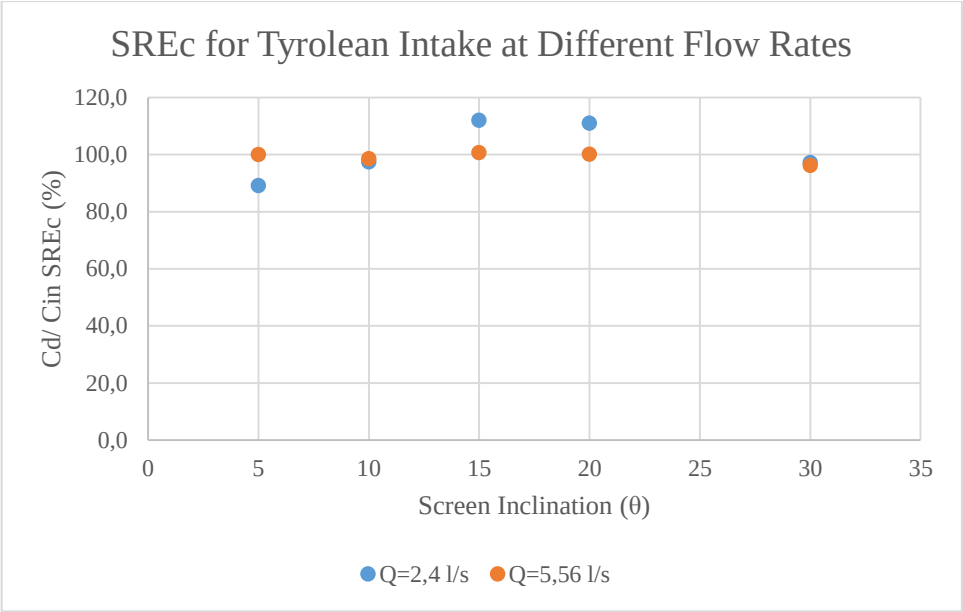

Figure 77. SREc (Cd / Cin) values for the Tyrolean type intakes in case of different flow rates and screen inclinations

Table 26. Summerized results for Tyrolean intake

Screen Inclination	Q = 2.4 l/s		Q = 5.56 l/s	
	SRE (%)	SREc (%)	SRE (%)	SREc (%)
5	15.7	89.2	11.5	100.0
10	18.0	97.4	20.4	98.6
15	22.5	112.0	23.2	100.7
20	28.3	111.0	27.9	100.2
30	41.7	97.2	34.9	96.3

4.1.2.2. Results from Uniform Sediment Distribution Studies in Case of Constant Sediment Mass and Constant Incoming Flow

In the previous part of this presented study, the sediment related studies that were performed under the inflow of constant sediment concentration have been analyzed and discussed. In this part, we will discuss the results that were obtained for the constant sediment amount.

In order to perform constant sediment experiments, two different incoming flow rates that are 2.4 l/s and 5.56 l/s were used. During the experiments, 300 g sediment was fed into the main channel. The feeding time took 30 s in all experiments. In that part, some graphs will be given as an example and all the results will be given as tables. Comparison of the results for the fixed sediment mass is given in Table 27.

Table 27. Comparison for results of fixed concentration and fixed mass

	Screen Inclination	**R1600(1) SRE (%)**	**R1200(1) SRE (%)**	**R800(1) SRE (%)**	**Tyrolean SRE (%)**
Q_{in} = 2.4 l/s and S_{in} = 300 g	5	21.7	5.0	26.8	15.7
	10	37.8	5.6	23.9	18.0
	15	45.3	14.0	47.6	22.5
	20	52.8	17.5	58.1	28.3
	25	50.6	17.8	58.3	
	30	49.3	23.7	65.1	41.7
	Screen Inclination	**R1600(1) SRE (%)**	**R1200(1) SRE (%)**	**R800(1) SRE (%)**	**Tyrolean SRE (%)**
Q_{in} = 5.56 l/s and S_{in} = 300 g	5	61.4	41.7	63.9	8.8
	10	72.0	57.3	72.3	13.3
	15	74.4	65.1	80.7	20.3
	20	80.6	66.9	84.6	24.4
	25	85.9	70.8	87.5	
	30	90.3	78.2	86.3	36.5
	Screen Inclination	**R1600(1) SRE (%)**	**R1200(1) SRE (%)**	**R800(1) SRE (%)**	**Tyrolean SRE (%)**
Q_{in} = 5.56 l/s and S_{in} = 695 g	5	58.9	42.1	65.4	11.5
	10	71.3	56.2	73.8	20.4
	15	76.3	65.1	82.5	23.2
	20	78.5	65.8	84.1	27.9
	25	82.7	64.9	85.3	
	30	87.9	69.8	89.6	34.9

As can be seen from Table 27, it is clearly seen that the SRE performance of the Coanda screens increases with increasing the flow rate when the sediment mass is fixed. However, this is not valid for the Tyrolean type intake. Unlike with this situation, when

the incoming flow is constant and the sediment mass that is fed to the main channel is increased from 300 g to 695 g, the SRE performances of the screens do not show any significant change.

4.1.2.3. Results Obtained from Sediment Composition Studies

In order to see the effect of sediment composition on screen performance, 4 different sediment compositions were prepared. Sediment sizes that were used in the compositions range in between 0.5 mm to 2 mm. Experiment for compositon-1 was performed under 5.56 l/s and 7.96 l/s incoming flow rates and 695 g sediment was fed to the system. Experiments for compositions (2, 3, and 4) were performed under 5.56 l/s and 7.96 l/s incoming flow rates and 800 g sediment was fed to the main channel. R800(1) type Coanda screen was used during these experiments. In addition, because the previous results show that the best performances for SRE are obtained at the steeper screen slopes, the experiments were performed for 20^o, 25^o, and 30^o screen inclinations.

4.1.2.3.1. Sediment Composition – 1

In the case of the sediment composition – 1, the ratio of the sediment groups in the composition was selected randomly. Results for the experiment of sediment composition – 1 is given in Table 28.

Table 28. Results of the R800(1) type Coanda intake for sediment composition - 1

Sediment Group	0.5 – 0.71		0.71 – 1		1 – 1.7		1.7 – 2	
Screen Slope	Excluded Sed. (g)	SRE (%)	Excluded Sed. (g)	SRE (%)	Excluded Sed. (g)	SRE (%)	Excluded Sed. (g)	SRE (%)
20	81.3	62.5	257.5	85,8	193.9	97	64.9	99.8
25	87.6	67.4	265.3	88.4	195.8	98	64.85	99.8
30	93.4	71.8	269,2	89.7	195.6	97.8	64.82	99.7

The purpose of using 695 g sediment is comparing the results with uniform sediment experiment results. The results will be compared in Table 29. As can be seen in Table 29, the SRE performances are similar for both type experiments.

Table 29. Comparison of Results for R800(1) type intake in case of the uniform and composition sediment experiments

Screen Inclination	Sediment Composition Experiment		Uniform Sediment Experiment	
	Tot. excl. sed. (g)	SRE (%)	Tot. excl. sed. (g)	SRE (%)
20	597.6	86.0	584.2	84.1
25	613.6	88.3	592.8	85.3
30	623.0	89.6	622.8	89.6

This sediment composition – 1 experiment is also repeated for the R1600(1) type Coanda intake. The detailed results for the sediment groups forming the sediment composition are given in Table 30.

Table 30. Results of the R1600(1) type Coanda intake for sediment composition - 1

Sediment Group	0.5 – 0.71		0.71 – 1		1 – 1.7		1.7 – 2	
Screen Slope	Excluded Sed. (g)	SRE (%)	Excluded Sed. (g)	SRE (%)	Excluded Sed. (g)	SRE (%)	Excluded Sed. (g)	SRE (%)
20	82.8	63.7	263.2	87.7	195.1	97.5	64.8	99.7
25	86.6	66.6	263.1	87.7	194.9	97.5	64.7	99.6
30	93.7	72.1	273.0	91.0	196.4	98.2	64.8	99.6

As it can be seen from the results, it is clear that the SRE performance of the R800(1) type Coanda intake and R1600(1) type intake is similar. Table 31 shows that the comparison of the results obtaining from the experiments of uniform sediment and experiments of composition – 1 for R1600(1) type Coanda intake. Similar with the R800(1) type Coanda intake, R1600(1) screen showed good performances and exclude approximately 90% of the total sediment.

Table 31. Comparison of results for 1600(1) type intake in case of the uniform and composition sediment experiments

Screen Inclination	Sediment Composition Experiment		Uniform Sediment Experiment	
	Tot. excl. sed. (g)	SRE (%)	Tot. excl. sed. (g)	SRE (%)
20	605.8	87.2	545.5	78.5
25	609.4	87.7	574.7	82.7
30	627.9	90.3	611.2	87.9

4.1.2.3.2. Sediment Composition – 2

In the case of sediment composition – 2, all the particle groups in the sediment composition are adjusted so that their weights are equal to each other. Because, the details of the compositions have been given in Chapter 3, here only the results will be given. The results of Sediment Composition – 2 are given in Table 32 and Table 33.

Table 32. Results of the R800(1) type Coanda intake in case of composition - 2

Sediment Group	0.5 – 0.71		0.71 – 1		1 – 1.7		1.7 – 2	
Screen Slope	Excluded Sed. (g)	SRE (%)	Excluded Sed. (g)	SRE (%)	Excluded Sed. (g)	SRE (%)	Excluded Sed. (g)	SRE (%)
20	122.8	61.4	160.3	80.2	194.0	97.0	199.61	99.8
25	136.5	68.2	168.07	84.0	194.5	97.2	199.56	99.8
30	145.7	72.8	176.88	88.4	196.0	98.0	199.72	99.9

Half of the amount of sediment used in the sediment composition experiment is designed to pass through the gaps between the screen bars. According to the results, the screen shows the best performances at 30^{o} screen inclination for all sediment group cases. The screen even shows good performance for removing the sediment which has a smaller diameter than the opening between the screen bars. Screen exclude 72.8% of the sediment group of (0.5 – 0.71) and also exclude 88.4% of the sediment group of (0.71 – 1). In

addition, approximately all of the sediment which has a diameter that greater than the screen opening is excluded from the screen. During the experiments, any serious clogging effect which affects the WCP is not observed. When we consider the total excluded sediment case, the screen excludes nearly 90% of the sediment.

Table 33. Results for the R800(1) type Coanda intake in case of total excluded sediment

Screen Inclination	Total Excluded Sediment	
	Excluded Sediment (g)	SRE (%)
20	676.8	84.6
25	698.6	87.3
30	718.2	89.8

4.1.2.3.3. Sediment Composition – 3

In the case of sediment composition – 3, the sediment size that is smaller than 1 mm bar opening is increased from 50% to 75% for investigating the effect of finer sediment on the bar opening. The results of the experiments are given in Table 34 and Table 35.

Table 34. Results of the R800(1) type Coanda intake in case of composition - 3

Sediment Group	0.5 – 0.71		0.71 – 1		1 – 1.7		1.7 – 2	
Screen Slope	Excluded Sed. (g)	SRE (%)	Excluded Sed. (g)	SRE (%)	Excluded Sed. (g)	SRE (%)	Excluded Sed. (g)	SRE (%)
20	191.7	63.9	243.7	81.2	95.4	95.4	99.8	99.8
25	206.2	68.7	261.0	87.0	97.9	97.9	99.8	99.8
30	224.3	74.8	261.1	87.0	97.6	97.6	99.8	99.8

Although the summation of the sediment groups of (0.5 – 0.71) and (0.71 – 1) are increased to 75%, the screen shows good performance for sediment exclusion. When, we

compare the SRE performances of this study with the SRE performances of composition – 2, it is seen that the screen shows similar results. This means that even the sediment diameters are equal to half of the bar opening, the screen can exclude up to 75% of this sediment for 30^o screen inclination. When the sediment diameters approach to the bar opening distance, the exclusion rate of the sediment increases. If the sediment diameter is greater than the bar opening, the sediment exclusion performance which is also named as SRE performance almost increases to 100%.

Table 35. Results for the R800(1) type Coanda intake in case of total excluded sediment

Screen Inclination	Total Excluded Sediment	
	Excluded Sediment (g)	SRE (%)
20	630.6	78.8
25	664.9	83.1
30	682.7	85.3

Table – 35 shows that the screen excludes 85.3 % of the total sediment at the 30^o screen inclination. When we compare the results which are gathering from the composition experiments, the screen shows similar performances for the total excluded sediment and SRE.

4.1.2.3.4. Sediment Composition – 4

For the case of composition – 4 experiments, the ratio of the sediment groups of (0.5 – 0.71) and (0.71 - 1) to the total sediment was kept at 75% similar with the previous example. However, the ratio of the (0.71 – 1) group of sediment in the mixture is decreased, while the ratio of the (0.5 – 0.71) group of sediment in the mixture is increased. In this way, the d_{50} of the mixture is reduced to 0.70 mm. This d_{50} value was 0.80 mm for the case of sediment composition – 3 and 1 mm for sediment composition – 2. The sediment distribution curves of the sediment mixture groups have been given in Conducting Experiment part which is the sub caption of Chapter 3.

Results for sediment groups is given in Table 36 and results for total sediment composition is given in Table 37. According to the results, the screen shows similar performances with the previous sediment composition experiments for the case of each individual sediment groups and total sediment composition. Like with the previous examples the screen shows better SRE performances with increasing the screen slope.

Table 36. Results for individual sediment groups in the composition – 4

Sediment Group	0.5 – 0.71		0.71 – 1		1 – 1.7		1.7 – 2	
Screen Slope	Excluded Sed. (g)	SRE (%)	Excluded Sed. (g)	SRE (%)	Excluded Sed. (g)	SRE (%)	Excluded Sed. (g)	SRE (%)
20	265.4	66.4	154.5	77.3	94.5	94.5	99.6	99.6
25	290.8	72.7	167.9	84.0	98.1	98.1	99.8	99.8
30	292.0	73.0	176.0	88.0	98.3	98.3	99.9	99.9

Table 37. Results for sediment composition - 4 in case of total sediment

Screen Inclination	Total Excluded Sediment	
	Excluded Sediment (g)	SRE (%)
20	614.1	76.8
25	656.6	82.1
30	666.1	83.3

Even the screen shows similar performances for all sediment composition cases, it can be said that decreasing the amount of sediment group which has smaller diameter than the space between the screen bars, the general SRE performances of the intake structure increases. SRE_C is a dimensionless parameter and it is the ratio of the diverted concentration to the incoming flow concentration. Because the less concentration in the diverted water is desired, best performance is obtained from sediment composition – 1 in case of total sediment. The effect of sediment compositions on the SRE is given in Figure 78 and the effect of sediment compositions on the SRE_C is given in Figure 79 for the total amount of sediment.

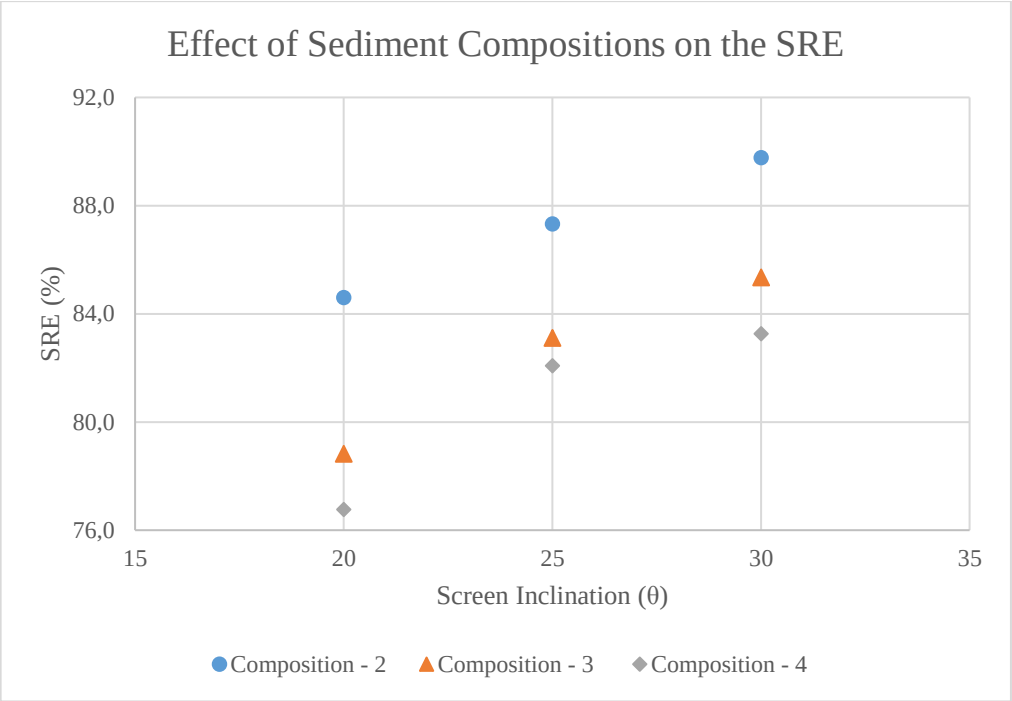

Figure 78. Comparison for Sediment Release Efficiency of R800(1) type Coanda intake for different sediment composition cases

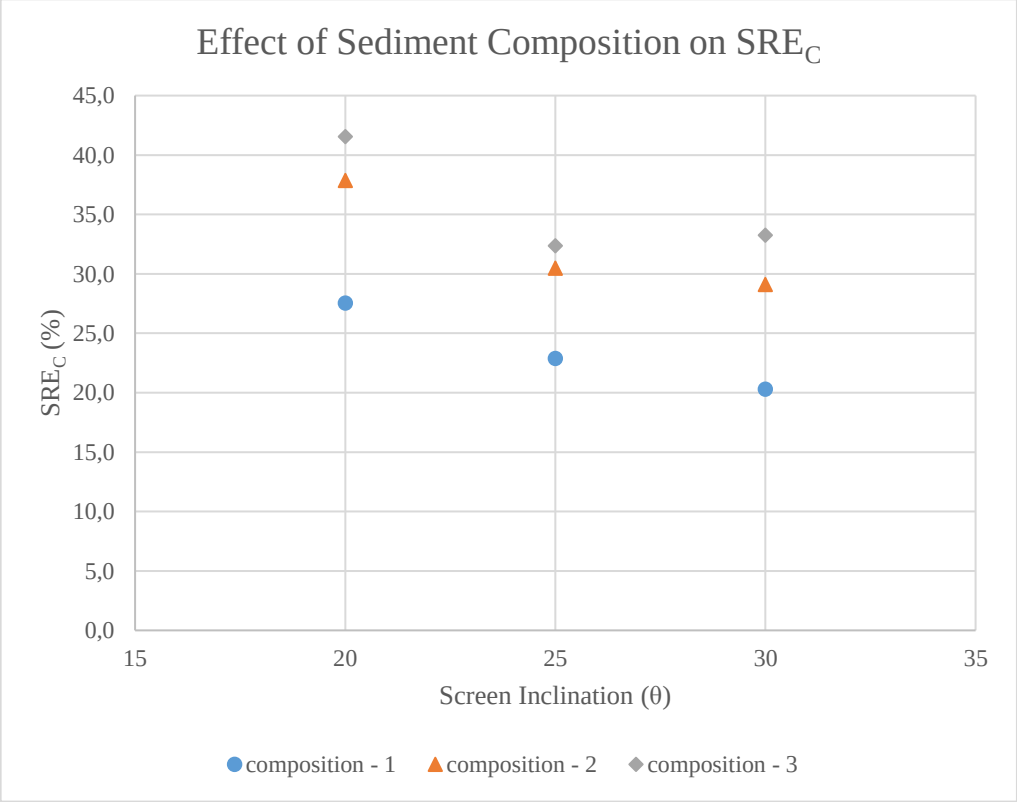

Figure 79. Effect of sediment composition on the SRE$_C$ for R800(1) type Coanda intake

CHAPTER 5

ANALYSIS METHODS

In the previous part, the effect of the screen features and flow conditions such as screen inclination, void ratio, screen curvature radius, and incoming flow rate and their effects on the screen performances were examined and discussed. In this part, we deal with the statistical analysis to obtain equations for the WCP and SRE performances of the screens using the data which are obtained from the experimental studies. In addition to this, the relation of important dimensionless parameters which are called the Froude number based on screen opening (Fr_e) and Qd/Qin will be investigated. First, we start with the statistical analysis of Water Capture Performance (WCP) for both Coanda and Tyrolean intakes. After than statistical analysis for Sediment Release Efficiency (SRE) for Coanda intakes will be investigated.

5.1. Dimensional Analysis

As mentioned earlier, there are two basic mechanisms, the shearing effect and orifice effect, which cause the incoming flow to be directed through the screen to the collecting channel. The first mechanism is that the screen bars placed perpendicular to the flow direction are bent with an angle which is also called wire tilt angle. This design causes a projection at the base layer of the flow and directs the flow downward with the shear effect. This shear effect primarily depends on the screen inclination and the velocity of the flow passing through the screen.

The second mechanism is the orifice effect, as it is mentioned earlier. The pressure of the water to the bottom causes water to pass through the gaps between the screen bars. It is known that the thickness of the water layer on the screen is directly proportional to the pressure at the bottom. The orifice effect also depends on the void ratio. Another factor that enhances the orifice effect is the curved design of the Coanda intakes. Here,

the pressure on the screen surface increases with the effect of the centrifugal force and causes an increase in the amount of water that is diverted by the screen.

Both mechanisms act simultaneously to different degrees depending on the properties of the screen surface and flow on the screen. In order to reveal which mechanism will be characterized by which dimensionless parameter, all the effective dimensional independent parameters are listed below in Equation 5.1. Here A denotes any dependent dimensional variable f denotes a general function.

$$A=f\{\alpha, \theta, R,h_0,p,Q_t,L,a,e,V,g,\rho,\rho_s,\upsilon,\sigma,d_{50},\sigma_D\} \tag{5.1}$$

Where;

α = wire tilt angle, θ = screen slope, R = screen curvature radius, h_0 = flow depth at the beginning of the screen, p = accelerator plate height, Q_t = total incoming flow, L = screen length, a = distance between centerline of the two consecutive bars, e = gap distance between two consecutive bars, V = velocity of incoming flow at the beginning of the screen, g = gravitational acceleration, ρ = density of water, ρ_s = density of sediment, υ = kinematic viscosity, σ = surface tension, d_{50} = median of the sediment diameter, σ_D = uniformity coefficient.

Since the Q_t can be calculated as a function of flow depth and flow velocity it can be subtracted from Equation 5.1. Similarly, viscosity can be neglected in case of turbulent flow, as it is often seen in nature. In this case, Equation 5.2 can be written with the parameters at hand.

$$A=f\{\alpha, \theta, R,h_0,p,L,a,e,V,g,\rho,\rho_s,\sigma,d_{50},\sigma_D\} \tag{5.2}$$

If R is chosen for the geometric variable, V is chosen for kinematic variable and ρ is chosen for the dynamic variable as repeating parameters and the Vaschy-Buckingham theorem is applied, Equation 5.3 can be written as given below.

$$\pi(A)=f\left\{\alpha,\theta,\frac{h_0}{R},\frac{p}{R},\frac{L}{R},\frac{a}{R},\frac{e}{R},\frac{V}{\sqrt{gR}},\frac{\rho_s}{\rho},\frac{\rho V^2 R}{\sigma},\frac{d_{50}}{R}\right\} \quad (5.3)$$

Since the sediment type to be used in the experiments will not change, ρs/ ρ can be taken as a constant. When the dimensionless parameters are rearranged, the following Equation 5.4 can be reached. Dimensionless parameters affecting flow on the Coanda screen are given in Table 38.

$$\pi(A)=f\left\{\alpha,\theta,\frac{ho}{R},\frac{p}{R},\frac{L}{R},\frac{a}{R},\frac{e}{R},\frac{V}{\sqrt{gR}},\frac{\rho V^2 R}{\sigma},\frac{d50}{R}\right\} \quad (5.4)$$

Table 38. Dimensionless parameters affecting flow on Coanda Screen

Dimensionless Parameters	Description
α	Wire tilt angle
θ	Screen slope
p / R	The ratio of accelerator plate to screen curvature
L / R	The ratio of screen length to the screen curvature
a / e	Void ratio
e / R	Ratio of the bar opening to curvature radius
$Fr = \frac{V}{\sqrt{g.ho}}$	Froude number
$Fr_R = \frac{V}{\sqrt{g.R}}$	Froude number based on screen curvature
$We = \frac{\rho V^2 R}{\sigma}$	Weber number
d_{50} / h_0	Relative porosity

Any dimensional and dependent parameter to be examined within the scope of this study, such as Water Capturing Performance (WCP), can be written in terms of dimensionless independent parameters as given in Equation 5.5. Dependent dimensionless parameters are listed in Table 39.

$$\pi(Qi)=\frac{Qi}{Qt}=f\left\{\alpha,\ \theta,\ \frac{p}{R},\ \frac{L}{R},\ \frac{a}{e},\frac{e}{R},\frac{V}{\sqrt{g.h_0}},\ \frac{V}{\sqrt{g.R}},\frac{\rho V^2 R}{\sigma},\ \frac{d_{50}}{h_0}\right\} \tag{5.5}$$

Table 39. Dependent dimensionless parameters on Coanda screen

Dimensionless Parameters	Explanation
$WCP = \frac{Qi}{Qt}$	Water Capturing Performance
$SRE = \frac{Si}{St}$	Sediment Release Efficiency

Qi = withdrawn water discharge

Si = withdrawn sediment amount with water

Qt = total water discharge

St = total sediment amount in the main channel

5.1.1. Froude Number Based on Bar Opening (Fr_e)

Following this analysis, a non-dimensional parameter, square of the Froude number based on bar opening, Fr_e is calculated by Equation 5.7.

$$Fre = \sqrt{\frac{\left(\frac{Qi}{L}\right)^2}{e^3.g}} \tag{5.7}$$

Where Q_i is the approaching flow rate, L is the width of the rack, e is the bar spacing and g is the gravitational acceleration.

Values of Froude number based on bar opening are plotted against nondimensionalized diverted discharge for various rack angles. In this study, the data

obtained from the R800(1), R800(2), and R800(3) are used to plot the graph. Figure - 80 shows that for lower (approximately 50) diverted discharge reaches maximum values and decreases as the increases. Also, it can be concluded from studies that, for the rack angles greater than 15 degrees, the rack angle did not have a significant effect on the results. These can be seen in Figure – 80 with more details.

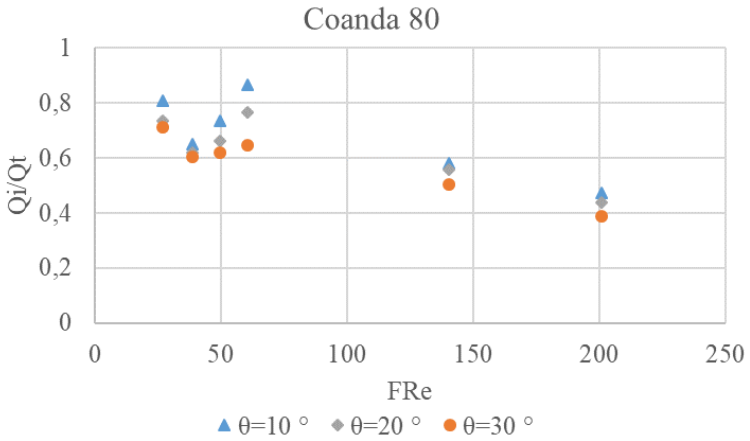

Figure 80. Variation of diverted discharge ratios with Froude numbers based on bar opening for three different rack angles.

5.2. Analysis of Experimental Data by Multiple Linear Regression

Using the data from the previously published studies and results gathered from experiments of this presented study, the Water Capture Performance for the Tyrolean type intake is related to independent variables such as void ratio, rack slope, Froude number based on bar opening and the ratio of the bar opening to the screen legth. For this purpose; multiple linear regression analysis is utilized. In the analysis, four independent variables: rack angle, θ, (X_1), ratio of bar opening to the screen length, e/l, (X_2), void ratio, m, (X_3), and Froude number based on bar opening, Fre, (X_4), are used to predict the Water Capturing Performances (WCP) of the intakes. Regression coefficients are calculated and the prediction model for the diverted flow rate is established as in the following equation by the multiple linear regression analysis. The formation of the equation is given in Equation 5.8.

$$Y=a + bX_1 + cX_2 + dX_3 + eX_4$$

(5.8)

Using the data from the current experiments presented in this paper, multiple linear regression analysis is utilized to predict Water Capture Performance and the Sediment Release Efficiency for Coanda type intakes. In the analysis, six independent variables: screen slope (θ), void ratio (m), ratio of the bar opening to the curvature radius (w/R), ratio of the screen length to the curvature radius (L/R), Froude number based on screen curvature $(V/(g.R)^{0.5})$, and Weber number based on screen curvature radius $((\rho V^2R)/\sigma)$ are used to predicting the Water Capture Performance of the intakes. As for the prediction of Sediment Release Efficiency, screen slope (θ), void ratio (m), ratio of the bar opening to the curvature radius (w/R), ratio of the screen length to the curvature radius (L/R), Froude number based on screen curvature $(V/(g.R)^{0.5})$, Weber number based on screen curvature radius $((\rho V^2R)/\sigma)$ and the ratio of the D_{50} to bar opening (D_{50}/e) are used to predict the Sediment Release Efficiency. Regression coefficients are calculated and the prediction models for the Water Capture Performance and Sediment Release Efficiency are established by the multiple linear regression analysis.

5.2.1. Results of the WCP for Coanda and Tyrolean Intakes

A total of 85 experiment data from three studies (Castillo 2017; Yılmaz 2017 and our results) are used in the analysis to predict the WCP of the Tyrolean type intakes. Statistical analysis leads to the following equation relating WCP to rack angle (θ); ratio of bar opening to screen length (e/L); void ratio (m); and Froude number based on bar opening is given in Equation 5.9.

$$WCP= 119.1 - 0.59(\theta) - 13.5\left(\frac{e}{L}\right) - 205.9(m) - 0.00048(Fr_e)$$

(5.9)

The adjusted variance value is 0.68 for the analysis indicating that the diverted discharge is predicted well based on the independent parameters. Results of the multiple

linear regression analysis used to predict the WCP in Tyrolean intakes are presented in Table 40. The comparison of the predicted WCP values with the monitored values is plotted in Figure 81.

Table 9. Summary output table for the multiple linear regression analysis for predicting the WCP in Tyrolean type intakes.

Summary Output					
Regresyon Statistics					
Çoklu R	0,86781287				
R Kare	0,75309917				
Ayarlı R Kare	0,74075413				
Standart Hata	9,4452697				
Gözlem	85				
ANOVA					
	df	*SS*	*MS*	*F*	*Significance F*
Regression	4	21769,49414	5442,374	61,00418	1,5631E-23
Residual	80	7137,049578	89,21312		
Total	84	28906,54372			
	Coefficients	*Standart Error*	*t Stat*	*P-value*	*Lower %95*
Intercept	119,081479	4,640805949	25,65965	2,32E-40	109,845981
X Variable 1	-0,5926322	0,196884463	-3,01005	0,003493	-0,9844448
X Variable 2	-13,464981	48,79674827	-0,27594	0,783306	-110,573605
X Variable 3	-205,8571	19,10667017	-10,7741	3,06E-17	-243,880582
X Variable 4	-0,0004752	6,63102E-05	-7,16606	3,4E-10	-0,00060714

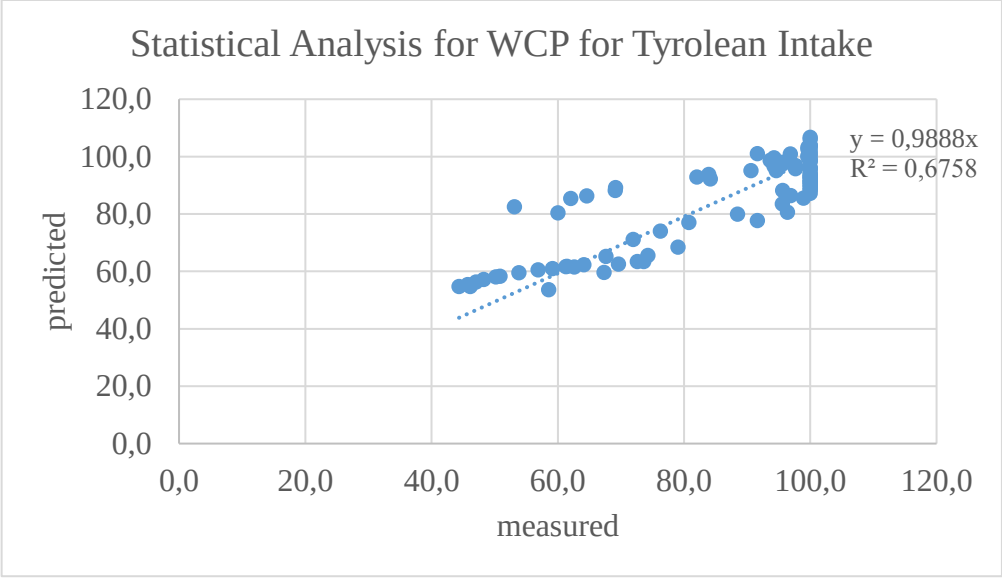

Figure 81. Comparison of monitored WCP values with the WCP predicted by the statistical model

Multiple linear regression is also utilized to derive a formulation for Water CapturePerformance, of the Coanda intakes. The statistical analysis leads to the Equation 5.10.

$$WCP=128-0.555(\theta)-121.8(m)+11255\left(\frac{e}{R}\right)-36\left(\frac{L}{R}\right)-114.3\left(\frac{V}{\sqrt{g.R}}\right)-0.00187\left(\frac{\rho V^2 R}{\sigma}\right) \quad (5.10)$$

The adjusted variance value was 0.93 for the analysis indicating that the diverted discharge was predicted well based on the independent parameters. Results of the multiple linear regression analysis used to predict the WCP in Coanda intakes are presented in Table 41. The comparison of the predicted WCP values with the monitored values is plotted in Figure 81.

Table 10. Summary output table for the multiple linear regression analysis for prediction the WCP for Coanda intakes

Summary Output					
Regression Statistics					
Multiple R	0,9633396				
R Square	0,9280232				
Adjusted R Sq	0,9138464				
Standart Error	4,6297846				
Observations	108				
ANOVA					
	df	*SS*	*MS*	*F*	*Significance F*
Regression	7	27913,18441	3987,598	217,0384	1,69572E-57
Residual	101	2164,925423	21,43491		
Total	108	30078,10984			
	Coefficients	*Standart Error*	*t Stat*	*P-value*	*Lower %95*
Intercept	127,96522	5,293969174	24,17189	8,7E-44	117,4634119
X Variable 1	-0,554968	0,052171762	-10,6373	3,55E-18	-0,658463219
X Variable 2	-121,7578	62,84746464	-1,93735	0,055495	-246,430313
X Variable 3	11255,001	2672,245599	4,211814	5,51E-05	5953,984756
X Variable 4	-36,04914	9,340592657	-3,85941	0,000201	-54,57835964
X Variable 5	-114,2906	15,20485961	-7,51672	2,34E-11	-144,4530014
X Variable 6	-0,001874	0,000239776	-7,81598	5,36E-12	-0,002349734

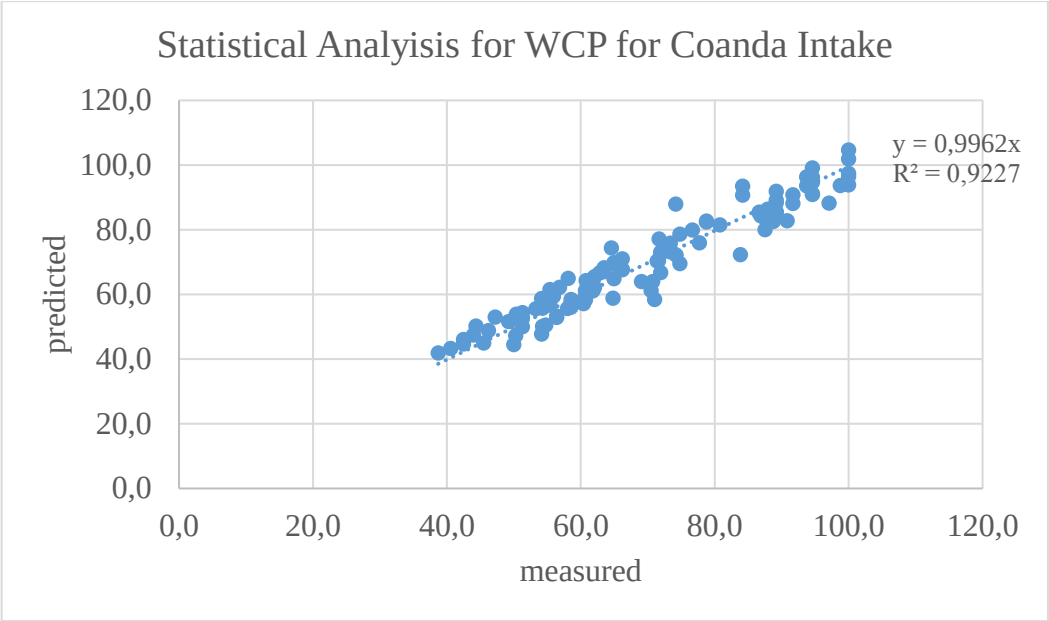

Figure 82. Comparison of monitored WCP values with the WCP values predicted by the statistical model

5.2.2. Results of the SRE for Coanda Intakes

The prediction model for the sediment release efficiency is established by the multiple linear regression analysis. The statistical analysis leads to the Equation 5.11 relating Sediment Release Efficiency to screen slope (θ), void ratio (m), ratio of the bar opening to the curvature radius (w/R), ratio of the screen length to the curvature radius (L/R), Froude number based on screen curvature $(V/(g.R)^{0,5})$, Weber number based on screen curvature radius $((\rho V^2 R)/\sigma)$ and the ratio of the D_{50} to bar opening (D_{50}/e).

$$SRE=-143.3+0.95(\theta)+1102.9(m)-30945\left(\frac{e}{R}\right)+56.1\left(\frac{L}{R}\right)+207.1\left(\frac{V}{\sqrt{g.R}}\right)+0.0018\left(\frac{\rho V^2 R}{\sigma}\right)+91.5\left(\frac{d50}{e}\right) \quad (5.11)$$

The adjusted variance value was 0.82 for the analysis indicating that the SRE was predicted well based on the independent parameters. Results for the multiple linear regression analysis are presented in Table – 41. The comparison of the predicted results

which is gathered from the multiple linear regression analysis and the measured results is given in Figure – 82.

Table 42. Summary output table for the multiple linear regression analysis for prediction the SRE for Coanda intakes

Summary Output					
Regression Statistics					
Multiple R	0,912070981				
R Square	0,831873474				
Adjusted R Squa	0,820104617				
Standart Error	11,04179138				
Observations	108				
ANOVA					
	df	*SS*	*MS*	*F*	*gnificance*
Regression	7	60325,39	8617,912	70,68431	7,07E-36
Residual	100	12192,12	121,9212		
Total	107	72517,5			
	Coefficient	*andart Erro*	*t Stat*	*P-value*	*Lower %95*
Intercept	-143,274477	35,65468	-4,01839	0,000114	-214,012
X Variable 1	0,953026584	0,124427	7,65933	1,22E-11	0,706167
X Variable 2	1102,91561	308,3617	3,576694	0,000538	491,1347
X Variable 3	-30944,9867	8255,856	-3,74825	0,000298	-47324,4
X Variable 4	56,10938266	25,3306	2,215083	0,029023	5,854196
X Variable 5	207,1385238	36,26851	5,71125	1,16E-07	135,1828
X Variable 6	0,001833664	0,000572	3,205941	0,001808	0,000699
X Variable 7	91,52371117	22,36975	4,091405	8,69E-05	47,14276

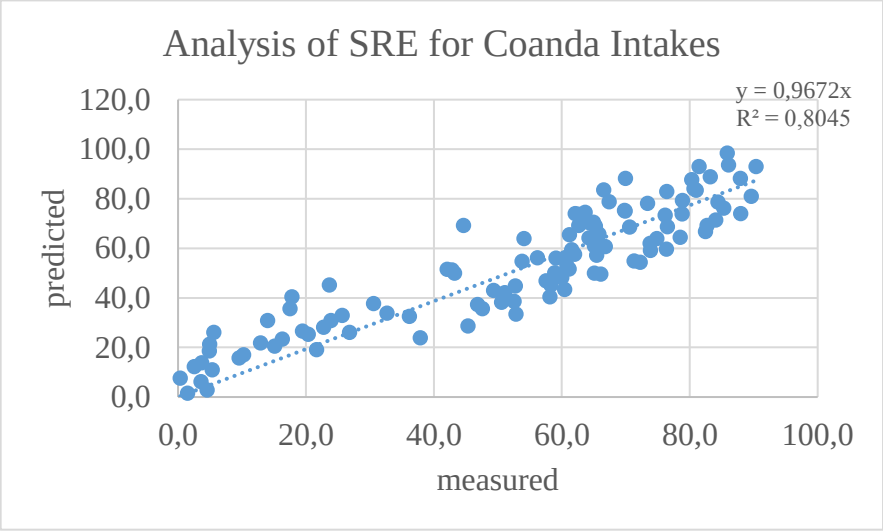

Figure 83. Comparison of monitored SRE values with the SRE values predicted by the statistical model

CHAPTER 6

CONCLUSION

In this study effects of some independent parameters on the Water Capturing Performance and Sediment Release Efficiency of Coanda intake were investigated by experimental studies. Also, some experimental studies were performed for the Tyrolean type intake for comparison of the performances with Coanda intakes. In addition to experimental studies, statistical analyses were performed to obtain a relation between independent parameters and the WCP and SRE.

From both experimental and statistical results, the following conclusions are presented;

1. The WCP values of the Coanda screens are decreasing with increasing the screen slope. Screens were tested for 5^{o} to 30^{o} screen inclinations, for future studies the screens can be tested with steeper screen slopes.

2. Although increasing the incoming flow rate increases the diverted water discharge, WCP is decreasing with increasing the incoming flow rate for a fixed screen length of 60 cm.

3.The WCP and diverted discharge values are increasing with increasing the void ratio of the screen.

4. The screen curvature radius and type of the screen which have been defined as the ratio of the sagging distance to the curvature radius of the intake structure (x/R) directly affect the diverted flow rate and the WCP of the Coanda screens. The best diverted water and WCP values were obtained from the R1200 type Coanda screens in this presented study. However, more different types of Coanda screens can be tested in order to obtain more data about this subject.

5. Similar to the Coanda intakes, the diverted water flow is decreasing with increasing the screen inclination for the Tyrolean type intake.

6. Opposite of the diverted water flow case, the diverted sediment amount is decreasing with increasing the screen inclination for the Tyrolean intake.

7. The SRE values are increasing by increasing screen inclination. The best performances

were obtained from the experiments that were done with the R800 type Coanda intake. This shows that the screen type very effective on the diverted sediment amount and SRE. For obtaining more accurate results, in future studies effect of screen curvature radius on the SRE can be investigated by more experiments.

8. The SRE values also increase with increasing the incoming flow rate.

9. The effect of the SRE and the void ratio of the screen are inversely proportional to each other. Increasing the screen void ratio decreases the SRE of the screen.

10. In the case of Tyrolean intake, the effects of the screen inclination and the incoming flow rate are in similar manner with their effect on Coanda screens. Increasing the screen inclination decreases the diverted sediment amount and increases the SRE value, increasing the incoming flow rate also increases the SRE value and decrease the diverted sediment amount.

11. Tyrolean intake shows the worst performance for the SRE when it is compared with the Coanda type intakes.

12. The SRE_C which can be expressed as the ratio of the diverted concentration to the incoming concentration is decreasing with increasing the screen inclination.

13. The SRE_C value is decreasing with increasing the incoming flow rate. However, after a certain point of the incoming flow rate, changing the incoming flow rate does not affect significantly the SRE_C under the conditions of fixed screen length.

14. The void ratio also significantly affects the SRE_C value. Increasing the void ratio generally causes to increase in the SRE_C value.

15. However, there is an interesting point. For example, the SRE_C values for the incoming rate of 7,96 l/s is less than the incoming flow rate of 2,4 l/s but, it is higher than the incoming flow rate of 5,56 l/s. Reason for this can be explained in such way, as we discussed it in previous parts, the Coanda screens have same and fixed screen length which is equal to 60 cm. Addition to this, the experiments were carried out under the by-pass flow conditions. Because the screens have limited capacity for diverting water, after a point of incoming flow rate the diverted water amounts come closer to each other. It is observed at the incoming flow cases of 5,56 l/s and 7,96 l/s where the results for the diverted water discharge values are close to the each other. At same time, because of the SRE_C depends on both diverted discharge and sediment amounts sometimes it can be observed that the SRE_C value of incoming flow case of 5,56 l/s is greater than the SRE_C value of 7,96l/s incoming flow. On the other hand, in general manner the SRE_C value is decreasing with increasing the incoming flow rate. It can

be recommended that more experiments can be performed with using the screens which have different screen lengths in the further studies.

16. Addition to the experimental studies, statistical analyses were performed for obtaining relations between the independent parameters and the dependent parameters of WCP and SRE.

17. Statistical analysis of WCP was performed for both Coanda and Tyrolean type intakes and the statistical analyses for the SRE was performed for only Coanda type intakes.

18. The adjusted variance value of the equation that was derived for the WCP of Tyrolean intake is 0,68 and the adjusted variance value of the equation that was derived for the WCP of Coanda intake is 0,93. The results indicate that the WCP is predicted well based on the independent parameters.

19. The adjusted variance values of the SRE for Coanda intakes are 0,82. The results show that SRE is predicted well based on the independent parameters.

20. Despite the accuracy of the equations for WCP and SRE are acceptable, more experiments can be performed to obtain much more data which will be used in the statistical analysis for improving these derived relations.

REFERENCES

Amruthur, Ramamurthy, Weimin Zhu, and B. L. Carballada. 1994."Flow past a two-dimensional lateral slot." *J. Envir. Engrg.,* (ASCE) 120(6): 1632–1638.

Bouvard, M. 1953 "Debit d'une grille par en dessous ." *Houille Blanche,* no. 3: 290-291.

Bouvard, M. 1992. "Mobile Barrages and Intakes on Sediment Transporting Rivers." *IAHR.* BR Rotterdam, The Netherlands: Monograph Series by A. A. Balkema.

Braun Maschinenfabrik, Accessed on December 17, 2019 https://www.braun- tech.com/upload/filecache/ basochhu_1_4eb43d92e9a2bc8ff3922a78b0c6a30a.jpg

Brunella, Sandro, Will Hager, and Hans-Erwin Minor. 2003."Hydraulics of Bottom Rack Intake." *Journal of Hydraulic Engineering.* 129, no. 1: 2-10.

Castillo, Luis and Juan Tomas Garcia Bermejo. 2016. "Estudio experimental y numérico de los sistemas de captación de fondo." Universidad Politécnica de Cartagena Departamento de Ingeniería Civil, (Spanish), 111-115.

Castillo, Luis, Jose Carillo, and Juan Tomas Garcia. 2013 "Comparison of clear water flow and sediment flow through bottom racks using some lab measurements and CFD methodology." *Proc. Seven River Basin Management.* Wessex Institute of Technology New Forest.

Castillo, Luis, Juan Tomas García, and José Carrillo. 2013."Experimental measurements of flow and sediment transport through." Civil Engineering Department, Universidad Politécnica de Cartagena, Hidr@m I+D+i Group.

Chow, Ven Te. 1959. *Open Channel Hydraulics.* New York: McGraw-Hill.

Dagan, Gedeon 1963."Notes sur le calcul hydraulique des grilles par-dessous." *Houille Blanche,* no. 1: 59-65.

Drobir, Helmut 1981. "Entwurf von Wasserfassungen im Hochgebirge." *Österreichische Wasserwirtschaft*, 243-253.

Drobir, Helmut, V. Kienberger, and N. Krouzecky. 1999."The wetted rack length of the Tyrolean weir." *IAHR-28th Congress.* Graz, Austria.

Frank, J. 1959."Fortschritte in der hydraulic des Sohlenrechens." *Der Bauingenieur*: 12-18.

Frank, J., Obering Von, and Erlangen. 1956 "Hydraulische Untersuchungen für das Tiroler Wehr. " *Der Bauingenieur*. no. 31: 96-101.

Garot, F. 1939."De Watervang met liggend rooster. " *De Ingenieur in Nederlandsch Indie.* Volume 6, no. 7: 115-132.

Gherardelli. 1956."Sul calcolo idraulico delle griglie di fondo." *Energia Elettrica*: 1347.

Huber, Dorothee. 2005 "BEDUIN Project (Better Design of Intakes)." Norwegian Water Resources.

Hydroscreen Co. LLG, Accessed on December 15, 2019 http://www.hydroscreen.com/# sthash.fFGLJ11I.dpbs

Kirschmer, Otto. 1926. "Untersuchungen über den Gefällsverlust an Rechen, vol.1." Mitteilungen des hydraulischen Instituts der TH München, Munich, Germany.

Krochin, and Sviatoslav. 1978. "Diseño Hidráulico." Quito, 97-106.

Madoux, Ract, M. Bouvard, J. Molbert, and J. Zumstein. 1955."Quelques réalisations récentes de prises en-dessous à haute altitude en Savoie." *La Houille Blanche* 6: 852-878.

Maraş, Cihan. 2017."Design of Bottom Rack and Coanda Intakes and Application on İlbank A.Ş. Projects." Expertise Thesis, Iller Bankası Anonim Sirketi, 15.

Marchi De. 1947 "Profili longitudinali della superficie libera delle correnti permanenti lineari con portata progressivamente crescente o progressivamente

decrescente entro canali di sezione costante." *Ricerca scientifica e ricostruzione.*, febrero-marzo: 203-208.

May, Don. 2015. "Sediment Exclusion from Water Systems Using a Coanda Effect Device. " *International Journal of Hydraulic Engineering*, no. 4(2): 23-30.

Mostkow, Michel. 1957. "Sur le calcul des grilles de prise d'eau. " *La Houille Blanche*, no. 4: 569-576.

Nakagawa, Hiroji. 1969. "On Hydraulic performance of bottom diversión Works." Bulletin of Disaster Prevention Research Institute, Kyoto University.

Nasser, M. S., P. Venkataraman, and Amruthur Ramamurthy. 1980. "Flow in a channel with a slot in the bed." *J. Hydr Res.* 18(4): 359–367.

National Geographic" Roman Aqueducts", Accessed on December 14, 2019 https://www.nationalgeographic.org/ encyclopedia/roman-aqueducts/

Noseda, G. 1956b."Correnti permanenti con portata progressivamente decrescente, defluenti su griglie di fondo." *L'Energia Elettrica*: 565-584.

Noseda, G. 1956a."Correnti permanenti con portata progressivamente decrescente, defluenti su griglie di fondo." *L'Energia Elettrica*: 41-51.

Orth, J., E. Chardonnet, and G. Meynardi. 1954."Étude de grilles pour prises d'eau du type en-dessous." *Houille Blanche*, no. 3: 343–351.

Plastok "Wedge Wire Screen", Accessed on December 15, 2019 http://www.plastok.co.uk/wp- content/ uploads/2014/06/wedge_wire_03.jpg

Progress Industry Group "Slotted Wedge Wire Screens"
Accessed on December 15, 2019
https://encrypted- tbn0.gstatic. com/images?q=tbn:ANd9GcRPcPnNxd3duUObf o1CcPM2o_3SxJL09lX5YRXfuGZB715SlMZe0g&s

Raudkivi, A.J. 1993."Hydraulic structures design manual." *IAHR*: 92-105.

ResearchGate " Falling water being re-directed by a spoon"
Accessed on December 15, 2019
https://researchgate.net/figure/f-Falling-water-being-re-directed-by-a-spoon-As-there-is-a-lack-of-appropriate-data-and_fig4_338117108

Ressiad, Accessed on 15 December, 2019
http://www.ressiad.org.tr /images/genel/gzp01.jpg

Righetti, M., and S. Lanzoni. 2008."Experimental Study of the Flow Field over Bottom Intake Racks." *Journal of Hydraulic Engineering*, no.1: 15-22.

Righetti, M., R. Rigon, and S. Lanzoni. 2000."Indagine sperimentale del deflusso attraverso una griglia di fondo a barre longitudinali." *Proc., XXVII Convegno di Idraulica e Costruzioni Idrauliche.* Genova, Italy. 112-119.

Simmler, H. 1978."Technische Universität Graz." für Wasserwirtschaft und konstruktiven Wasserbau., Technische Universität Graz.

Sotelo, G. 2004. *Hidráulica General*. Fundamentos Edit: Limusa Noriega Editores Volumen I .

Structurae International Database and Gallery of Structures "Sadd-el-Kafara Dam", Accessed on December 14, 2019
https://structurae.net/en/structures/sadd-el-kafara-dam

Vargas, V. 1998."Tomas de fondo." *XVIII Congreso Latinoamericano de Hidráulica.* Oaxaca, Méjico, octubre.

Venkataraman, P. 1977."Divided flow in channels with bottom openings." *J. Hydr. Div.* (ASCE), no. 103(2): 1900–1904.

Wahl, Tony. 2003. *Design guidance for coanda-effect screens*. Bureau of Reclamation, Technical Service Center, Water Resources Research Laboratory, Denver.

Wahl, Tony. 2001."Hydraulic Performance of Coanda-Effect Screens." *Journal Of Hydraulic Engineering* 127, no. 6: 480-488.

Wahl, Tony, Robert K. Weir, Hohn K. Cerise, Brian Sauer, and Jack Wergin.2004. "Labor-Saving Debris and Fish Screens. " *Water Q&M Bulletin*, June 5-6.

Wahl, Tony. 2017. *Improving Coanda - Effect Screen Technology*. Hydraulic Investigations and Laboratory Services Group U.S. Department of the Interior. Bureau of Reclamation. Denver.

White, J.K, J.A Charlton, and Caw Ramsay. 1972. "On the design of bottom intakes for diverting stream flows. " *Proceedings of the Institution of Civil Engineers*, London, 45-337.

Wild Metal GmbH "Hydropower Metal Constructions",
Accessed on December 15, 2019
https://www.wild-metal.com/sites/default/files/styles/contentbilder/public/referenzbilder/prischeralm_wildmetal_stahlwasserbau.jpg?itok=t6TEy0qN

Yıldız, Ali. 2016. "Tirol Tipi Savaklarda Akımın Deneysel ve Sayısal Modellenmesi." Yüksek Lisans Tezi, İnşaat Mühendisliği Ana Bilim Dalı, Selçuk Üniversitesi, Konya.

Yılmaz, Nazlı Aslıcan. 2010. "Hydraulic Characteristics of Tyrolean Weir." Master of Science in Civil Engineering, Middle East Technical University, Ankara.

APPENDIX A

Table 43. Results of the R800(1) type Coanda intake

R800(1) Coanda Screen Qi=2.4 l/s and Si=300 g					
θ	**Qd (l/s)**	**Sd (g)**	**WCP (%)**	**SRE (%)**	**SREc (%)**
5	2.33	219.6	97.1	26.8	75.4
10	2.08	228.3	86.7	23.9	87.8
15	1.89	157.3	78.8	47.6	66.6
20	1.84	125.6	76.7	58.1	54.6
25	1.72	125.2	71.7	58.3	58.2
30	1.55	104.7	64.6	65.1	54.0
R800(1) Coanda Screen Qi=5.56 l/s and Si=300 g					
θ	**Qd (l/s)**	**Sd (g)**	**WCP (%)**	**SRE (%)**	**SREc (%)**
5	3.68	108.2	66.2	63.9	54.4
10	3.23	83.0	58.1	72.3	47.6
15	3.16	57.9	56.8	80.7	33.9
20	3.11	46.2	55.9	84.6	27.5
25	3.08	37.6	55.4	87.5	22.6
30	2.80	41.1	50.4	86.3	27.2
R800(1) Coanda Screen Qi=5.56 l/s and Si=695 g					
θ	**Qd (l/s)**	**Sd (g)**	**WCP (%)**	**SRE (%)**	**SREc (%)**
5	3.68	240.2	66.2	65.4	52.2
10	3.23	182.1	58.1	73.8	45.1
15	3.16	121.9	56.8	82.5	30.9
20	3.11	110.84	55.9	84.1	28.5
25	3.08	102.2	55.4	85.3	26.5
30	2.80	72.2	50.4	89.6	20.6
R800(1) Coanda Screen Qi=7.96 l/s and Si=995 g					
θ	**Qd (l/s)**	**Sd (g)**	**WCP (%)**	**SRE (%)**	**SREc (%)**
5	4.32	361.7	54.3	63.7	67.0
10	3.76	210.6	47.2	78.8	44.8
15	3.53	192.8	44.3	80.6	43.7
20	3.50	167.0	44.0	83.2	38.2
25	3.38	138.6	42.5	86.1	32.8
30	3.08	141.0	38.7	85.8	36.6

Table 44. Results of R800(2) and R800(3) types Coanda intakes

R800(2) Coanda Screen Qi=2.4 l/s and Si=300 g					
θ	**Qd (l/s)**	**Sd (g)**	**WCP (%)**	**SRE (%)**	**SREc (%)**
5	2.4	295.6	100.0	1.5	98.5
10	2.37	289.2	98.8	3.6	97.6
15	2.27	284.0	94.6	5.3	100.1
20	2.2	271.4	91.7	9.5	98.7
25	2.14	254.8	89.2	15.1	95.3
30	2.13	239.0	88.8	20.3	89.8
R800(2) Coanda Screen Qi=5.56 l/s and Si=695 g					
θ	**Qd (l/s)**	**Sd (g)**	**WCP (%)**	**SRE (%)**	**SREc (%)**
5	4.32	443.7	77.7	36.2	82.2
10	4.08	369.8	73.4	46.8	72.5
15	3.98	339.95	71.6	51.1	68.3
20	3.68	295.2	66.2	57.5	64.2
25	3.61	270	64.9	61.2	59.8
30	3.45	274	62.1	60.6	63.5
R800(2) Coanda Screen Qi=7.96 l/s and Si=995 g					
θ	**Qd (l/s)**	**Sd (g)**	**WCP (%)**	**SRE (%)**	**SREc (%)**
5	5.63	565.0	70.7	43.2	80.3
10	4.83	460.2	60.7	53.8	76.2
15	4.66	382.9	58.5	61.5	65.7
20	4.62	356.0	58.0	64.2	61.6
25	4.49	346.2	56.4	65.2	61.7
30	4.32	372.3	54.3	62.6	68.9
R800(3) Coanda Screen Qi=2.4 l/s and Si=300 g					
θ	**Qd (l/s)**	**Sd (g)**	**WCP (%)**	**SRE (%)**	**SREc (%)**
5	2.4	286.4	100.0	4.5	95.5
10	2.4	299.0	100.0	0.3	99.7
15	2.27	292.4	94.6	2.5	103.0
20	2.25	269.3	93.8	10.2	95.8
25	2.25	261.3	93.8	12.9	92.9
30	2.2	241.7	91.7	19.4	87.9
R800(3) Coanda Screen Qi=5.56 l/s and Si=695 g					
θ	**Qd (l/s)**	**Sd (g)**	**WCP (%)**	**SRE (%)**	**SREc (%)**
5	4.83	468	86.9	32.7	77.5
10	4.49	330.1	80.8	52.5	58.8
15	4.16	275	74.8	60.4	52.9
20	4.08	278	73.4	60.0	54.5
25	4.00	272.5	71.9	60.8	54.5
30	3.97	264.2	71.4	62.0	53.2
R800(3) Coanda Screen Qi=7.96 l/s and Si=995 g					
θ	**Qd (l/s)**	**Sd (g)**	**WCP (%)**	**SRE (%)**	**SREc (%)**
5	5.91	569.2	74.2	42.8	77.0
10	5.18	407.0	65.1	59.1	62.9
15	5.00	330.5	62.8	66.8	52.9
20	4.92	386.3	61.8	61.2	62.8
25	4.92	354.9	61.8	64.3	57.7
30	4.81	299.9	60.4	69.9	49.9

Table 45. Results of R1200(1) type Coanda intake

R1200(1) Coanda Screen Qi=2.4 l/s and Si=300 g					
θ	**Qd (l/s)**	**Sd (g)**	**WCP (%)**	**SRE (%)**	**SREc (%)**
5	2.4	285.2	100	5.0	95.1
10	2.27	283.2	94.6	5.6	99.8
15	2.14	258.1	89.2	14.0	96.5
20	2.14	247.5	89.2	17.5	92.5
25	2.18	246.7	90.8	17.8	90.5
30	2.10	229.0	87.5	23.7	87.2
R1200(1) Coanda Screen Qi=5.56 l/s and Si=300 g					
θ	**Qd (l/s)**	**Sd (g)**	**WCP (%)**	**SRE (%)**	**SREc (%)**
5	4.66	174.8	83.8	41.7	69.5
10	4.16	127.97	74.8	57.3	57.0
15	4.00	104.7	71.9	65.1	48.5
20	3.84	99.24	69.1	66.9	47.9
25	3.92	87.5	70.5	70.8	41.3
30	3.95	65.4	71.0	78.2	30.7
R1200(1) Coanda Screen Qi=5.56 l/s and Si=695 g					
θ	**Qd (l/s)**	**Sd (g)**	**WCP (%)**	**SRE (%)**	**SREc (%)**
5	4.66	402.6	83.8	42.1	69.1
10	4.16	304.6	74.8	56.2	58.6
15	4.00	242.8	71.9	65.1	48.6
20	3.84	237.7	69.1	65.8	49.5
25	3.92	243.6	70.5	64.9	49.7
30	3.95	209.9	71.0	69.8	42.5
R1200(1) Coanda Screen Qi=7.96 l/s and Si=995 g					
θ	**Qd (l/s)**	**Sd (g)**	**WCP (%)**	**SRE (%)**	**SREc (%)**
5	5.16	551	64.8	44.6	85.4
10	4.66	377.2	58.5	62.1	64.8
15	4.49	324.6	56.4	67.4	57.8
20	4.36	332.8	54.8	66.6	61.1
25	4.31	299.14	54.1	69.9	55.5
30	3.62	184.5	45.5	81.5	40.8

Table 46. Results of R1600(1) type Coanda intake

R1600(1) Coanda Screen Qi=2.4 l/s and Si=300 g					
θ	**Qd (l/s)**	**Sd (g)**	**WCP (%)**	**SRE (%)**	**SREc (%)**
5	2.27	235	94.6	21.7	82.8
10	2.02	186,5	84.2	37.8	73.9
15	2.02	164	84.2	45.3	65.0
20	1.78	141.5	74.2	52.8	63.6
25	2.08	148.3	86.7	50.6	57.0
30	1.89	152.12	78.8	49.3	64.4
R1600(1) Coanda Screen Qi=5.56 l/s and Si=300 g					
θ	**Qd (l/s)**	**Sd (g)**	**WCP (%)**	**SRE (%)**	**SREc (%)**
5	4	115.8	71.9	61.4	53.6
10	3.61	83.9	64.9	72.0	43.0
15	3.53	76.8	63.5	74.4	40.3
20	3.38	58.3	60.8	80.6	31.9
25	3.08	42.3	55.4	85.9	25.4
30	3.01	29.25	54.1	90.3	18.0
R1600(1) Coanda Screen Qi=5.56 l/s and Si=695 g					
θ	**Qd (l/s)**	**Sd (g)**	**WCP (%)**	**SRE (%)**	**SREc (%)**
5	4	285.7	71.9	58.9	57.1
10	3,61	199.5	64.9	71.3	44.2
15	3,53	164.6	63.5	76.3	37.3
20	3,38	149.5	60.8	78.5	35.4
25	3,08	120.3	55.4	82.7	31.2
30	3,01	83.8	54.1	87.9	22.3
R1600(1) Coanda Screen Qi=7.96 l/s and Si=995 g					
θ	**Qd (l/s)**	**Sd (g)**	**WCP (%)**	**SRE (%)**	**SREc (%)**
5	4.81	371.7	60.4	62.6	61.8
10	4.08	211	51.3	78.8	41.4
15	3.92	155.2	49.2	84.4	31.7
20	3.68	189.1	46.2	81.0	41.1
25	3.38	120.5	42.5	87.9	28.5
30	3.23	95.9	40.6	90.4	23.8

Table 46. Results for R1600(2) type Coanda intake

R1600(2) Coanda Screen Qi=2.4 l/s and Si=300 g					
θ	**Qd (l/s)**	**Sd (g)**	**WCP (%)**	**SRE (%)**	**SREc (%)**
5	2.40	288.9	100.0	3.7	96.3
10	2.27	285.4	94.6	4.9	100.6
15	2.14	251.2	89.2	16.3	93.9
20	2.14	231.8	89.2	22.7	86.7
25	2.11	223.0	87.9	25.7	84.5
30	2.10	208.3	87.5	30.6	79.4
R1600(2) Coanda Screen Qi=5.56 l/s and Si=695 g					
θ	**Qd (l/s)**	**Sd (g)**	**WCP (%)**	**SRE (%)**	**SREc (%)**
5	4.08	328.7	73.4	52.7	64.5
10	3.68	235.79	66.2	66.1	51.3
15	3.53	193.1	63.5	72.2	43.8
20	3.45	182	62.1	73.8	42.2
25	3.42	174.7	61.5	74.9	40.9
30	3.38	163.4	60.8	76.5	38.7
R1600(2) Coanda Screen Qi=7.96 l/s and Si=995 g					
θ	**Qd (l/s)**	**Sd (g)**	**WCP (%)**	**SRE (%)**	**SREc (%)**
5	4.83	456.9	60.7	54.1	75.7
10	4.24	292.6	53.3	70.6	55.2
15	4.08	237.65	51.3	76.1	46.6
20	4.08	264.72	51.3	73.4	51.9
25	4.00	235.16	50.3	76.4	47.0
30	3.98	196.00	50.0	80.3	39.4